Appendix E: Water Team Final Report

Martha Conklin

Roger Bales

Phil Saksa

Sarah Martin

Ram Ray

December 15, 2015

Table of Contents

List of Tables

List of Figures

Executive Summary

Part I of this chapter addresses water quantity measurement and modeling to determine the impacts of forest fuel treatments and wildfire on hydrologic fluxes. For this study, a spatially explicit hydro-ecologic model, based on observed data, was used to scale from small to large catchments. The Regional Hydro-Ecologic Simulation System (RHESSys) was calibrated using headwater catchment observations of climate, snow, soil moisture, and stream discharge for the three pre-treatment water years (2010-2012), which encompassed wet, average, and dry precipitation conditions. The successful headwater calibrations were then transferred to the fireshed scale, based on geologic similarities between catchments. Changes in forest structure were determined by differences in Leaf Area Index (LAI), overstory canopy cover, and understory shrub cover.

Implementation of Strategically Placed Landscape Treatments (SPLATs) at Last Chance resulted in a vegetation decrease of 8% leading to runoff increases of at least 12% for the initial 20 years, falling to 9.8% by year 30, when compared to the no treatment scenario. Predicted vegetation growth following SPLATs showed the reduced biomass densities only lasted for about 10 years; after 10 years runoff decreased to pre-treatment levels. Two other modeled scenarios were also assessed: fire without SPLATs reduced vegetation by 49.8% while fire with SPLATs reduced vegetation by 38.1%, increasing runoff respectively by 66.7% and 54.9%.

SPLAT implementation at Sugar Pine resulted in a 7.5% decrease in vegetation, but increases in runoff were less than 3% compared to the no treatment scenario over 30 years. Predicted vegetation growth following SPLATs again showed the reduced biomass densities only lasted for about 10 years. Fire without SPLATs reduced vegetation by 42.5% while fire with SPLATs reduced vegetation by 39.5%, increasing runoff by 15.2% and 13.1% respectively.

Implementing SPLATs, both with and without wildfire, had a greater effect on annual runoff in Last Chance than in Sugar Pine. The difference in the two study area responses can largely be attributed to the differences in precipitation rates. Changes in vegetation at Sugar Pine had minimal effect on annual evapotranspiration rates, suggesting the forest is more water-

limited than at Last Chance, where changes in evapotranspiration were more closely linked to forest density. This response can be illustrated using the scenario of greatest vegetation change, wildfire without SPLATs, where a 42.5% reduction in Sugar Pine vegetation led to a 2.9% decrease in evapotranspiration. The 49.8% reduction in Last Chance vegetation resulted in a 22.8% decrease in evapotranspiration. Although the high-intensity fires can result in greater vegetation reductions and lead to increased runoff, these results did not specifically address water quality issues related to these wildfires such as soil erosion into the stream channel, hydrophobic soils, and elevated snowmelt rates.

Management implications of this work include the need for more spatially distributed measurements of the water balance components (particularly snow depth and soil moisture). Having a model calibrated with multiple variables allowed us to upscale from a headwater basin to an ungauged basin to capture fireshed responses to forest treatments. In our study, the most effective areas for forest treatments, with the goal of increasing water yield, are forests without significant water limitations.

Part II of this chapter addresses water quality measurements that were made to determine potential effects of treatments on water quality which could impact aquatic life and downstream water resources. Stream water temperature, conductivity, turbidity, and dissolved oxygen were recorded at 15-minute intervals using continuous recoding sensors from water year 2010 to water year 2013 in all four watersheds. Additional grab samples were collected and analyzed on a bi-weekly to bi-monthly basis for major ion chemistry and stable isotope chemistry. Movement of channel bed material was measuring using load cell pressure sensors and also recorded at 15-minute intervals for water years 2012-2014.

Water temperature, conductivity, and major ion concentrations were found to be higher in the 2012 and 2013 concurrent- and post-treatment water years respectively (referred hereafter in this chapter as the post-treatment period), however, these years were dry years and these patterns are typical of drought conditions. Dissolved oxygen remained fairly stable throughout the years of the study. Water chemistry parameters were found to all be within healthy ranges for aquatic

life with the exception of low dissolve oxygen values during very low flows of dry years when stream flow was intermittent.

Much of the water quality measurement effort was focused on turbidity and bedload movement due to the healthy ranges for other water quality parameters and a lack of sources for chemical pollutants in these headwater systems. The observed timing of turbidity verses discharge event peaks indicates that sediment is coming from localized in-channel sources that are easily transported (Martin et al., 2014). Data trends are indicative of accumulation and depletion periods tied to high and low flows. Because SPLATs were light and set far back from stream channels we hypothesized that any changes in water quality (namely turbidity) due to treatments would be due to changes in stream discharge. Mean peak turbidity values were compared for pre- and post- treatment periods in the treatment watersheds but no significant difference was found. This may have been due in part to small sample sizes and large standard deviations caused by the infrequent and episodic nature of sediment movement in these streams. Channel bed movement data trends are indicative of the channel bed acting as temporary storage for sediment, but that it remains stable over the long term. The treatments as implemented were not intensive enough to show an increase in discharge during a low precipitation year and SPLATS as implemented in SNAMP had no detectable effect on turbidity.

Management implications of the water quality study point to the heterogeneity of flowpaths in these headwater catchments. Parameters from one headwater catchment may not translate to a nearby catchment. To capture this heterogeneity, spatially explicit measurements are necessary.

I: Water Quantity Observations and Modeling

Introduction

The movement of water through mountainous catchments in the western United States is dependent on the interplay of climate, vegetation, and subsurface processes. Characterizing these components and their influence on snowpack and water supply is a priority for effective management of land and water resources. In this study, two pairs of headwater catchments (1.0-2.5 km^2) were instrumented and monitored. One catchment in each pair received prescribed thinning. Using the parameters derived from these headwater basins, the hydrologic effect of treatments at the fireshed scale (17-35 km^2) was modeled.

The risk of high-intensity wildfire in the Sierra Nevada is increasing (Miller et al., 2009) because of changes in climate (Westerling et al., 2006) and high vegetation densities compared to the previous century (Collins et al., 2011b). There is a need to restore the resiliency of the forest to pressures of climate and wildfire by applying localized integrated management (Stephens et al., 2013). The collective impacts of forested-watershed management, wildfire, and climate will modify the responses of evapotranspiration and runoff in these mountain catchments. As the major source of California's annual water supply (CA Department of Water Resources, 2013), predicting the changes in Sierra Nevada runoff in response to forest vegetation management, disturbance, and growth is a priority.

Fuels treatments can be used in Sierra Nevada mixed-conifer forest to reduce wildfire hazard (Stephens, 1998; Stephens and Moghaddas, 2005), and Collins et al. (2011a) showed the effectiveness of fuels treatments on burn probabilities was reduced after 20 years of regrowth. Runoff response to fuels treatments depends on the pattern and magnitude of prescribed fire (Robichaud and Waldrop, 1994; Robichaud, 2000; Fernandez et al., 2008), shrub removal (Fernandez et al., 2008), and thinning (Robles et al., 2014). The runoff response to wildfire depends on similar characteristics, such as location in the catchment, fire intensity, and fire severity (Ice et al., 2004). The rate of vegetation regrowth will affect long-term runoff effects (Potts et al., 2010; Hawthorne et al., 2013). Shakesby and Doerr (2006) note that post-fire runoff

research at the watershed scale tends to focus on changes to peak flows and erosion potential more than on water yield.

Reviewing catchment studies of vegetation treatment effects on stream discharge, Stednick (1996) and Bosch and Hewlett (1982) show that removal of forest vegetation typically increases runoff and storm event discharge peaks, but the magnitude of change and period of impact depend upon the amount of vegetation removal, post-treatment precipitation levels, and the rate of vegetation re-growth. In seasonally snow-covered basins, tree removal not only impacts evapotranspiration, but also local energy balances that affect the patterns of snow ablation in a forest (Macdonald, n.d.; Ellis et al., 2013) . Long-term experimental treatments implemented in the continental snowpack of the Rockies have shown some indication of increasing runoff. Harvesting 23.7% of the 16.7-km^2 Coon Creek Watershed in Wyoming resulted in a mean annual runoff increase of 7.6-cm (17%) for the 5 years following treatments (Troendle et al., 2001). Harvesting 25% of a 21.3-km^2 lodgepole forest in Utah revealed a 14.7-cm (52%) increase in annual runoff, after 20 years of post-treatment monitoring (Burton, 1997). Lastly, reviewing 28 years of post-treatment monitoring after harvesting 40% of the 8-km^2 Fool Creek Watershed in Colorado, Troendle and King (1985) observed a mean increase of 8.2-cm (28%) in annual runoff.

Multiple regressions of runoff response to forest treatments, mean annual precipitation, mean annual runoff, and runoff fraction from 31 experimental catchments in the western United States were applied to model treatment effects in the Sierra Nevada (Marvin, 1996), and show that a 10% increase in mixed-conifer zone harvesting would have no statistical significance on annual runoff (-0.2 - 1.2 cm). Marvin (1996) notes that it is more difficult to determine effects of treatments on runoff in the arid west than the catchments used by Bosch and Hewlett (1982). Stednick (1996) suggests that 20% of a forest needs to be treated, generally, required to detect changes in runoff. Using existing literature, Kattelmann et al. (1983) qualitatively hypothesize that removing all vegetation in the Sierra could increase runoff 30 - 40%, while managing National Forest land specifically for water production could increase runoff by 2 - 6%. Constraints of management, access, and economics lower this qualitative estimate to about 0.5 -

2% (0.3 - 1.2 cm), and Kattelmann et al. (1983) instead emphasize the benefit of treatments in delaying snowpack ablation.

Forest management to reduce fire risk requires the thinning of dense vegetation, removal of ladder fuels, and prescribed burning or mastication to reduce understory shrubs. This modification of the vegetated landscape has an impact on the energy inputs leading to snowpack melt (Black et al., 1991; Essery et al., 2008; Pomeroy et al., 2009; Lawler and Link, 2011) and the rate of water transferred to the atmosphere through evapotranspiration (Zhang et al., 2001; Moore et al., 2004; Biederman et al., 2014; Brown et al., 2014). Annual runoff and evapotranspiration rates in the Sierra Nevada are dependent on elevation and latitude. In the eight basins of the Kings River Experimental Watershed, Hunsaker et al. (2012) calculated a mean annual runoff fraction ranging from 0.23 to 0.53, resulting in a loss term ranging from 47% to 77% of the annual precipitation. In a separate study, evapotranspiration loss in two Providence Creek sub-catchments was 76 cm (63%) of a 122 cm precipitation year, also estimated using a water balance calculation (Bales et al., 2011). Goulden et al. (2012) calculated a 44% evapotranspiration loss from a mean 98.4 cm of precipitation in the larger watershed of the Upper Kings River using eddy covariance measurements expanded with remote sensing normalized difference vegetation index (NDVI).

Research into the application of hydrologic modeling to ungauged basins has been the focus of recent studies (e.g., Sivapalan, 2003; Wagener and Montanari, 2011; Hrachowitz et al., 2013), given the increasing use of modeling tools and decreasing emphasis on measurements in hydrology (Silberstein, 2006). One approach for modeling basins lacking observations has been to transfer model parameters from another instrumented basin (van der Linden and Woo, 2003; Heuvelmans et al., 2004; Bárdossy, 2006). There are a number of attributes that can be considered when regionalizing model parameters from gauged basins, including spatial proximity, physical similarity, and regression of model parameters and physical characteristics (Merz and Blöschl, 2004; Bao et al., 2012). Studies comparing the methods have noted that parameters of some gauged (donor) basins can be completely transferred to ungauged (receiver) watersheds based on spatial proximity and hydrologic similarity (Kokkonen et al., 2003; Parajka et al., 2005), which eliminates the necessary assumption of linearity associated with the

regression method (Parajka et al., 2005). For the purpose of this study, a spatially explicit model was used to maximize available spatial data and to scale from small to large catchments. The Regional Hydro-Ecologic Simulation System (RHESSys; C. L. Tague and Band, 2004) was specifically chosen due to its use in research applications of forest and mountain hydrology over a range of geographical regions (Hartman et al., 1999; Mackay, 2001; Zierl et al., 2006; Hwang et al., 2008; Tague et al., 2009).

The U.S. Forest Service, the largest public land manager in the Sierra Nevada, has undertaken efforts to incorporate adaptive management into the institution's land management practices (e.g., Bormann et al., 1994, 2007). One of these land-management approaches, Strategically Placed Landscape Treatments (SPLATs; Bahro and Barber, 2004), are fuels treatments designed to disrupt fire paths and reduce overall fire severity. A fireshed generally spans thousands of acres, and is determined by landscape fire characteristics such as regime, history, risk, and potential behavior (Bahro and Barber, 2004). Development of forest-management strategies should incorporate water yield into the management framework (Adams, 2013). Explicit quantification and verification of water-balance response to vegetation management and disturbance is required, however, in order for management of forests and water to succeed. Development of regional prediction and verification tools are also needed to transfer observed hydrologic conditions to unmonitored firesheds and projected forest-vegetation conditions.

Our objective in this study was to estimate the impacts of the implemented fuels treatments (SPLATs) and the impacts of wildfires, modeled with and without fuels treatments, on runoff at the fireshed scale. Our study design was to monitor the water balance in small headwater catchments, using distributed measurements of snow and soil moisture with stream discharge, to calculate the annual water-balance. From the intensive measurement program, we would then be able to produce a well-constrained hydrologic model to assess the water balance response to vegetation disturbances at the fireshed scale. To complete these objectives, we needed to determine the factors controlling hydrologic response to changes in vegetation, and assess the transferability of a well-calibrated headwater catchment hydrologic model (0.7-2.4 km^2) to the fireshed scale (17-35 km^2).

Study Sites

Two sets of paired headwater study catchments within two larger study areas were have been instrumented with continuously recording observation equipment (Figure E1, Table E1). Big Sandy Creek (treatment) and Speckerman Creek (control) are the paired headwaters in the Sierra National Forest. The headwaters drain to the South Fork of the Merced River which is adjacent to the firesheds located in the Lewis Fork of the Fresno River (referred to as Sugar Pine).

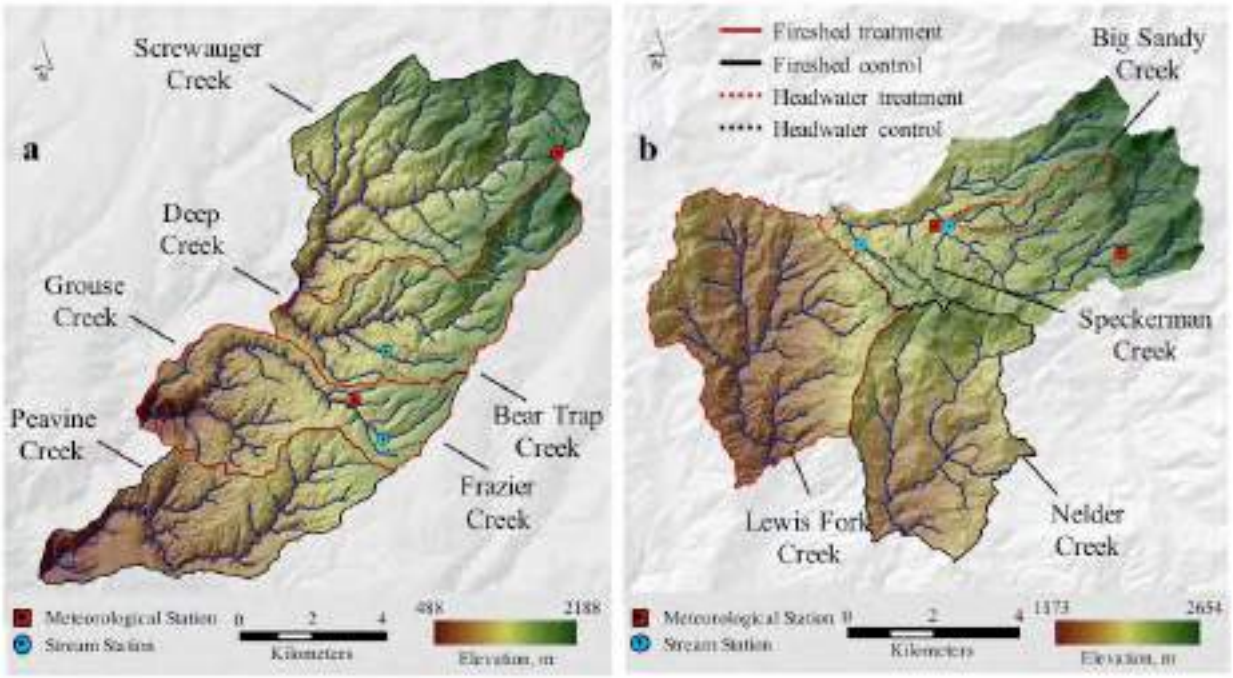

Figure E1: Location of the study catchments: Last Chance in Tahoe National Forest (a) and Sugar Pine in Sierra National Forest (b).

Bear Trap Creek (treatment) and Frazier Creek (control) are the other set of paired headwaters in the Tahoe National Forest, and are nested within the firesheds draining to the Middle Fork of the American River (referred to as Last Chance). Frazier and Bear Trap catchments are underlain by upper elevation Miocene-Pliocene volcanic and lower elevation sedimentary bedrock of the Shoo Fly complex (Saucedo and Wagner, 1992). The bedrock underlying the Big Sandy and Speckerman catchments consists of plutonic Early Cretaceous Bass Lake Tonalite (Bateman, 1989). Fireshed elevations range from 488 m to 2188 m (Table E2), transitioning from rain to

snow dominated precipitation, and vegetation communities are mainly comprised of mixed-conifer forests (Tables E3, E4).

Table E1 : Physiographic features of the four headwater study catchments.

Catchment	Area (km^2)	Outlet Elev (m)	Drainage Basin	Type
Bear Trap	1.4	1560	American R.	Treatment
Frazier	1.8	1604	American R.	Control
Big Sandy	2.2	1776	Merced R.	Treatment
Speckerman	1.9	1720	Merced R.	Control

Table E2: Physiographic features of the fireshed catchments.

Study Area	Catchment	Area (km^2)	Elevation (m)	Type
Last Chance	Screwauger	34.5	1167 – 2018	Control
	Deep	21.6	658 – 2188	Treatment
	Grouse	21.3	658 – 1847	Treatment
	Peavine	22.2	488 – 1847	Control
Sugar Pine	Lewis	24.4	1173 – 2088	Treatment
	Nelder	17.7	1390 – 2179	Control

Table E3: The vegetation composition of Last Chance firesheds.

Vegetation Community	Screwauger (%)	Deep (%)	Peavine (%)	Grouse (%)
Low Shrubs	0.0	0.1	0.0	0.0
High Shrubs	0.2	0.0	0.0	0.0
Open True Fir	4.3	3.2	1.1	0.1
Pine Forests	6.1	2.9	2.6	2.4
Cedar Forests	14.3	7.0	6.0	3.8
Young Mixed Conifer	13.6	8.9	6.0	2.8
Mature Mixed Conifer	61.5	77.9	84.3	90.9

Table E4: The vegetation composition of Sugar Pine firesheds.

Vegetation Community	Lewis (%)	Nelder (%)
Open Pine-Oak Woodland	0.0	0.0
Live Oak-Pine Forest	5.9	2.2
Mature Mixed Conifer Forest	88.2	79.1

Closed-canopy Mixed Conifer Forest	5.9	18.7

Soils in Last Chance are well drained, containing Crozier-Cohasset, Crozier-McCarthy-Cohasset, Crozier-Mariposa-Cryumbrepts, and Hurlbut-Deadwood complexes (Soil Survey Staff, 2011). Sugar Pine soils are also well drained, containing Ledford family-Entic-Xerumbrepts, Chaix-Chawanakee, and Umpa families (Soil Survey Staff, 2011). Texture analysis from the 128 soil samples <1-m below the surface show the soils at Last Chance to be categorized as loam or sandy loam, with soils at Sugar Pine being categorized as sand or sandy loam. Mixed-conifer forest at Last Chance is dominated by White Fir (*Abies concolor*), Ponderosa Pine (*Pinus ponderosa*), Douglas Fir (*Pseudotsuga menziesii*), and Sugar Pine (*Pinus lambertiana*) with understory including Incense Cedar (*Calcedrous decrrens*), Huckleberry Oak (*Quercus vacciniifolia*) and Dwarf Rockcress (*Arabis parishii*). Mixed-conifer forest at Sugar Pine is dominated by Ponderosa Pine (*Pinus ponderosa*), Incense Cedar (*Calocedrous decurrens*), California Black Oak (*Quercus kelloggii*), White Fir (*Abies concolor*), and Sierra Live Oak (*Quercus wislizeni*) with understory including Mountain Misery (*Chamaebatia foliolosa*) and Dwarf Rockcress (*Arabis parishii*).

Methods

Sierra Nevada Adaptive Management Project

For the purposes of completing a water balance and constraining hydrologic model parameters, the following instruments were installed using the same methods at each site. One upper and one lower elevation meteorological station recording conditions of precipitation, temperature, wind speed/direction, and radiation close to the extremes of the headwater elevation ranges were installed at Last Chance and Sugar Pine. Precipitation measured at the installed meteorological stations used the tipping bucket method, so accurate records were limited to rainfall-only events. Comprehensive precipitation data from both rain and snow events for water balance characterization and model input were from the Blue Canyon meteorological station operated by the US Bureau of Reclamation, 22 km to the northeast of Last Chance. In Sugar Pine, the Poison Ridge meteorological station also operated by the US Bureau of Reclamation, 8 km to the southeast, was used for precipitation input. Precipitation levels were assumed to be

uniform across the headwater basins. In this document, precipitation refers to the combination of rain and snow falling in the watersheds, and Snow Water Equivalent (SWE) refers specifically to precipitation falling as snow.

Distributed snow depth (15/site) and soil moisture (64/site) sensors installed around the meteorological stations and discharge sites recorded measurements at 15-minute intervals over a range of elevation, slope, aspect and forest cover, similar to the design used in later installations by Bales et al. (2011) and Pohl et al. (2014). Bear Trap and Big Sandy watersheds did not have continuous SWE measurements available within the basin. Instead, observed snow depth from the distributed sensors was converted to snow water equivalent using a linear relationship between the Day of Year and percent water from the nearest snow pillow at a similar elevation, following the methods of Liu et al. (2013). Daily mean SWE was calculated for the entire watershed using the converted snow water equivalent for each sensor and the average basin elevation.

Stream stage was recorded at each headwater catchment outlet by pressure-sensitive water depth recorders. Stream discharge was then measured at each location at multiple stages to develop the stage-discharge rating curve to calculate daily observed discharge for each stream. Discharges were measured over a range of flows during the four years, with a minimum of 16 data points available at each watershed outlet. A majority of measurements were recorded at low to medium stream discharge, while higher discharges are generally under-represented. Discharge in this water quantity section are reported as area-normalized discharge in centimeters, to directly relate annual precipitation inputs to runoff outputs. Discussing water quality results in the next section, we report discharge in cubic meters per second, to relate the tractive force of discharge to in-channel sediment displacement.

Strategically Placed Landscape Treatments (SPLATs; Bahro and Barber, 2004) are designed to disrupt fire paths and reduce overall fire severity. SPLATs were implemented in the fall of 2012 in accordance with the record of decision for the Sierra Nevada Forest Plan Amendment (2004). Changes in forest vegetation were determined by differences in Leaf Area Index (LAI) and Canopy Cover (CC) calculated from LiDAR and vegetation plot data collected

before and after treatments (Appendix A-FFEH in this report). Waveform LiDAR products that would be able to estimate understory vegetation were unavailable, so understory shrub cover was incorporated into the model using a linear equation developed by the fire and forest health team, based on their forest plot measurements (Equations 1, 2); we assumed these relationships in overstory and understory structure were constant in all model scenarios. Shrub cover was calculated in each vegetation community type for Last Chance (Equation 1, $R^2 = 0.16$) and Sugar Pine (Equation 2, R^2=0.25) as

$$SC = 63.079 - 0.244 \times BA - 0.257 \times CC \quad [1]$$

$$SC = 55.273 - 0.294 \times BA - 0.256 \times CC \quad [2]$$

where SC is Shrub Cover (%), BA is Basal Area (m^2/ha) and CC is Canopy Cover (%). Although the correlation coefficients are relatively low, the equations produce an expected trend of increasing shrub cover with decreasing overstory forest cover and density.

Leaf area index and vegetation cover modify transpiration rates by changing the total amount of vegetation, modify snowmelt rates by changing the amount of light that reaches the snowpack (Equations 4-6), and on a smaller magnitude change interception and evaporation rates. Forest thinning in the treatment areas consisted of removing trees below 76.2-cm Diameter at Breast Height through a combination of cable and mechanical thinning. Mastication and prescribed ground burning were not specifically done in the headwater catchments, although they were used within the treated firesheds.

The RHESSys model (Tague and Band, 2004) combines a meteorological forcing model (MTN-CLM; Hungerford et al., 1989), biogeochemical cycling model (BIOME-BGC; Running and Hunt, 1993), and hydrological model (TOPMODEL; Beven and Kirkby, 1979 or DHSVM; Wigmosta et al., 1994). Explicit flow routing using DHSVM was used for the simulations in this study. The spatial environment in the model is created using a 20-m DEM, soil layer from the USDA-NRCS soil survey geographic survey (SSURGO) database (Soil Survey Staff, 2011), and a vegetation layer created from a combination of LiDAR canopy point clouds and forest plot data (Appendix A-FFEH in this report). Daily minimum and maximum temperature data were input

from the on-site meteorological stations and precipitation was input from the closest-reference stations detailed above.

Modeling the impact of vegetation on catchment water balance is focused on the following equations. Vegetation density affects interception, transpiration, and the surface energy balance. Transpiration rates are impacted as LAI is used to scale up the rate of stomatal conductance to the landscape patch (Equation 3; Jarvis, 1976). The limitations of maximum stomatal conductance for sunlit and shaded canopy are calculated as linear scalars

$$gs = f(ppfd) f(CO_2) f(LWP) f(vpd) gs_{\max}(LAI) \quad [3]$$

where *gs* is stomatal conductance (m/s), *ppfd* is photosynthetic flux density, CO_2 is carbon dioxide, *LWP* is Leaf Water Potential, *vpd* is vapor pressure deficit, and gs_{max} is maximum conductance. The surface energy balance for snowmelt is affected by a Beer's law approximation of the amount of incoming shortwave radiation (Equations 4, 5), combined with longwave radiation (Equation 6). Incoming direct (K_{direct}) and diffuse ($K_{diffuse}$) shortwave radiation to the snowpack surface are calculated as

$$K_{direct} = (1 - \propto_{direct})(1 - \alpha \propto_{direct}) K_{direct'} (1 - corr\ exp^{-ext_{coef}}) \quad [4]$$

$$K_{diffuse} = (1 - \alpha_{direct}) K_{diffuse'} \{1 - exp^{-[(1-GF)PAI]^{0.7}} + S_c\} \quad [5]$$

where α_{direct} is the vegetation-specific albedo, $K_{direct'}$ and $K_{diffuse'}$ are direct and diffuse solar radiation at the top of each vegetation layer, *corr* is an option correction factor for low sunlight angles with sparse canopy, ext_{coef} is the Beer's Law extinction coefficient, *GF* is the canopy gap fraction, *PAI* is the Plant Area Index, and S_c is the scattering coefficient. Longwave radiation is calculated as

$$L = 41.868[ess_{atm} \sigma (T_{air} + 272)^4 - 663] \quad [6]$$

where ess_{atm} is the emissivity of the atmosphere , σ is the Stefan-Boltzmann constant, and T_{air} is the air temperature (*K*).

For each scenario, we used the four water years of observed meteorological inputs (2010-2013) to produce a mean annual value of runoff, evapotranspiration, and groundwater. Four vegetation scenarios were considered: an untreated forest, a forest with SPLATs implemented, an untreated forest following a simulated wildfire, and a forest with SPLATs implemented following a simulated wildfire. Vegetation growth in each scenario was projected for 30-years using the Forest Vegetation Simulator (FVS; Dixon, 2002), where a point-in-time snapshot of the vegetation conditions was captured at 0, 10, 20, and 30 years. The four water years of meteorological observations were simulated for each vegetation condition to capture the range of dry to wet precipitation conditions that occurred during this study. Post-fire vegetation scenarios start at 10 years, allowing for a decade of growth following the simulated wildfire events, and avoid issues such as soil hydrophobicity, reduced soil infiltration capacity, and diminished litter cover that can occur immediately after fire. We differed from the exact FVS scenarios by adding in the shrub cover as outlined above, because understory vegetation can be an important additional source of transpiration loss following the disturbance events modeled in this study.

The stream outlets draining the study firesheds were not gaged due to the remote and steep terrain. The stream discharge site closest to the Last Chance firesheds drains the North Fork of the Middle Fork (NFMF) of the American River (Figure E2), an area of 230.2 km^2 of which 43.2% are the study firesheds. Discharge monitoring data were provided by the Placer County Water Agency (PCWA). The closest monitored stream discharge for the Sugar Pine firesheds is on the Lewis Fork (Figure E3, USGS gage 11257040). The Lewis Fork discharge site is just north of its confluence with the Fresno River in Oakhurst, CA, and drains an area of 84.2 km^2, of which 50% are the study firesheds.

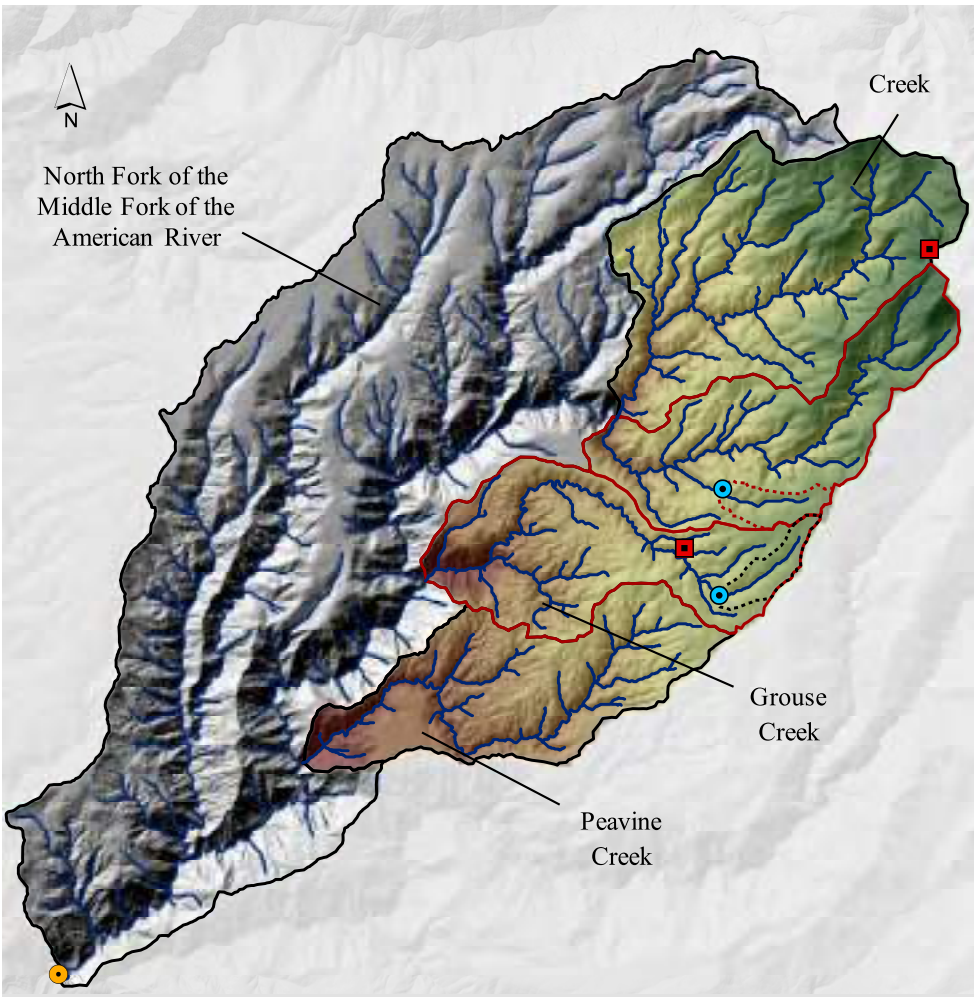

Figure E2: Location of the closest stream gage station to the firesheds, the North Fork of the Middle Fork (NFMF) of the American River, for comparing discharge to the headwater sites of Bear Trap and Frazier in Last Chance. Placer County Water Agency (PCWA) provided NFMF stream gage data. Colored basins with red boundaries are treated; those with black boundaries are controls. Headwater basins have dashed boundaries.

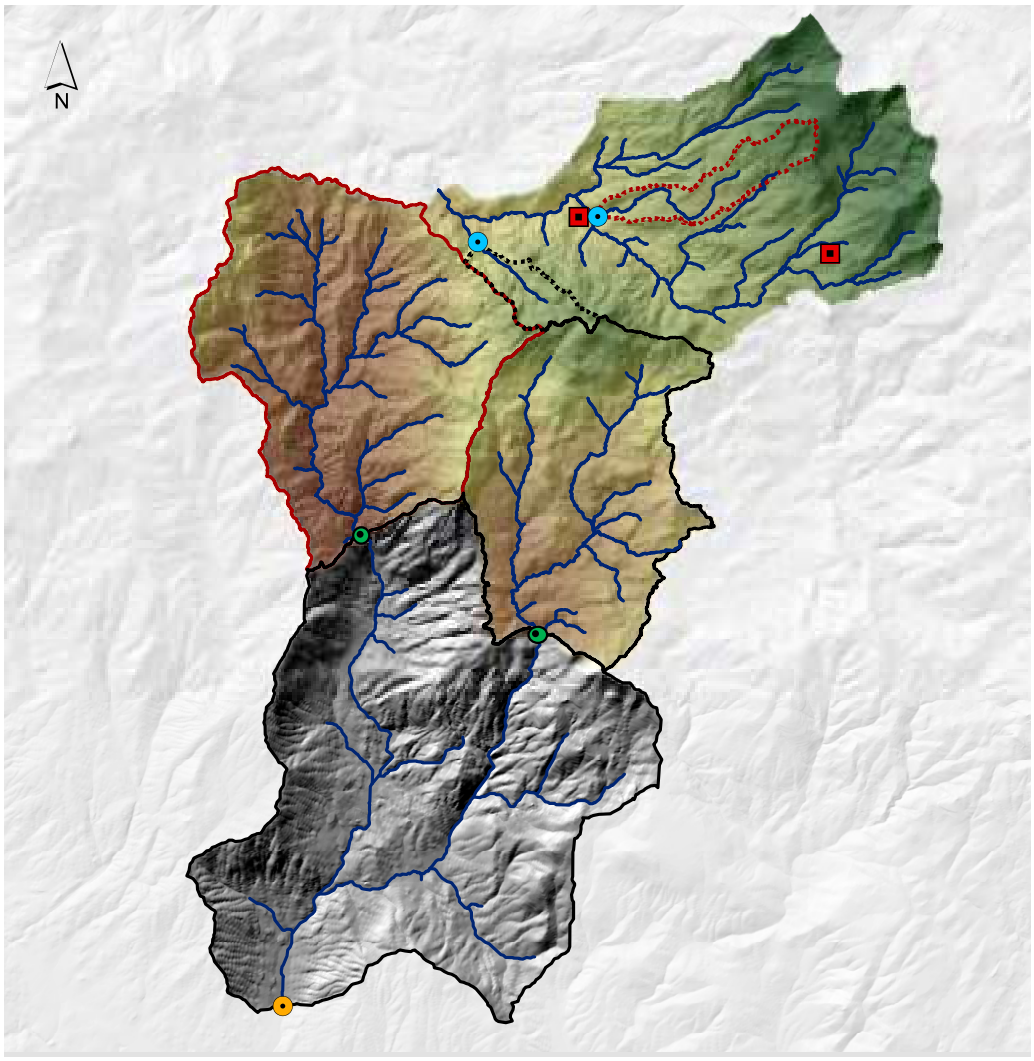

Figure E3: Location of the closest stream gage station to the firesheds, the Lewis Fork of the Fresno River (USGS gage 11257040), for comparing discharge to the headwater sites of Big Sandy and Speckerman in Sugar Pine. Colored basins with red boundaries are treated; those with black boundaries are controls. Headwater basins have dashed boundaries.

The direct transfer of calibrated model parameters has been shown to be a preferred method of simulating nearby ungauged basins with similar physiographic characteristics (Kokkonen et al., 2003; Parajka et al., 2005). There are a number of attributes that can be considered when regionalizing model parameters for an ungauged basin, including spatial proximity, physical similarity and regression of model parameters. The headwater and fireshed

catchments in this study have similar geologic and vegetation characteristics. The Last Chance firesheds are underlain by upper-elevation Miocene-Pliocene volcanic and lower-elevation sedimentary bedrock of the Shoo Fly complex (Saucedo and Wagner, 1992). The bedrock underlying the Sugar Pine catchments consists of plutonic Early Cretaceous Bass Lake Tonalite (Bateman, 1989). They do differ in elevation range and basin size; the lower elevation range in the larger catchments result in more rain and faster winter runoff, which was reflected in the observations and model results. Goulden and Bales (2014) note that lower-elevation basins in the Sierra Nevada also have a higher potential evapotranspiration because of the warmer winter temperatures.

Initial comparison of flow duration curves for the two headwater streams and the NFMF of the American River showed that headwaters and downstream sites have similar slopes for 80% of the flow probabilities (water years 2010-2013, Figure E4). This suggests that for 20% of conditions, discharge at different scales and between basins is controlled by different flow paths, or paths with different flow lengths.

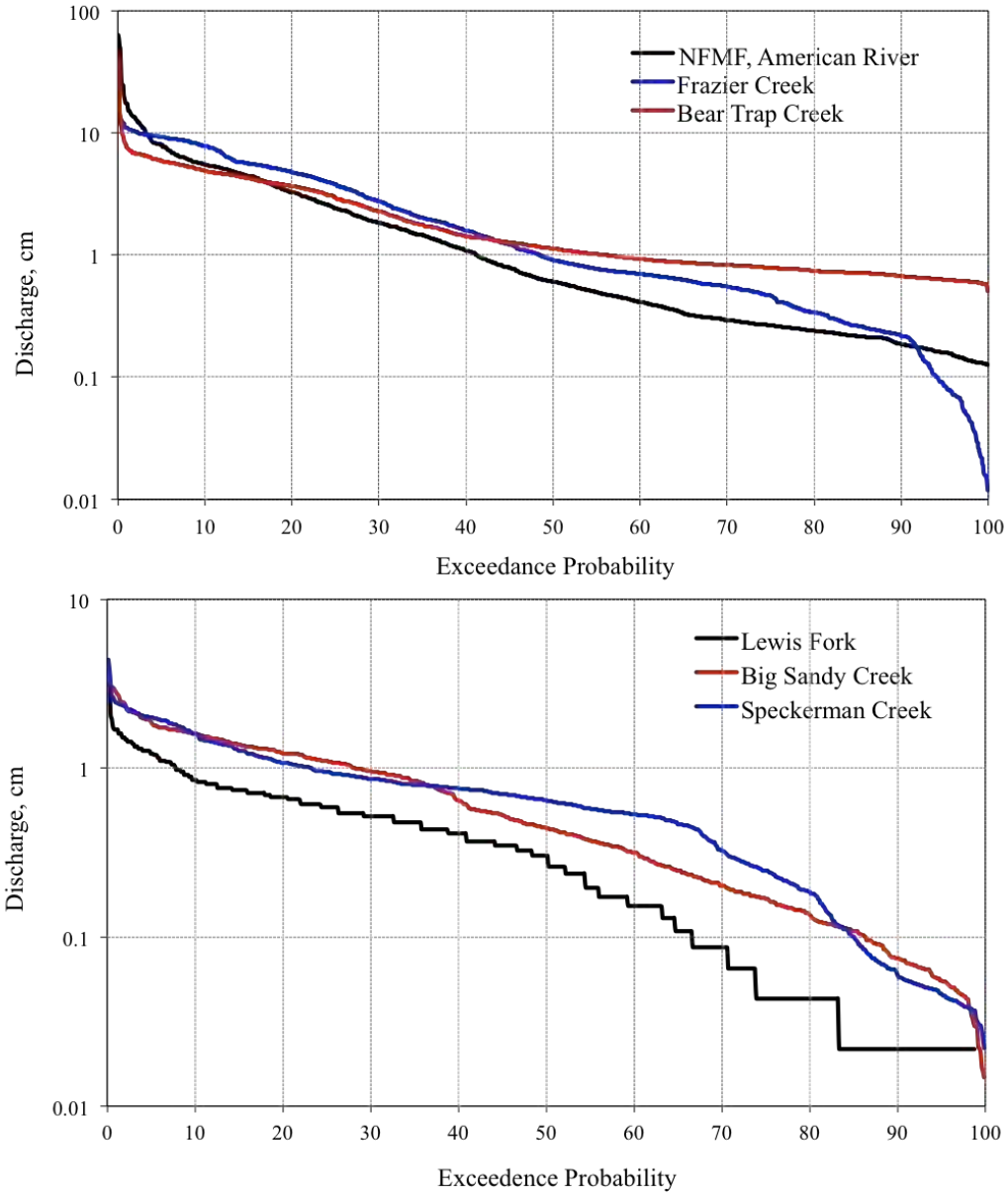

Figure E4: Flow duration curves for the headwater sites compared to the closest stream gaging site for the firesheds in Last Chance (a) and Sugar Pine (b). Discharge is normalized over the watershed area for direct comparison.

As flow drops below the 10th percentile, the slope of the line representing the relationship between discharge and probability becomes more parallel between headwaters and the NFMF. This suggests that the behavior of these headwater basins is more similar to the hydrologic behavior of the NFMF at normalized discharges of less than 10 cm, until flow probabilities increases to above the 90th percentile, where discharge values for Frazier drop rapidly. This drop

is due to the stream becoming ephemeral during extreme drought conditions in 2013. A comparison of the hydrographs of the headwaters and the NFMF of the American River show that peak discharge and subsequent recessions occurred at approximately the same time at both scales (Figure E5).

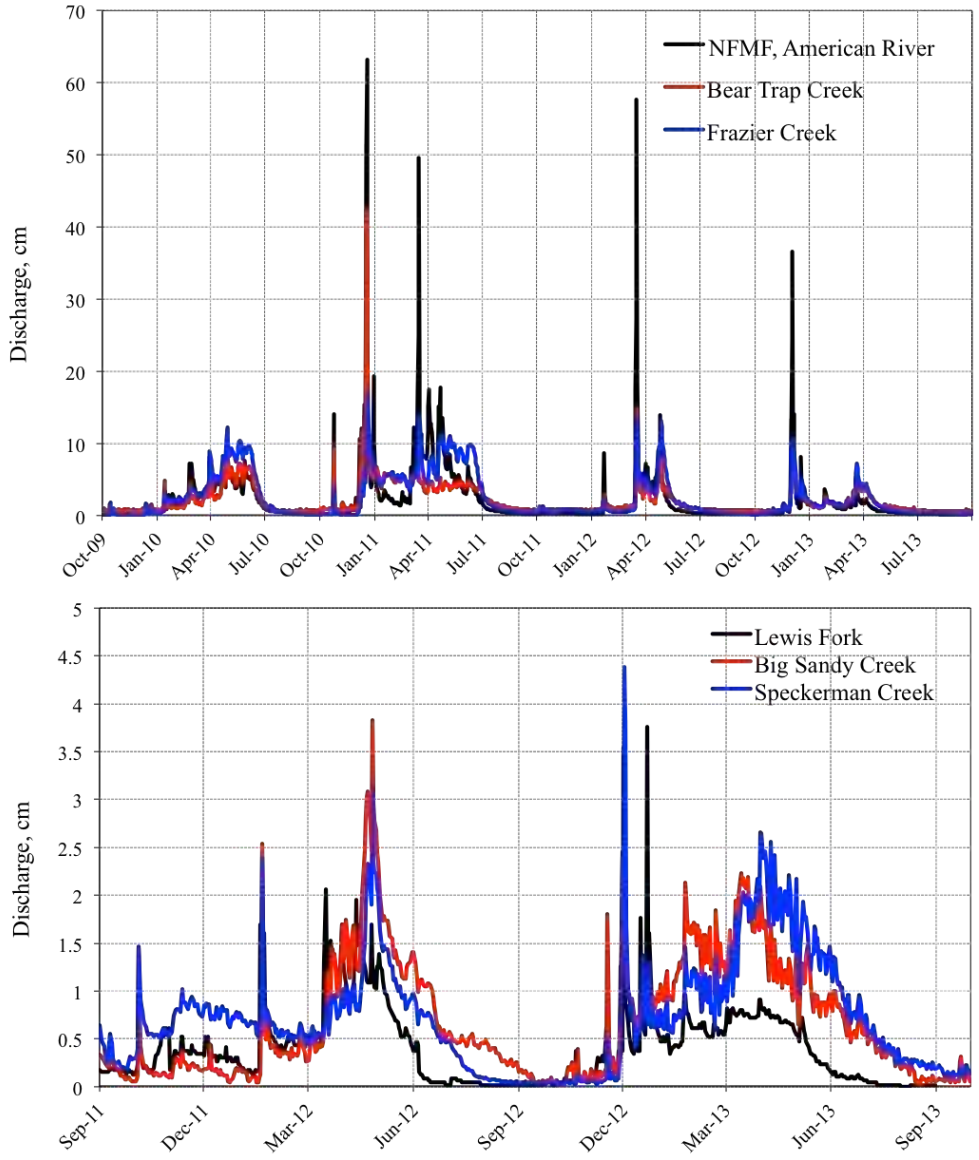

Figure E5: Discharge for the headwater and closest stream gaging site to the firesheds for Last Chance (a) and Sugar Pine (b). Discharge is normalized over the watershed area.

A direct comparison of area-normalized discharge between each headwater stream and the NFMF did not show a strong correlation between the headwaters and downstream sites (Figure

E6). However, using the predictive format of linear regression models with the full discharge record for the headwater streams, the headwaters acted as predictors for downstream stream discharge and were highly significant for all three models tested (Table E5). Bear Trap discharge explained more of the variability in the North Fork of the Middle Fork of the American River than Frazier, however, the combination of the two basins was shown to be the best fit model using the Akaike Information Criterion (AIC; Akaike, 1973) informed by Akaike Weights (Burnham and Anderson, 2002) (Table E5). AIC selection ranks the goodness-of-fit in the prediction models with penalties for increasing model complexity by adding terms (K), where a lower value indicates better performance. The AIC value is relative to the models being compared, and does not indicate an uniform standard for goodness-of-fit like the correlation coefficient (i.e., the lower AIC values in Table E6 do not indicate a better fit than the models in Table E5). Akaike Weights are a method of averaging the models together, such that the weights sum to 1, and a higher weight indicates additional information gained. The combined model explained 63.7% of the variability in the downstream discharge for the entire available data record, with the lowest AIC value and highest weight.

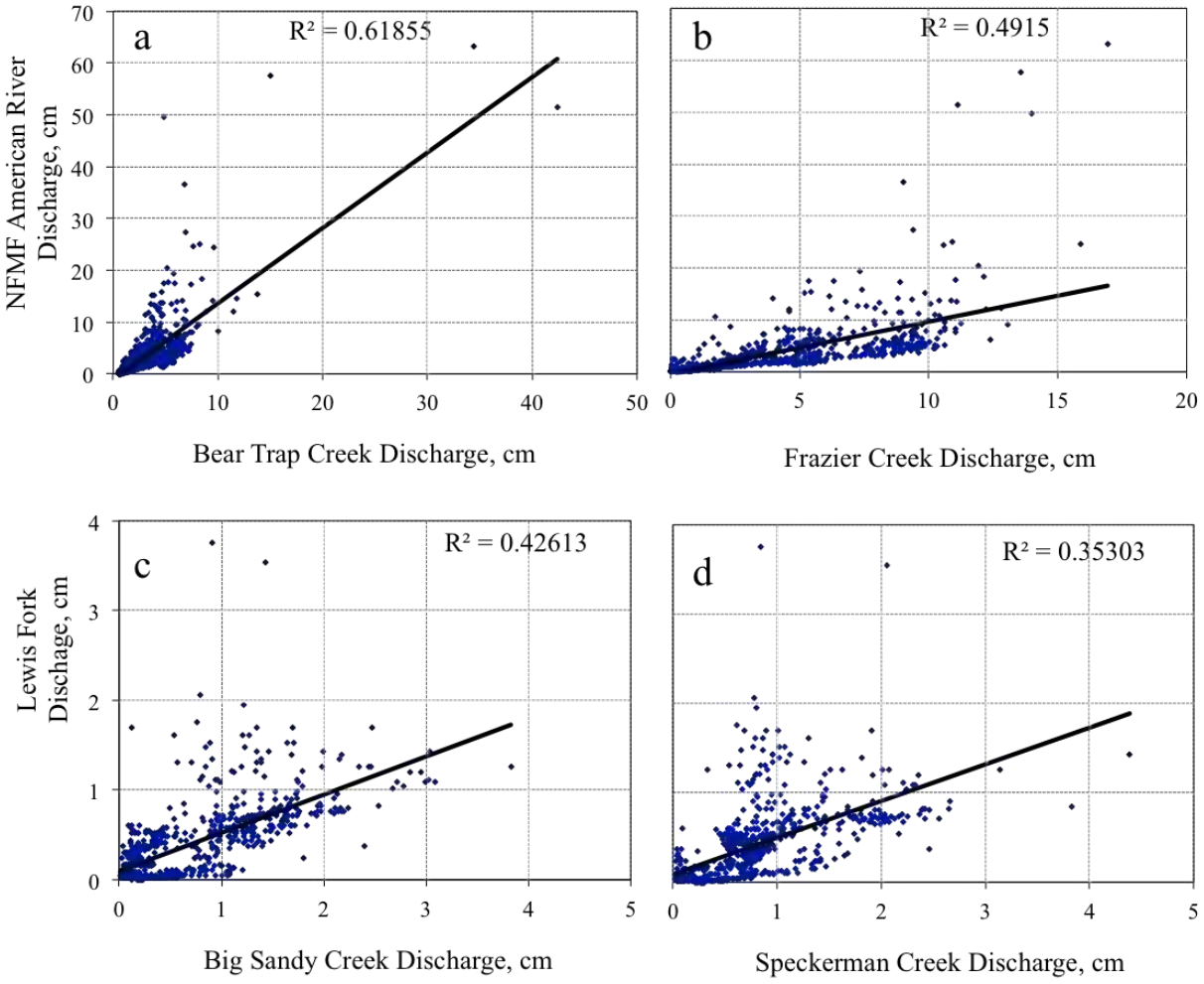

Figure E6: Linear relationships of area-normalized discharge between the headwaters and closest gaged stream sites to the firesheds in Last Chance (a, b) and Sugar Pine (c, d). Discharge is normalized over the watershed area.

Table E5: Results of AIC analysis of regression model between listed variables and discharge of the North Fork of the Middle Fork of the American River.

Variables	**K**	**AIC**	**Akaike Weight**	**r^2**
Bear Trap	3	6973.33	4.4×10^{-16}	0.618
Frazier	3	7393.36	2.7×10^{-107}	0.491
Bear Trap + Frazier	4	6902.602	0.999	0.637

When looking specifically at low flow conditions, a stronger correlation occurs between the basins (Table E6). During low flow conditions, Frazier explains more of the variability in the downstream discharge than Bear Trap, however model selection again shows that the linear regression model using both headwater streams provided the best fit. The combined regression model explains 93.2% of the variability seen in the NFMF area-normalized discharge data, again with the lowest AIC and highest Akaike Weight. This suggests that during low flow and baseflow conditions, the headwaters and full basin have statistically similar behavior.

Table E6: Results of the AIC analysis of the regression model between listed variables and discharge of the North Fork of the Middle Fork of the American River during low flow conditions.

Variables	K	AIC	Akaike Weight	r^2
Bear Trap	3	-914.15	9.1×10^{-100}	0.835
Frazier	3	-1307.62	2.5×10^{-14}	0.919
Bear Trap + Frazier	4	-1370.25	1	0.932

Flow Durations curves for the Sugar Pine sites show a similar relationship to those seen in the Last Chance sites (Figure E4). During high flow conditions, both headwater streams and the Lewis Fork of the Fresno show very different flow probabilities. However, as flow probability decreases below 20%, the slopes of the curves become more similar. The data for the Lewis Fork have a lower resolution and are likely affected by water withdrawals during the upper portions of the flow duration curve (California Environmental Protection Agency, 2014), which combined to reduce the similarity of the Lewis Fork to the headwater streams, although a relationship is still present. Additionally, a comparison of the hydrographs of the headwaters and the Lewis Fork show that peak discharge and subsequent recessions also occurred at approximately the same time at both scales (Figure E5), similar to the Last Chance sites.

A direct comparison of area-normalized discharge between each headwater stream and the Lewis Fork did not show a strong correlation between the headwaters and downstream sites (Figure E6). However, these hydrograph comparisons between the headwater sites and the Lewis Fork of the Fresno River were complicated by a number of factors including (1) numerous active water withdrawals upstream of the gaged site on the Lewis Fork, (2) low resolution of the Lewis

Fork data during low flow conditions (data were recorded in cubic feet per second with no decimal places), and (3) the headwater streams flow into the South Fork of the Merced River and do not have a direct surface hydrology connection with the firesheds, which drain into the Lewis Fork of the Fresno River. These complications have likely resulted in lower correlations between headwater streams and the downstream discharge site. However, the regression analysis between discharge of the headwater streams (predictor variables) and discharge of the Lewis Fork (response) still show a similar pattern to those seen in the Last Chance sites. During the period of available data, the combined discharges of Big Sandy and Speckerman were seen to be the best-fit model for discharge in the Lewis Fork (Table E7) and explained 43.5% of the variability in Lewis Fork Discharge, with the lowest AIC value and highest Akaike Weight.

Table E7: Results of AIC analysis of regression model between listed variables and discharge of the Lewis Fork of the Fresno River.

Variables	K	AIC	Akaike Weight	r^2
Big Sandy	3	404.76	0.002	0.425
Speckerman	3	496.01	3.3×10^{-23}	0.352
Big Sandy + Speckerman	4	392.49	0.997	0.435

During low flow conditions, the combined model is again the best fit. The ability of the headwater discharge values to predict Lewis Fork discharge during low flow increases, and is able to explain 61.0% of the variability of the Lewis Fork of the Fresno River (Table E8). This model is not as good of a fit as in the Last Chance sites due to a combination of the low resolution of the data and the large number of water withdrawals upstream of the site.

Table E8: Results of AIC analysis of regression model between listed variables and discharge of the Lewis Fork of the Fresno River during low flow conditions.

Variables	K	AIC	Akaike Weight	r^2
Big Sandy	3	-955.50	6.3×10^{-15}	0.593
Speckerman	3	-1005.93	5.6×10^{-4}	0.528
Big Sandy + Speckerman	4	-1020.91	0.999	0.610

Development of modeling approach at Providence Creek

RHESSys was initially tested in the Providence Creek catchments at the Kings River Experimental Watershed (KREW) using comparatively rich input datasets from the National Science Foundation's Southern Sierra Critical Zone Observatory (NSF-SSCZO), to prepare for SNAMP study simulations. Providence Creek catchments are in the Sierra National Forest (as is Sugar Pine), have similar elevation range (1758-2094 m) and area (0.49-1.32 km^2) (Figure E7; (Stuemky, 2010)) to SNAMP headwater catchments, but also have a longer period of discharge measurements (2003-2012), providing a better opportunity to evaluate model calibration. RHESSys was calibrated at P303 from 2003-2008 and evaluated for 2009-2012. Model results were also evaluated at P301 and P304 from 2003-2012 using the same soil and vegetation parameters from P303.

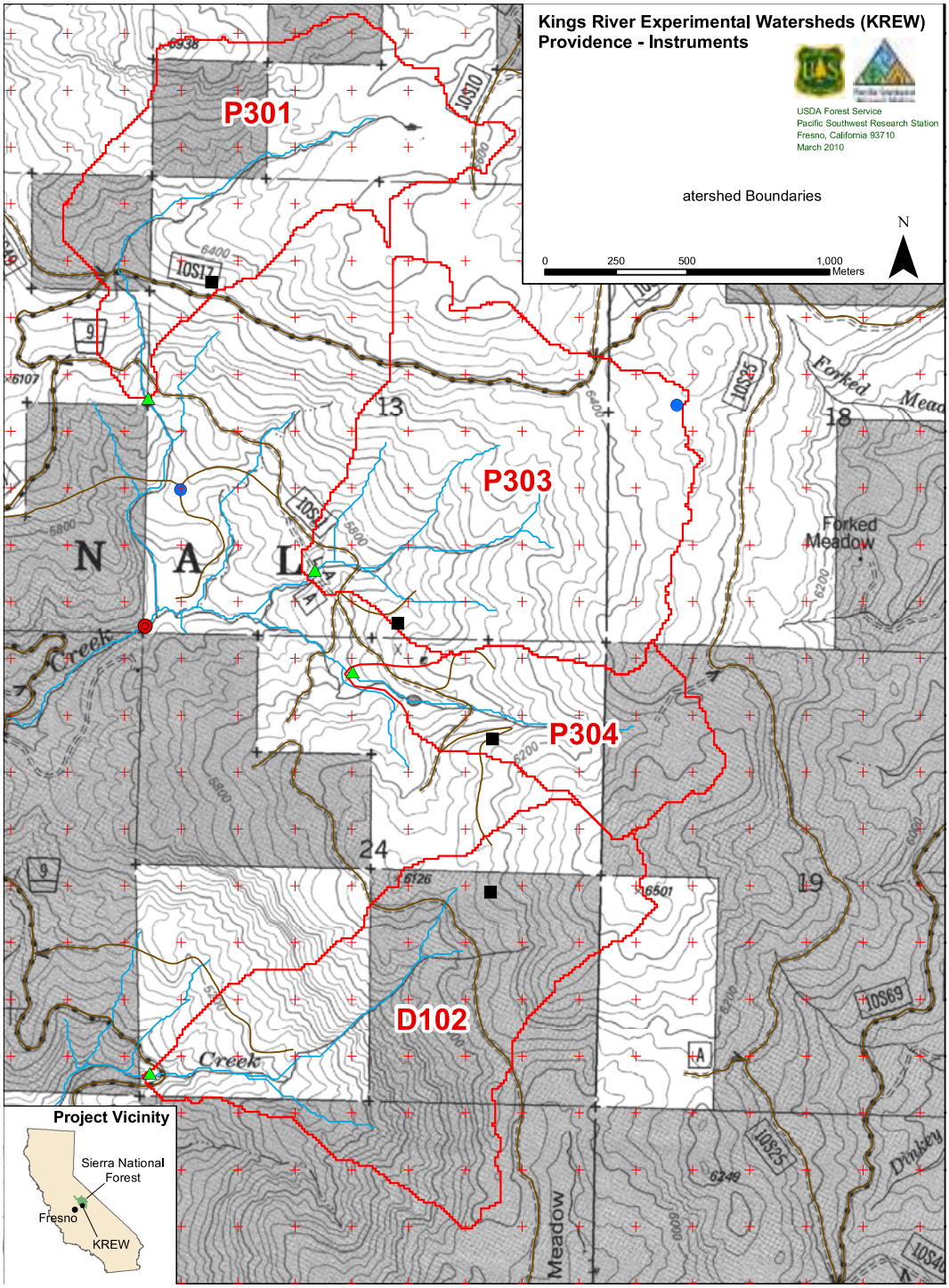

Figure E7: Providence Creek Catchments within the Kings River Experimental Watershed (KREW), Sierra National Forest (Map replicated from Stuemky 2010).

Table E9: Calibration parameters for Providence Creek catchments. The highest combination of Nash-Sutcliffe Efficiency (NS_e) and log-transformed NS_e ($logNS_e$) were used to determine optimal parameters.

Site	SMc	m	k	po	pa	gw1	gw2
P301	0.0004	0.18	4.5	0.3855	0.528	0.05-0.35	0
P303	0.0004	0.18	4.5	0.3855	0.528	0.05-0.35	0
P304	0.0004	0.18	4.5	0.3855	0.528	0.23-0.45	0.00005-0.0001

Note: For dry years (2007,2009) m=0.12, po=0.2455, SMc=0.0001

We used forcing datasets from two meteorological stations (Upper and Lower Providence, USFS Pacific Southwest Research Station) at P303. RHESSys was calibrated at a daily time-step, using one optimal set for wet and dry years at P303 catchment in order to establish the best parameters for the region (Table E9, Figure E8). The timing of water availability in the soil is critical in the partitioning of precipitation into transpiration and runoff. Model parameters were calibrated with 500 normally-distributed random sets, including hydraulic conductivity (k), decay of hydraulic conductivity with depth (m), and deep groundwater flow out of the basin (gw1) and groundwater flow to the stream (gw2). Parameters controlling soil properties of pore size index (po) and air entry pressure (pa) were manually calibrated to match soil storage observations and held constant. Groundwater inflow and outflow parameters (gw1,gw2), which vary with wet and dry soil and climate conditions, were modified annually. Calibration was completed for water years 2003-2008 to capture the range of wet to dry precipitation conditions, and evaluated for water years 2009-2012. Optimal calibration was determined by the highest combination of Nash-Sutcliffe Efficiency (NS_e; Nash and Sutcliffe, 1970) and log NS_e, which supports an improved statistical characterization of the seasonal periods of high and low flows (Table E10). Log NS_e is NS_e calculated on long transforms of the data and preferentially weights low values.

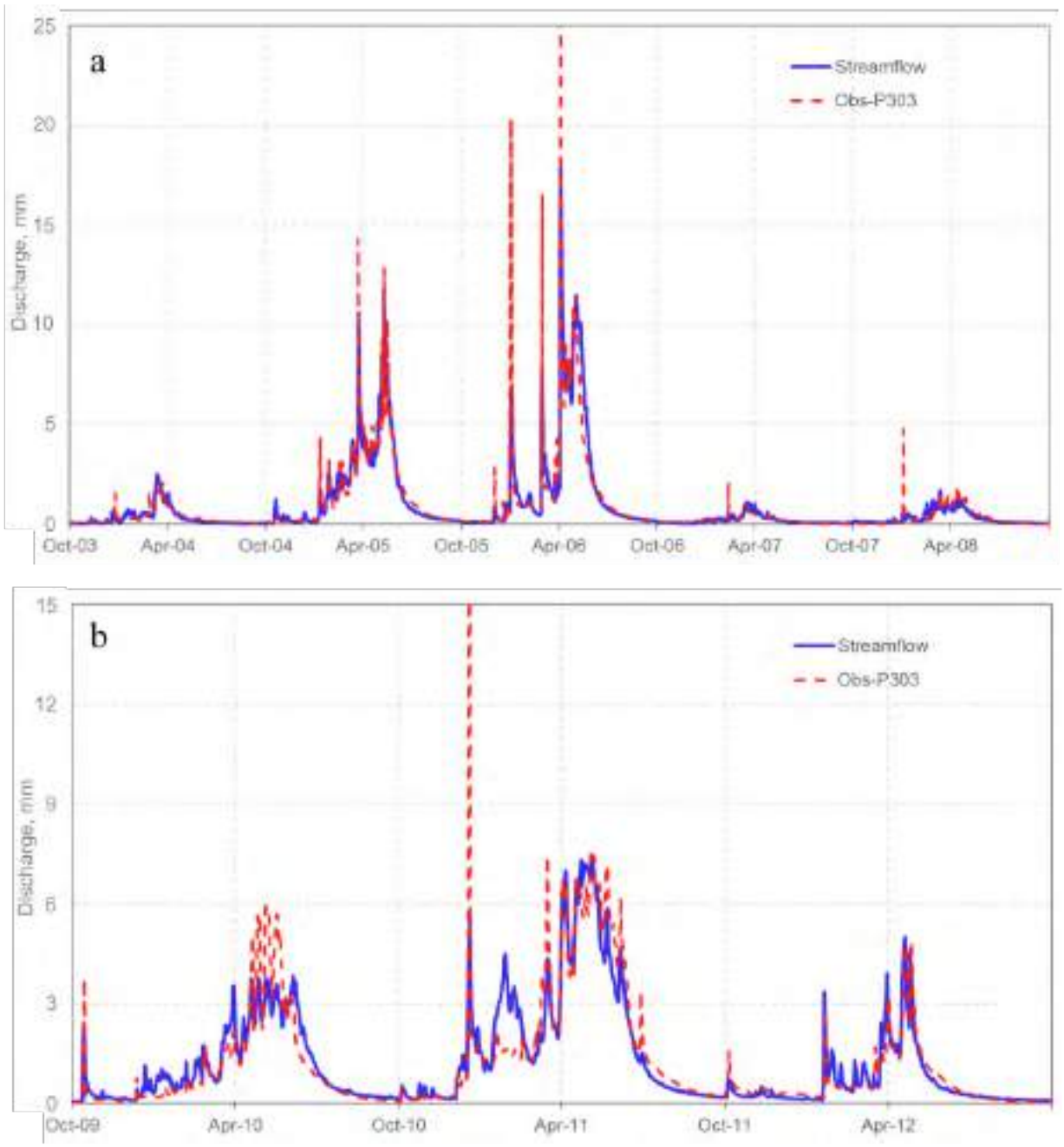

Figure E8: Model stream discharge calibration (a, 2003-2008) and evaluation (b, 2009-2012) for Providence Creek, catchment 303 (P303). Discharge is normalized over the watershed area.

Table E10: Calibration results for Providence catchment 303 (P303). Streamflow statistics of Nash-Sutcliffe Efficiency (NS_e) and log-transformed NS_e ($logNS_e$) were used to determine optimal parameters.

Providence 303	Snow NS_e	Stream NS_e	Stream $logNS_e$
Calibration (2003-2008)	0.92	0.84	0.87
Evaluation (2009-2012)	0.92	0.75	0.85
Overall (2003-2012)	0.92	0.81	0.86

Snow accumulation and melt was also calibrated in RHESSys, where snowmelt is calculated using energy inputs of temperature, radiation, and rainfall to the snowpack. We calibrated snow water equivalent (SWE) on a yearly basis at the specific 10-m patch, which overlapped with the snow pillow station, producing excellent agreement between observed and modeled SWE (NS_e = 0.92, Table E10). We then used the parameters for the temperature snowmelt coefficient (SMc) and radiation melt coefficient (RMc) that were calibrated at the snow pillow station for the entire watershed. Calibrated SWE used SMc = 0.0004 for wet years (2003-2006, 2008) and SMc=0.0001 for dry years (2007, 2009); RMC = 1.0 for all years except the dry 2007 year, where RMc=0.6.

Overall, the analysis shows very good agreement between observed and simulated stream discharge and SWE both for calibration and evaluation period at P303, with snow NS_e, stream NS_e and stream log NS_e > 0.75 (Figures E8, E9; Table E10). SWE observations were not available within P301 and P304. Using same calibrated snow, soil, and vegetation model from P303, the direct transfer of parameters to adjacent basins resulted in very good agreement between observed and simulated discharge (2003-2012) at P301 and P304 (NS_e=0.82; Figure E10).

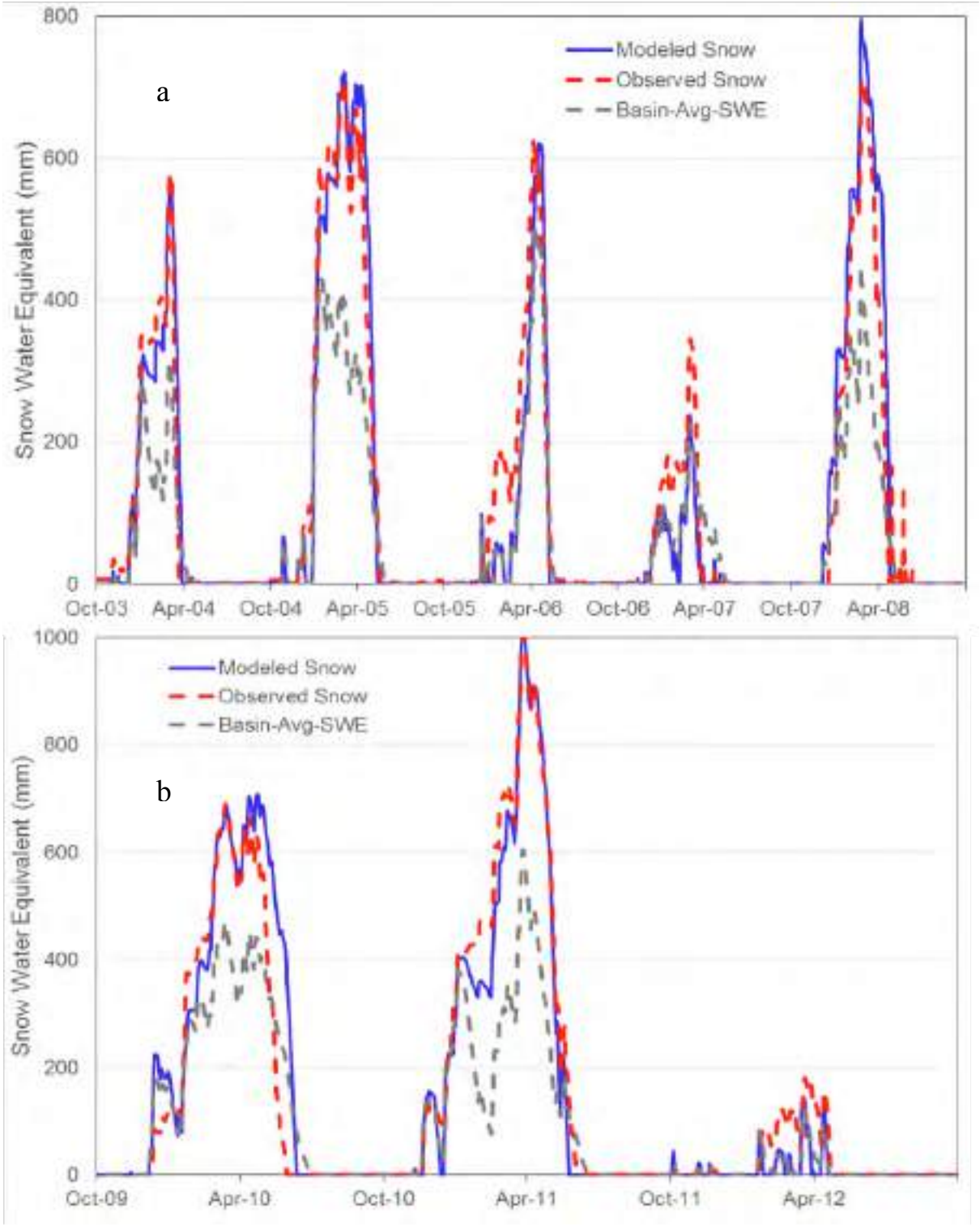

Figure E9: Model snow calibration (a, 2003-2008) and evaluation (b, 2009-2012) for Providence Creek, catchment 303 (P303). Discharge is normalized over the watershed area.

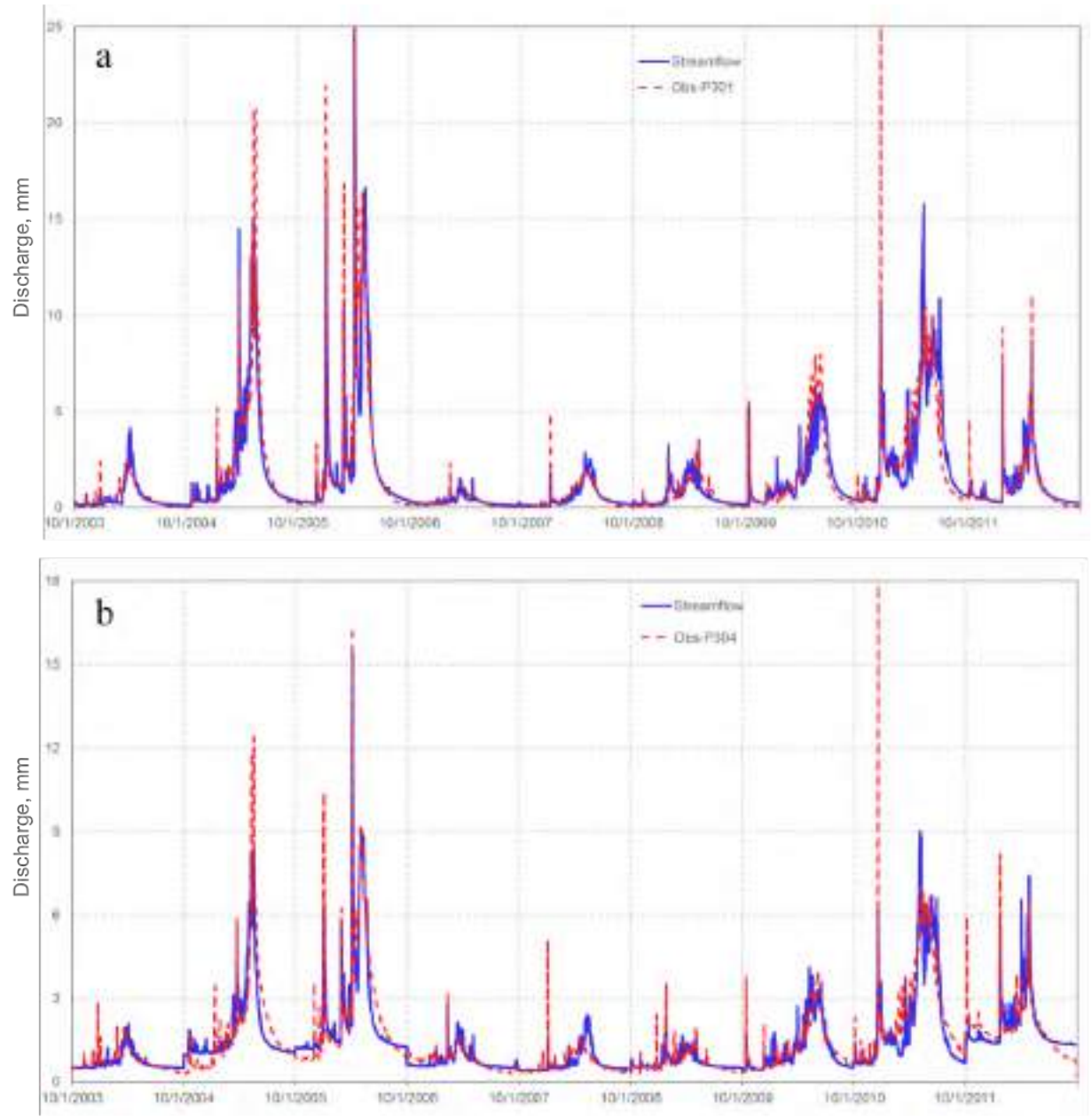

Figure E10: Model stream discharge evaluation for Providence Creek using parameters calibrated at P303 for catchment 301 (a, P301) and catchment 304 (b, P304). Nash Sutcliffe Efficiencies for both catchments were 0.82 (2003-2012). Discharge is normalized over the watershed area.

Results

Precipitation observed over the four water years was highly variable. The first water year measured (2010) showed average precipitation, high levels of precipitation occurred in 2011, and low amounts of precipitation fell during 2012-2013. Annual Precipitation in Last Chance ranged

160 cm (2012) to 275 cm (2011) (Table E11), which the California Department of Water Resources (DWR) 8-station Northern Sierra Precipitation Index shows was 60% to 140% of the long-term mean (1961-2010; California Department of Water Resources, 2014a). Sugar Pine had 83cm (2012) to 202 cm (2011) (Table E11) over the same time period, with the DWR 5-station San Joaquin Precipitation Index recorded as 61% to 160% of the long-term mean (1961-2010; California Department of Water Resources, 2014b). Note the consistently lower precipitation at the southern site.

At the higher elevation stations of Duncan Peak (2112 m) and Fresno Dome (2177 m), the respective snowfall consisted 69% and 52% of the precipitation over the four water years, while at the lower elevation stations of Bear Trap (1490 m) and Big Sandy (1780 m), respective snow fractions were at 41% and 40%. A grid survey of 119 points in the 1 km^2 around Duncan Peak was completed on March 23-26, 2009 to compare the mean and variability of distributed snow depth measurements with the surrounding landscape. The 7 wired snow depth sensors represented 20% of the variability measured with the survey, and a second survey on April 15 and 26, 2012 showed a similar amount of variability was represented by the sensors (24%). Nine additional sensors were installed before the 2012 survey with a new wireless network setup (Kerkez et al., 2012). The wireless network allowed placement of instruments at a distance from the data logger, extending observation locations to better represent the surrounding landscape, and resulted in an increased measurement of variability (61%, Figure E12). In both surveys, wired and wireless snow-depth sensors were close to the mean spatial value of snow depth over the 1-km^2 area surveyed.

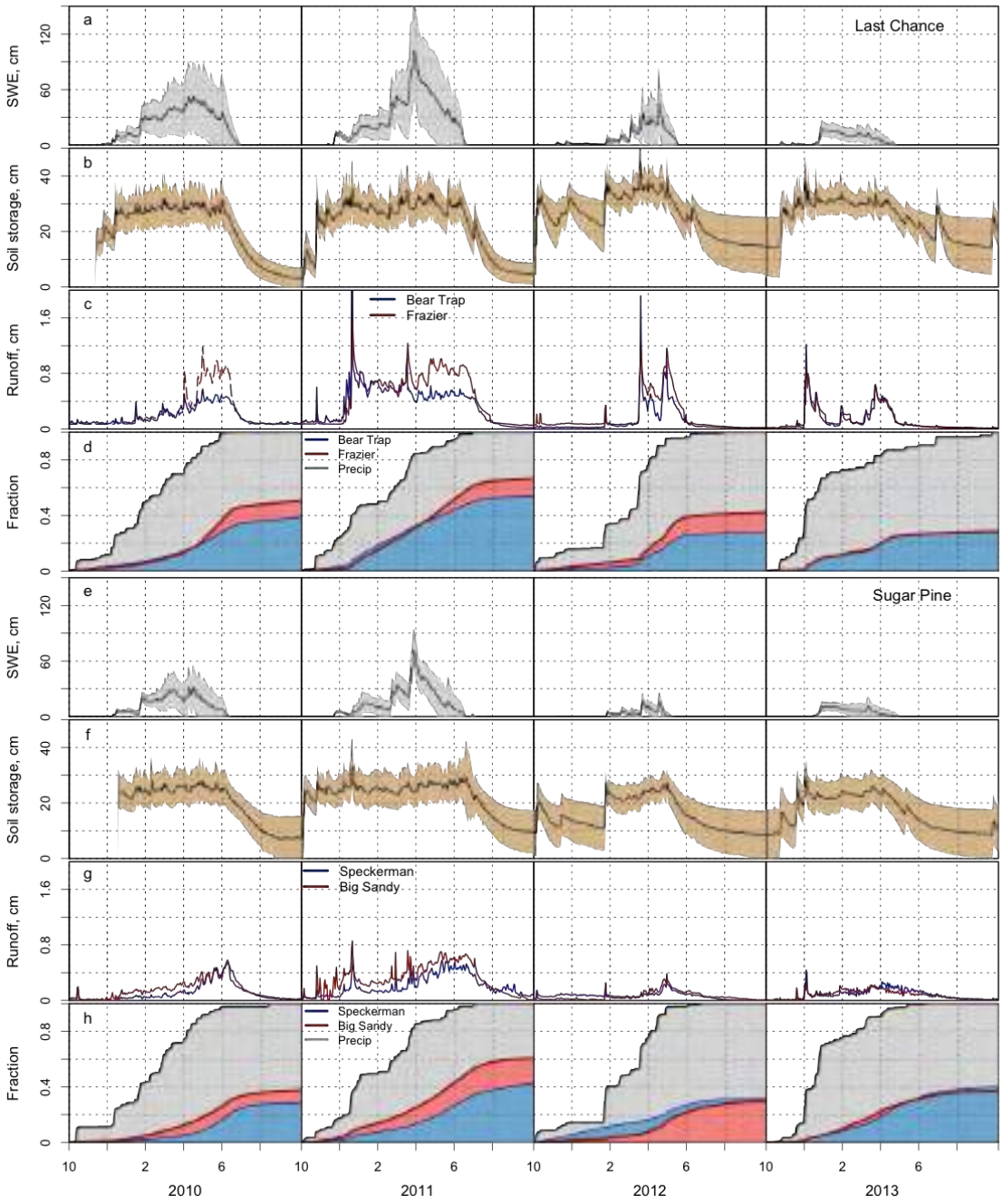

Figure E11: Daily snow water equivalent (SWE) (a, e), soil storage (b, f), and runoff (c, g) observations for the Last Chance and Sugar Pine sites during water years 2010-2013. Black lines show mean of distributed observations; shaded area shows one standard deviation. Cumulative precipitation and runoff are also shown as a fraction of precipitation for each year (e, h).

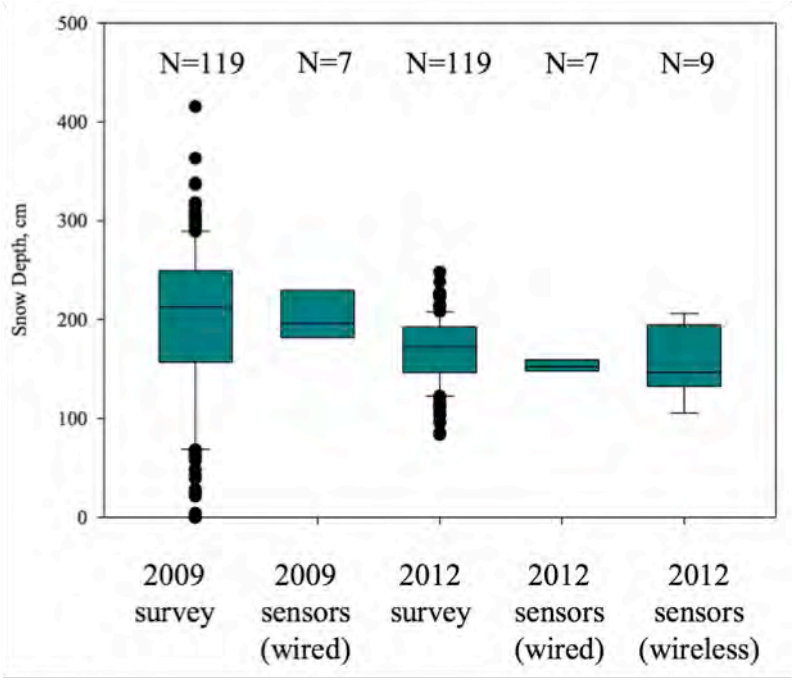

Max, cm	405	257	248	180	206
Mean, cm	212	208	168	155	160
Median, cm	226	196	172	152	146
Min, cm	0	176	83	141	105

Figure E12: Snow depths recorded during surveys around Duncan Peak in 2009 and 2012, with summary statistics in the table below. The wireless sensors (N=9) show an improved ability to capture snow variability over the original wired sensors (N=7). The boxes bound the 25th and 75th percentiles with a line for the median value in the middle. Error bars represent the 10th and 90th percentiles, with outliers shown as points.

Soil-moisture values increased with the first precipitation events of the water year, typically responding within the first few days of an event. Moisture values showed elevated moisture that was generally sustained through the entire wet season. Soils in the top 100 cm stored 20-30 cm of water during the wet winter season in Sugar Pine, while Last Chance soils stored 25-35 cm, the higher value likely reflecting the lower sand content in Last Chance. Soil storage recession started as early as day 200 in the dry years, but as late as day 270 in the wet year.

Table E11: Inter-annual variability of precipitation and runoff observed in the study watersheds.

Site	Catchment	Year	Precipitation, cm	Runoff, cm	Runoff Coefficient*
Last Chance	Bear Trap	2010	191	67	0.35
		2011	275	134	0.49
		2012	160	41	0.26
		2013	169	43	0.25
	Frazier	2010	191	88	0.46
		2011	275	167	0.60
		2012	160	66	0.39
		2013	169	44	0.26
Sugar Pine	Big Sandy	2010	152	52	0.34
		2011	202	112	0.55
		2012	83	23	0.28
		2013	85	29	0.34
	Speckerman	2010	152	39	0.26
		2011	202	77	0.38
		2012	83	36	0.29
		2013	85	31	0.36

*Runoff Coefficient is Water Yield divided by Precipitation

Annual stream discharge rates varied greatly, revealing annual runoff that was 3-4 times in high precipitation years (2011) compared to low precipitation years (2012, 2013). Similarly, the fraction of precipitation leaving the catchment as runoff was lowest in dry years and highest in wet years, ranging from 0.26-0.55 for Sugar Pine and 0.25-0.49 for Last Chance. Higher runoff fractions in Last Chance reflected the elevated precipitation (Table E11, Figure E11). To determine if the forest thinning had an effect on observed discharge, F-tests ($p < 0.05$) were calculated to analyze differences in the regression lines relating daily discharge at the control and treatment watersheds on an annual basis. Discharge was log-transformed to meet the assumption of normally distributed data. The results showed significant differences in the control-treatment stream discharge relationship, not only in the pre- and post-treatments years, but also for all four individual years (Figure E13), masking any post-treatment specific signal in discharge. This difference in behavior may reflect uncharacterized differences in subsurface storage properties. Between 2012 (pre-treatment) and 2013 (post-treatment) precipitation increased. In the Bear Trap catchment runoff increases between those two years, but for the Frazier catchment runoff decreases significantly. There are differences in the underlying geology for these two catchments, with more sedimentary bedrock under Frazier (Saucedo and Wagner, 1992). This

difference in behavior was not observed at the Sugar Pine catchments (Speckerman and Big Sandy).

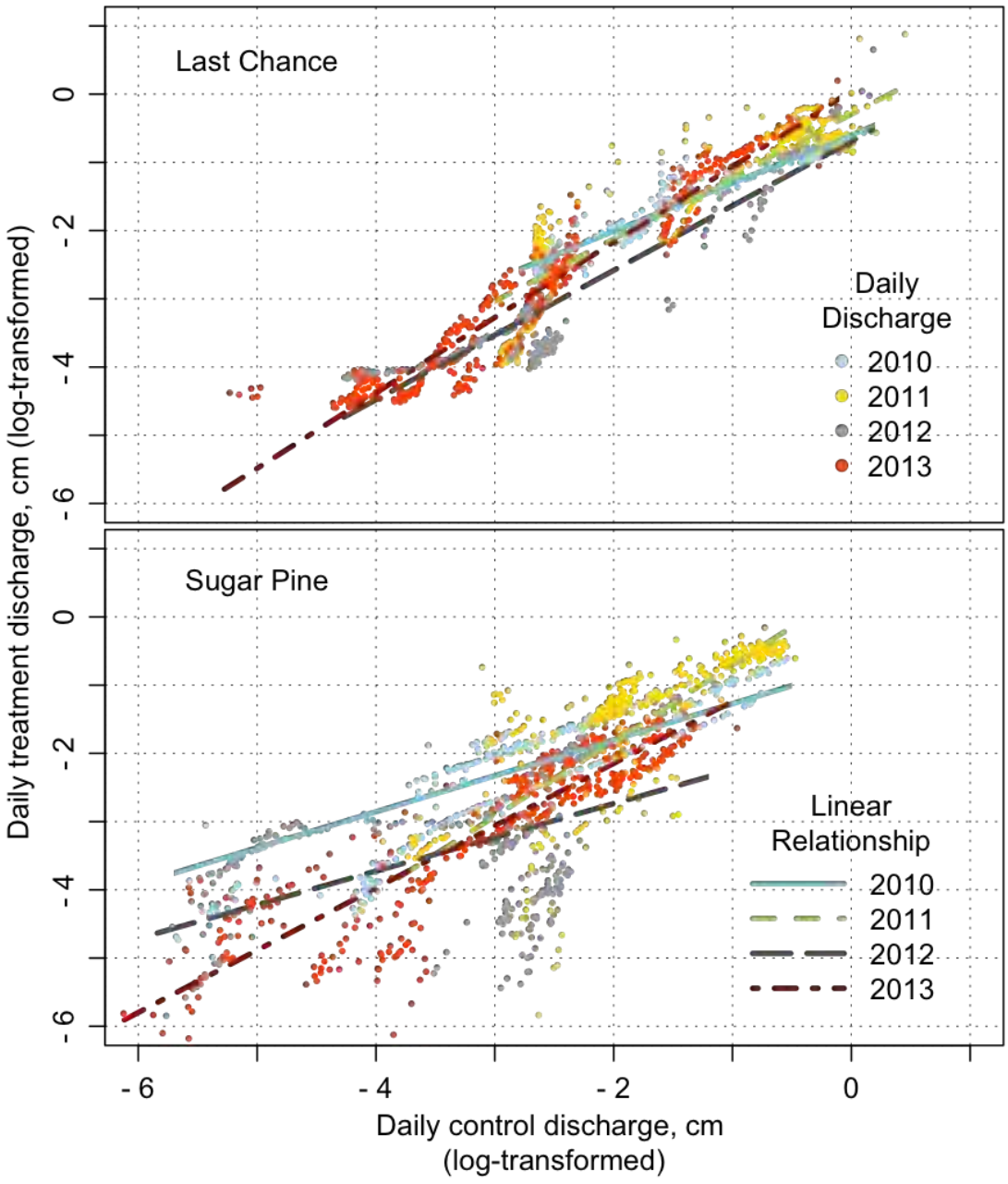

Figure E13: Log-transformed daily stream discharge (area-normalized) relationships in Last Chance and Sugar Pine. The linear relationship between the headwater control and treatment watersheds tested significantly different (F-test, $p<0.05$) every year, including pre-treatment (2010-2012) and post-treatment (2013) water years

Daily snowpack output from RHESSys was calibrated with basin-averaged SWE estimates, with precipitation specifically input as rain or snow, a radiation melt coefficient (RMc) of 0.4, and temperature snowmelt coefficient (SMc) of 0.0005 and 0.001 for Bear Trap and Big Sandy respectively. The timing of water availability in the soil is critical in the partitioning of precipitation into transpiration and stream discharge. RHESSys was calibrated with 5000 normally distributed random parameters sets, of which 6 (Bear Trap, Last Chance site) and 17 (Big Sandy, Sugar Pine site) sets met the criteria described below (Table E12, Figure E14). Parameters controlling soil physical properties of pore size index (po) and air entry pressure (pa), along with parameters controlling flow properties of hydraulic conductivity (k), decay of hydraulic conductivity with depth (m), vertical hydraulic conductivity (svk), and deep groundwater flow (gw1, gw2) were used for calibration. We were unable to calibrate Frazier and Speckerman catchments with the same sets of parameters. Scale up and the effects of treatments are based on the results from Bear Trap (for Last Chance) and Big Sandy (for Sugar Pine).

Table E12: Calibrated parameter ranges for Bear Trap and Big Sandy catchments, used for fireshed simulations. Streamflow statistics of Nash-Sutcliffe Efficiency (NS_e) and log-transformed NS_e ($logNS_e$) were used to determine acceptable parameter sets.

Parameter	Range	Bear Trap	Big Sandy
m	0 - 20	5.6 - 12.3	0.6 - 19.9
k	0 - 300	2.0 - 6.6	4.8 - 293.8
svk	0 - 300	7.0 - 249.9	2.8 - 293.4
po	0 - 3	1.4 - 3.0	0.1 - 3.0
pa	0 - 3	0.6 - 2.6	0.2 - 2.9
gw1	0 - 0.4	0.0 - 0.15	0.2 - 0.4
gw2	0 - 0.4	0.0 - 0.01	0.1 - 0.4
NS_e	-∞ - 1	0.60 - 0.64	0.67 - 0.78
$logNS_e$	-∞ - 1	0.75 - 0.84	0.62 - 0.70

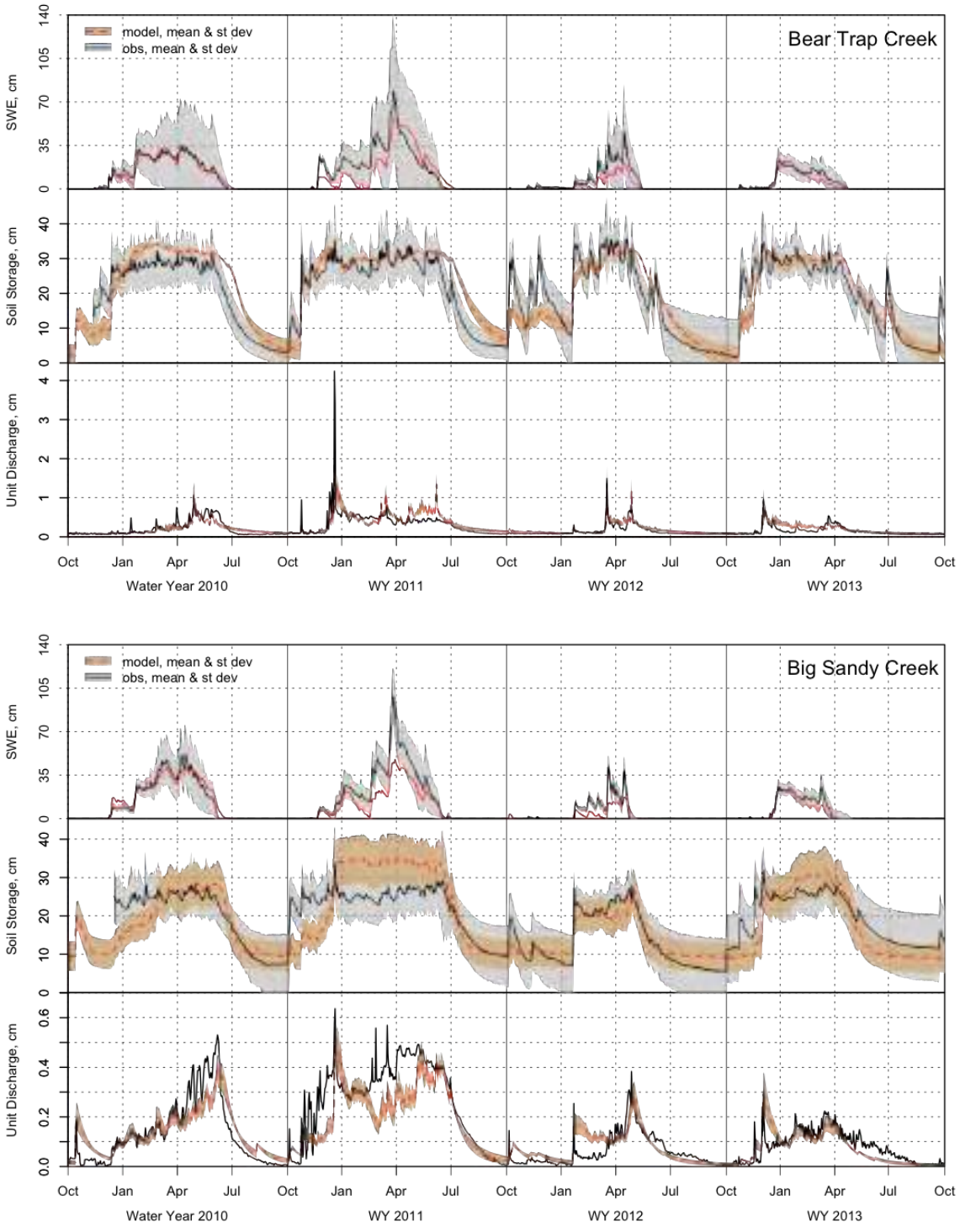

Figure E14: RHESSys daily snow water equivalent, root zone soil storage, and stream discharge calibrations (2010-2013) to mean observation values in Bear Trap (top panel) and Big Sandy (bottom panel) catchments. Discharge is normalized over the watershed area.

Model calibration was completed for water years 2010 - 2012, as all three years exhibited substantially different precipitation levels. Acceptable parameter sets were determined by comparing observed and modeled daily stream discharge using a Nash-Sutcliffe Efficiency (NS_e; Nash and Sutcliffe, 1970) and log NS_e greater than 0.60, and discharge within 20% of annual and 25% of August flows (similar to Garcia et al., 2013). These constraints support acceptable simulations of annual discharge, peak storm flow events, and the seasonal trends typical of a Mediterranean climate. Water year 2013 was post-treatment and could not be strictly considered an evaluation year, having an expected lower range of performance for Bear Trap (NS_e = 0.34 - 0.74, logNS_e = 0.68 - 0.79) and Big Sandy (NS_e = 0.2 7- 0.75, logNS_e = 0.29 - 0.81). Using multiple data sets for model constraint did not provide the highest model fit as we could have achieved by calibrating only discharge, but as Seibert and McDonnell (2002) mention, using multiple data sets produce a better overall model of catchment behavior.

Annual precipitation not accounted for in evapotranspiration or runoff was routed to subsurface groundwater storage. Groundwater flow routing comes from two sources, the calibrated groundwater parameters (gw1, gw2) and groundwater infiltration at the bottom of the soil column. The calibrated parameters control the fraction of water infiltrated to the soil that is routed to groundwater storage (representing macropore flow), and the fraction of groundwater storage released to stream discharge. The second source is groundwater infiltration at the bottom of the modeled soil column, which infiltrates at a rate proportional to soil saturation (higher saturation = faster groundwater infiltration). Longer periods of seasonal soil saturation, which can occur from reduced evapotranspiration, can result in higher groundwater loss. Shorter periods of soil saturation, which can occur from faster snowmelt, result in lower groundwater loss.

Model simulations show that implementation of SPLATs at Last Chance (fireshed scale) resulted in runoff increases of at least 12% for the initial 20 years compared to the no treatment scenario, reducing the effect to a runoff increase of 9.8% by year 30 (Table E13, Figure E15). Following SPLATs, mean LAI decreased 8.0%, including shrub cover (Table E13, Figure E16). Vegetation recovery following SPLATs returned LAI values and runoff to pre-treatment levels in

the first decade. Fire without SPLATs reduced vegetation by 49.8% while fire with SPLATs reduced vegetation by 38.1%, increasing respective runoff fractions by 66.7% and 54.9%.

Table E13: Model results of treatment scenarios for Leaf Area Index (LAI), Groundwater loss (GW), Evapotranspiration loss (ET), and Runoff (Q) in the Last Chance and Sugar Pine study sites, with the 95% confidence interval in parentheses. Precipitation listed for each study site was the mean annual precipitation over the four years of observation, water years 2010-2013.

Study Area	Treatment	Year	LAI	ET, cm	GW, cm	Q, cm
Last Chance (Precip = 199 cm)	No Treatment	0	7.0	122.9 (5.0)	20.9 (1.8)	55.1 (5.0)
		10	8.6	126.0 (5.0)	23.9 (1.8)	49.2 (5.1)
		20	10.0	127.7 (5.1)	26.1 (1.9)	45.2 (5.3)
		30	11.1	127.9 (5.2)	27.3 (1.9)	43.8 (5.4)
	Treatment	0	6.4	117.9 (4.8)	19.1 (1.7)	62.0 (4.7)
		10	7.7	121.7 (4.8)	21.5 (1.8)	55.9 (4.9)
		20	9.0	124.4 (4.9)	23.8 (1.8)	50.8 (4.9)
		30	10.1	125.4 (5.0)	25.3 (1.8)	48.3 (5.1)
	Treatment + Fire	10	4.3	99.7 (3.3)	14.2 (1.7)	85.1 (3.3)
		20	5.1	106.1 (3.7)	15.6 (1.7)	77.3 (3.7)
		30	5.9	111.6 (4.1)	17.0 (1.7)	70.4 (3.8)
	No Treatment + Fire	10	3.5	94.9 (3.3)	12.8 (1.7)	91.3 (3.3)
		20	4.2	101.7 (3.7)	13.9 (1.7)	83.4 (3.6)
		30	4.9	108.7 (4.1)	15.5 (1.7)	75.4 (3.9)
Sugar Pine (Precip = 130 cm)	No Treatment	0	9.0	64.8 (2.5)	24.0 (2.2)	41.2 (1.5)
		10	9.3	64.8 (2.5)	24.3 (2.2)	40.9 (1.5)
		20	10.0	64.8 (2.5)	24.7 (2.2)	40.5 (1.5)
		30	10.5	64.8 (2.5)	24.9 (2.2)	40.3 (1.5)
	Treatment	0	8.4	64.5 (2.4)	23.2 (2.3)	42.3 (1.6)
		10	8.8	64.5 (2.4)	24.1 (2.3)	41.4 (1.6)
		20	9.6	64.5 (2.4)	24.7 (2.3)	40.9 (1.5)
		30	10.2	64.5 (2.4)	25.0 (2.3)	40.5 (1.5)
	Treatment + Fire	10	5.5	64.6 (2.4)	18.8 (2.4)	46.6 (1.6)
		20	6.2	64.6 (2.4)	20.8 (2.4)	44.6 (1.6)
		30	6.9	64.6 (2.4)	22.1 (2.3)	43.3 (1.6)
	No Treatment + Fire	10	5.2	64.8 (2.5)	17.8 (2.5)	47.4 (1.6)
		20	5.9	64.8 (2.5)	19.9 (2.4)	45.3 (1.6)
		30	6.6	64.8 (2.5)	21.4 (2.4)	43.8 (1.6)

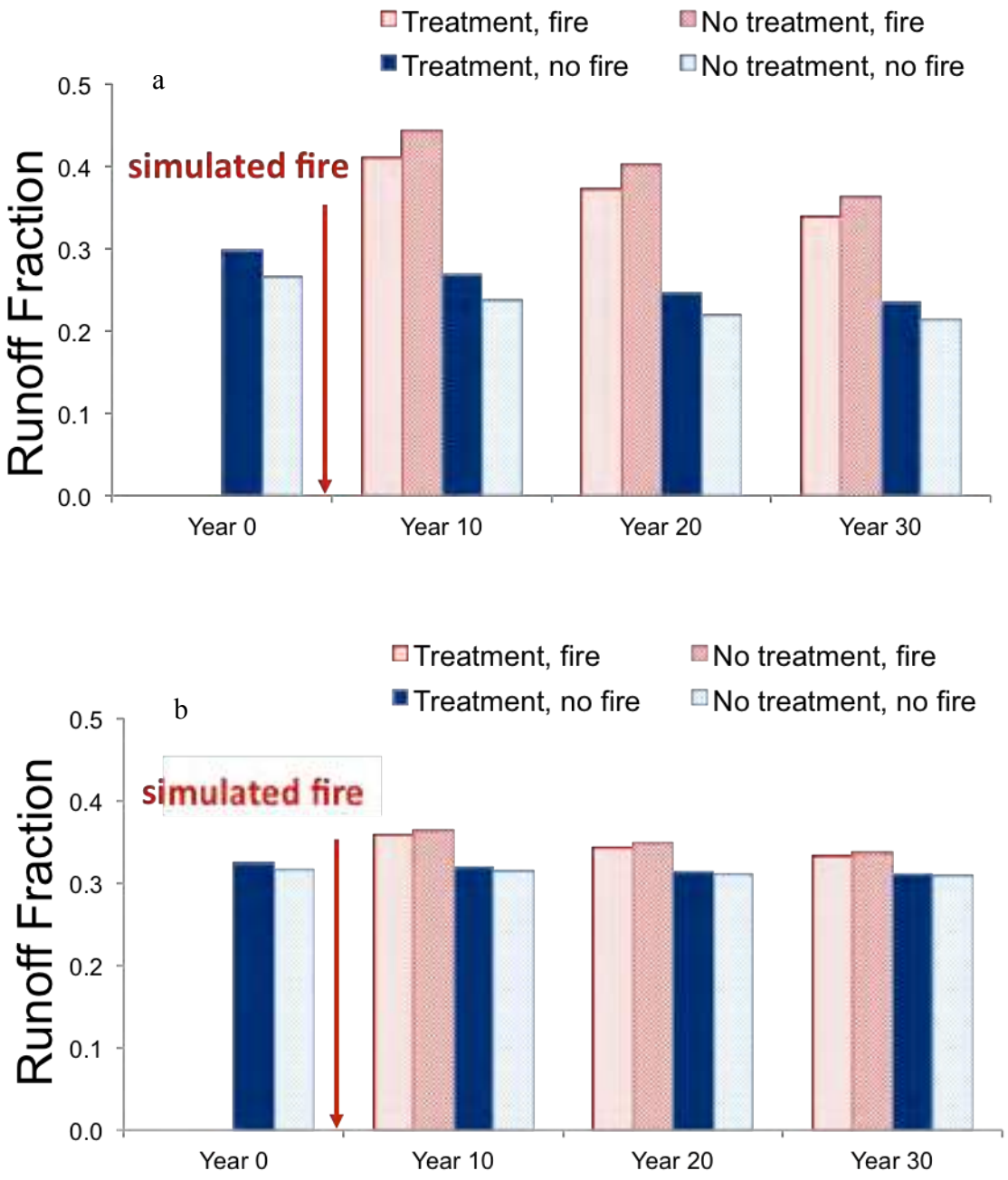

Figure E15: Changes in the runoff fraction of precipitation by treatment and time at Last Chance (a) and Sugar Pine (b). Results based on fire and forest growth simulations. Models were parameterized with plot-level tree lists and scaled to the fireshed using remote sensing. The simulated fire burns immediately after Year 0 is measured. Results for the treated fireshed only.

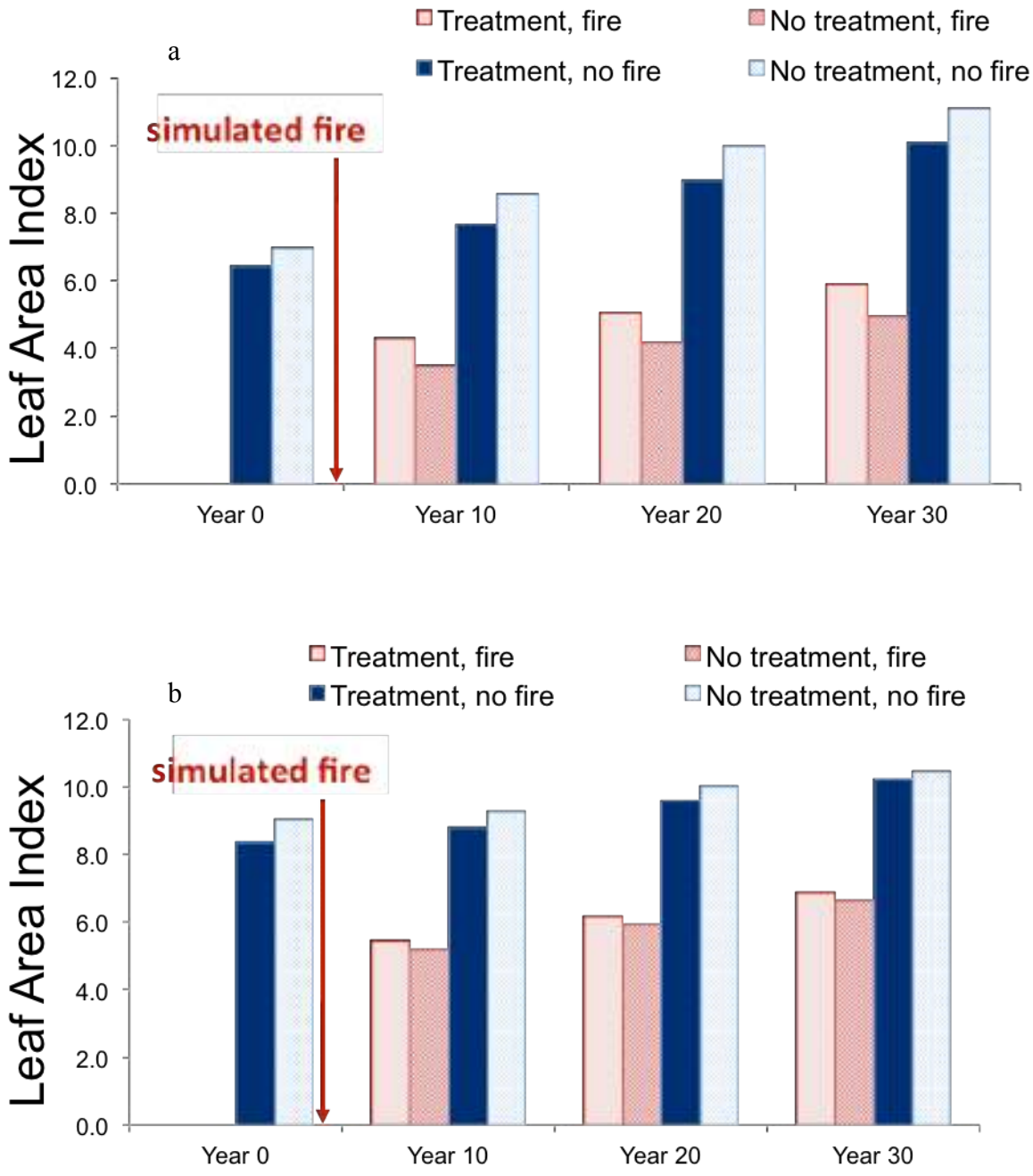

Figure E16: Changes in leaf area index by treatment and time at Last Chance (a) and Sugar Pine (b). Results based on fire and forest growth simulations. Models were parameterized with plot-level tree lists and scaled to the fireshed using remote sensing. The simulated fire burns immediately after Year 0 is measured. Results for the treated fireshed only.

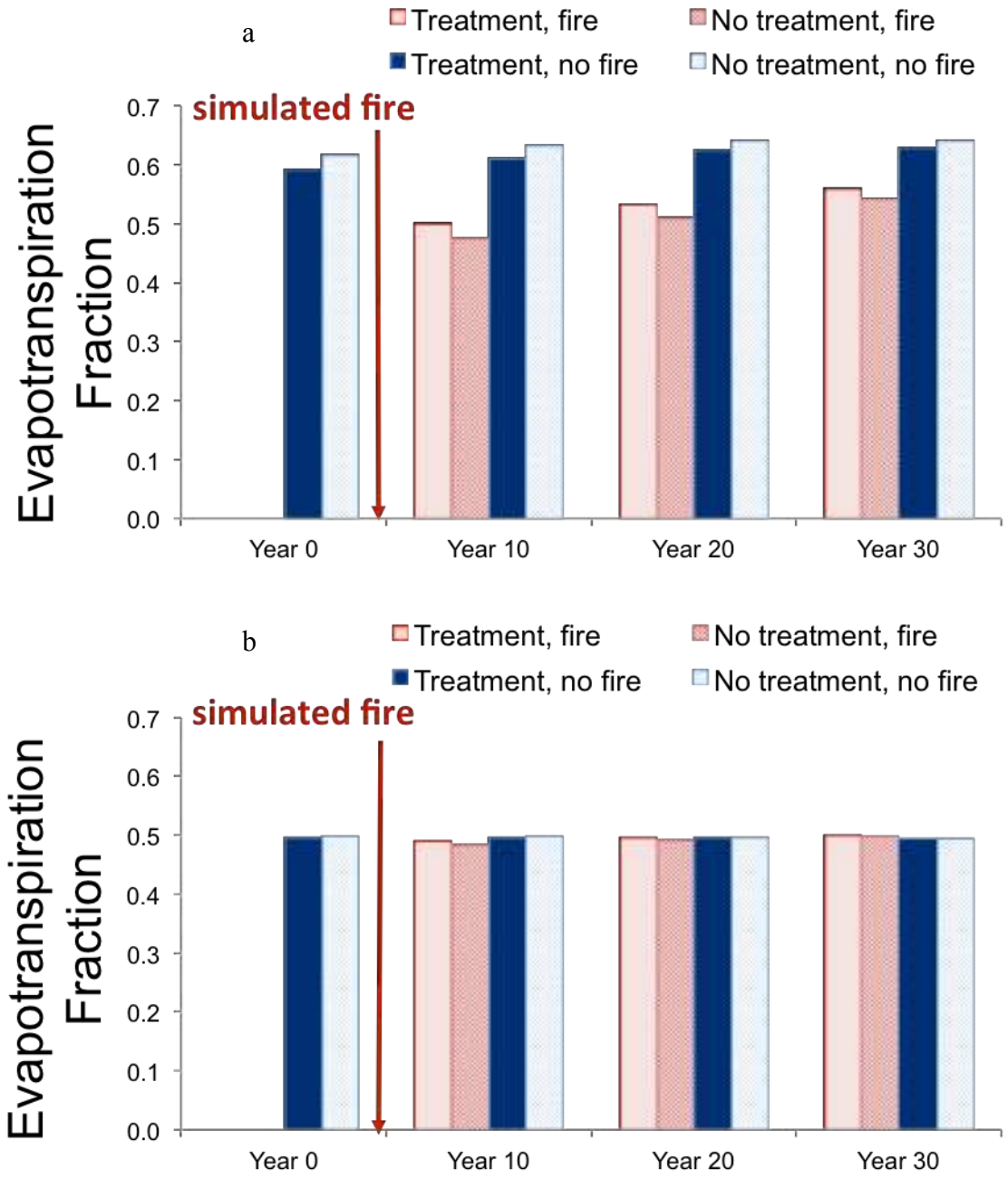

Figure E17: Changes in the evapotranspiration fraction of precipitation by treatment and time at Last Chance (a) and Sugar Pine (b). Results based on fire and forest growth simulations. Models were parameterized with plot-level tree lists and scaled to the fireshed using remote sensing. The simulated fire burns immediately after Year 0 is measured. Results for the treated fireshed only.

Model simulations of SPLAT implementation at Sugar Pine shows runoff increases of less than 3% compared to the no treatment scenario over 30 years (Table E13, Figure E15). SPLATs resulted in a 7.5% decrease in Sugar Pine LAI (Table E13, Figure E16). Vegetation re-growth following SPLATs again showed the reduced LAI only lasted for about 10 years, but runoff response was less impacted by the treatment vegetation than occurred Last Chance. Differences in mean LAI and runoff were less than 3% and 1% respectively after 30 years. Fire without SPLATs reduced vegetation by 42.5% while fire with SPLATs reduced vegetation by 39.5%, increasing respective runoff fractions by 15.2% and 13.1%.

Compared to studies in the Kings River basin (Bales et al., 2011; Goulden et al., 2012; Hunsaker et al., 2012), the closely located Sugar Pine sites had similar evapotranspiration rates (65 cm), but Last Chance showed high annual evapotranspiration (123 cm) resulting from high annual precipitation inputs (199 cm). Although the annual precipitation measured in the Last Chance region was high, the Blue Canyon meteorological station (1609 m elevation) was within the range of measurements reported by nearby stations including Drum Power House (1036 m elev., 159 cm annual precipitation), Hell Hole (1396 m elev., 121 cm precip.), and Huysink (2012 m elev., 216.2 cm precip.). Soil water storage and moisture patterns at both sites were similar to Bales et al. (2011), where the coarser soils of Sugar Pine resulted in lower water content than Last Chance.

This study found higher evapotranspiration in the fireshed model simulations, which have a lower elevation range than the headwaters, and are reflected in consistently lower annual runoff. Observations in the American catchments, however, show the North Fork of the Middle Fork has similar or higher rates of runoff than the Bear Trap headwater catchment for three out of the four water years. The differences in the observations and model results may be due to lower vegetation densities outside the measurement area of this study. Additionally, the increased winter runoff from greater amounts of precipitation falling as rain may reduce water availability later in the year, when forest water demand is higher (Tague and Peng, 2013).We also assessed the sensitivity of the RHESSys water-balance components to changes in individual LAI and canopy cover to determine controlling factors of model vegetation structure on water balance components. Pre-treatment LAI and canopy cover were each increased and decreased by

50%, similar to the highest magnitude of vegetation change, to identify water balance response to the individual changes in vegetation structure for Last Chance (Figure E18). Changes in LAI had lower magnitude effects on the water balance in comparison to changes in canopy cover. Both LAI and canopy cover had smaller impacts on snowpack and soil storage, but canopy cover changes impacted evapotranspiration and runoff extensively. Runoff increases and decreases were greatest during periods of high flow in response to simulated vegetation disturbances.

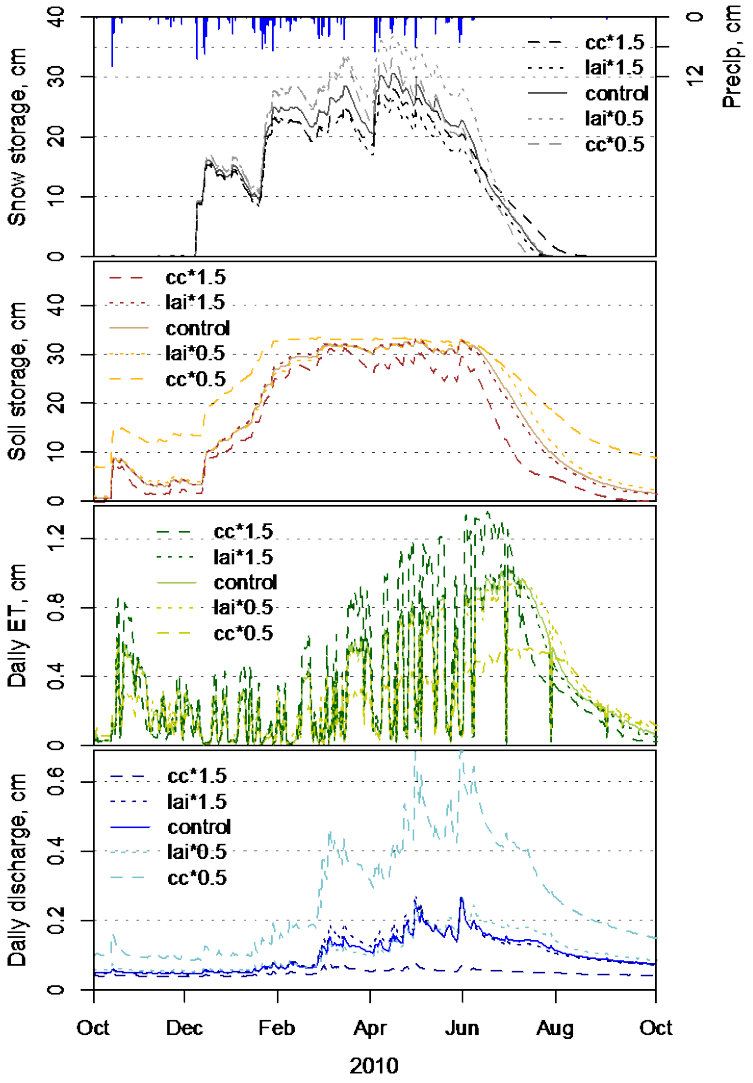

Figure E18: Changes in the water balance components when canopy cover or LAI was increased by 50% (lai*1.5, cc*1.5) or decreased by 50% (lai*0.5, cc*0.5) in Last Chance.

Discussion

Model results of SPLAT implementation, both with and without wildfire, had a greater effect on runoff in Last Chance than in Sugar Pine. The difference in the two study area responses can largely be attributed to the differences in precipitation rates, where Last Chance had approximately 50% higher mean annual precipitation than Sugar Pine. Changes in vegetation at Sugar Pine had minimal effect on annual evapotranspiration rates, suggesting the forest is more water-limited than at Last Chance, where changes in evapotranspiration were more closely linked to forest density. This difference in responses can be illustrated using the range of vegetation changes, where a 7.5% - 42.5% reduction in Sugar Pine vegetation led to a 0.5% - 2.9% decrease in evapotranspiration and a 2.7% – 15.2% increase in runoff (Figure E17). Alternatively, the 8.0% - 49.8% reduction in Last Chance vegetation resulted in a 4.1% - 22.8% decrease in evapotranspiration and a 12.0% - 66.7% increase in runoff (Figure E17). These results on the modeled effects on stream runoff are within the range reported from long-term studies in the continental climate of the Rockies, where a 25% harvest area led to a 52% increase in annual runoff (Burton, 1997) and a 40% harvest led to a 28% runoff increase (Troendle and King, 1985).

Although the treatments within the Last Chance are were light, lower precipitation rates in this lower-precipitation area may limit responses of runoff and ET to vegetation thinning. Running and Coughlan (1988) show that Forest-BGC, changes in LAI will scale directly with vegetative water use in areas that are not water limited (e.g., Last Chance), but variation in the higher range of LAI may not show a response in more water-limited systems.

Robles et al. (2014) calculated a 9-10% increase in runoff following thinning in ponderosa pine forests of central Arizona, with a 50% basal area decrease and 41 cm of winter precipitation. Their result follows the trend of higher runoff increases with higher precipitation in this study, given the 15.2% and 22.8% runoff increase with the 42.5% and 49.8% LAI decrease in the Lewis Fork (130 cm/yr) and the American (199 cm/yr), respectively. Zou et al. (2010) use this precipitation trend to suggest vegetation manipulations in the forested upper basin of the Colorado River have higher potential to increase runoff than lower basin landscapes, using previous forest thinning studies to propose a 6.3-25.0% potential runoff increase given a mean

precipitation of 40 cm. Robles et al. (2014) also estimated that runoff increases would be eliminated 6-7 years after thinning, similar to both sites in this study, where runoff increases from thinning were also absent following 10 years of vegetation regrowth.

High-intensity wildfire impacts on runoff can be greater than thinning, not only from the higher biomass removed, but also from the variability in burn severity, from light understory burns to stand-replacing crown fires. In a central Arizona ponderosa pine and mixed conifer forest, no increases in seasonal or mean annual streamflow were observed after a prescribed burn over 45% of the watershed (Gottfried and DeBano, 1990). Following a stand-replacing fire in central Washington, Helvey (1980) showed flow rates approximately doubled over the entire flow-duration curve.

In addition to vegetation impacts, wildfire can also reduce forest soil infiltration and hydraulic conductivity rates due to the formation of a hydrophobic surface layer (Robichaud, 2000). The few studies that address the persistence in soil water repellence have recorded the effect undetectable within a year (Huffman et al., 2001; Macdonald and Huffman, 2004) to six years after fire (Dyrness, 1976; Henderson and Golding, 1983). Soil recovery rates can depend on vegetation, as Cerdà and Doerr (2005) found soil stabilization under herb and shrub regrowth in as little as two years, but increasing hydrophobicity and runoff under Mediterranean pines over the decade of measurements. Wildfire effects were modeled starting 10 years after the fire event, at which time we assumed the post-fire impacts were no longer a factor, with stabilization of the soil and vegetation. The maximum runoff increase of 23% in response to the simulated post-fire vegetation reduction of nearly 50% in the American was likely mitigated by the increased understory vegetation cover, calculated in response to the reduced overstory.

Management Implications

The structure and density of forested watersheds in the Sierra Nevada impacts snowpack persistence, evapotranspiration loss, and runoff from precipitation. The contribution and fractioning of precipitation into these separate processes depends on annual precipitation and individual catchment physiography. Distributed measurements of snowpack and soil moisture in

the rain-snow transition zone, combined with discharge measurements, were successful in developing a modeling tool that can be used in estimating water balance response to projections of forest management and vegetation disturbance in the southern- and central-Sierra Nevada. The hydrologic model in this study was able contend with the short study period, high precipitation variability, and low post-treatment precipitation, to estimate evapotranspiration and runoff response over a range of vegetation densities.

Modeling tools cannot be developed, however, without the measurements required for constraining model estimates, and verification of projected responses. The highly variable range of snow depth and soil moisture values measured around the meteorological stations and stream discharge sites suggests distributed measurements are needed for representative observations. The snow depth survey around Duncan Peak found that the distributed measurements were successful at capturing a representative mean value, but also that only capturing a few measurements could lead to reporting non-representative high or low snow depth estimates. The inability to produce a calibrated model for two of the four-headwater basins suggests exactly that result. Although we were able to replicate the snow accumulation and ablation patterns we measured in our model simulations, the modeled stream discharge estimates did not match the observed values, suggesting a different snowmelt pattern or groundwater – surface water interactions within the basins than at the four locations we measured.

Calibrated models, constrained with observed data, were transferred to ungauged catchments with similar geology and hydrology. There are a number of uncertainties associated with modeling ungauged basins, but using a similar well-constrained model limits these uncertainties.

Model simulations suggest that treatments as implemented would increase runoff in the high precipitation region of Last Chance, but either treating a broader area or greater vegetation reductions over the same area may be necessary to measurably increase runoff in Sugar Pine. Given the single dry year of post-treatment precipitation, we were unable to verify the projected increases in runoff that the modeling estimated. Verification of responses would require long-term monitoring, to capture the range of precipitation conditions expected in this region of

Mediterranean climate, with periodic sequences of multiple wet or dry years. The stage-discharge relationship method we use is a common low-cost method used in hydrology research, but measurements that are more precise may be necessary to better capture effects of vegetation change for the wide range of interannual precipitation and stream discharge conditions present in the Mediterranean climate of the Sierra Nevada. Model sensitivity results also showed that forest disturbances would affect runoff the greatest during high-flow periods, which would likely exceed the established stage-discharge rating curves. The high-intensity fires modeled in this study can result in greater vegetation reductions and lead to increased runoff, however these results did not address potentially adverse issues related to these wildfires such as soil erosion into the stream channel, hydrophobic soils, and elevated snowmelt rates.

II: Water Quality

Introduction

In California, mountain catchments are not only important as a water source, but often as the dominant sediment source (State of California Sierra Nevada Conservancy). Poor water quality can be harmful to aquatic organisms and have adverse effects on water supply systems, downstream hydropower plants and industries, and water-related recreation. With the concern of overgrown forests and the increasing frequency of catastrophic fires (Miller et al., 2009), it is vital to understand water quality and sediment transport in forested mountain catchments so that we know how factors such as fire, grazing, timber harvesting, road construction, and climate change can impact downstream resources.

In undisturbed small, headwater, mountain catchments, sediment tends to be the primary water quality concern, as these systems typically lack significant sources of chemical pollutants. Sediment and sediment transport play a key role in aquatic-habitat quality, flood-control and water-supply infrastructure, nutrient cycling, contaminant transport, channel morphology, and overall channel stability (Dunne and Leopold, 1978). Information on sediment sources and transport can help policy makers and land/water managers target erosion prone areas or erosion prone time periods with control efforts such as Best Management Practices. Finally, an understanding of how sediment production and transport is affected by seasonal conditions (e.g., snow cover) is key to planning for seasonal precipitation changes associated with climate change.

Sediment yields in streams are controlled not only by discharge but also by erosion and transport. Sediment can come from hillslope or in-channel sources. On hillslopes and floodplains, the relevant sediment processes may consist of rain splash, sheet wash, landsliding, gullying, road erosion, snow creep, tree throw, and soil creep (including bioturbation). In-channel processes that can act on banks include mass failure of banks, freeze thaw cycles, drying and crumbling, and fluvial erosion during high flows (Leopold et al., 1995). In-channel erosion processes that act on the channel bed are generally a form of fluvial erosion (i.e., re-suspension or vertical incision). Previous work in stream systems similar to those in this study has

suggested that under normal conditions the hillslopes have low direct connectivity to the channels (Stafford, 2011). Instead, in-channel erosion of the bed and banks provides the direct link between sediment and stream. In other words, sediment may be mobilized and transported downslope, but is generally redeposited in riparian areas before reaching the stream channel. In-channel process then re-mobilize and transport material downstream, from in- or near-channel storage, during substantial discharge events. This assumption, however, may not hold for forested mountain headwater streams where hillslope processes such as landsliding occur with greater frequency, for time periods containing extreme events, or for land use changes such as road construction, extensive grazing, logging, or wildfire where moderate to severe impacts to the landscape occur.

Despite forested mountain catchments being an important water source world-wide, the majority of sediment transport theory has been developed on lowland systems and with flume work (Traylor and Wohl, 2000). Over the past several decades, most research on the relationships between precipitation, discharge, and sediment transport has been focused on single events (e.g., Sadeghi et al., 2008), or has been in predominately agricultural areas (e.g., Doomen et al., 2008; Rodriguez-Blanco et al., 2010; Gao and Josefson, 2012; Wilson et al., 2012; Soler et al., 2008), in small hillslope plots (e.g., MacDonald et al., 2004; Granger et al., 2011) or in areas with drastically different physiographic and climatic regimes from that of the Sierra Nevada (Gao and Josefson, 2012; Fang et al., 2011; McDonald and Lamoureux, 2009). The wide variety of land use, topography, and climate across existing studies has yielded mixed results. Several longer studies looking at multiple time scales have shown considerable temporal variation in sediment patterns. McDonald and Lamoureux (2009) found significant temporal variation in suspended sediment transport in High Arctic catchments that was linked to snow melt. For a medium sized basin in Central New York, Gao and Josefson (2012) found event and seasonal patterns to be too complex to identify sources or processes but that their system was generally supply limited. Iida et al. (2012) looked at hysteresis patterns associated with snow melt in a temperate mountain catchment in Japan. They found more sediment moved during the snow melt season than the rest of the year and that sediment depletion or a shift to more distant sediment sources occurred as the snow melt season progressed. Fang et al. (2011) found evidence of a hillslope source area in the Loess Plateau of China. Headwater and larger order

basins in southeast Australia were studied by Smith and Dragovich (2009), who suggested that differences in sediment hysteresis patterns were due to different rates of sediment transfer to larger order basins.

Work on the relationship between sediment and discharge in small, forested, mountain catchments with a Mediterranean climate has been limited. Seeger et al. (2004) showed for a basin in the central Spanish Pyrenees that seasonal differences in the sediment - discharge relationship were tied to antecedent conditions within the basin. In their work in the Lake Tahoe region, Langolis et al. (2005) showed that suspended sediment peaked fairly consistently on the rising limb of the hydrograph for the snow melt season, but they did not look at other seasons.

Forest fire impacts that affect water quality include increased hillslope erosion, increased in-channel erosion from greater discharges, increased availability and rapid transport of nutrients to streams, and loss of riparian vegetation impacting water temperatures (Lane et al., 2006; Shakesby and Doerr, 2006; Shakesby, 2011; Smith et al., 2011, Oliver et al., 2011). Lane et al. (2006) linked increased sediment exports for two basins in Australia to increased post-fire discharges. In a review of fire effects on water quality for forested catchments, Smith et al. (2011) reported first year post-fire suspended sediment exports varied from 1 to 1459 times unburned exports. Similarly, they reported wide ranges in total N and total P exports that represented 0.3 to 431 times unburned levels, but found that there was a low risk of N exceeding drinking water guidelines (Smith et al., 2011). Turbidity, N and P were all shown to increase in watersheds burned in the severe Angora wildfire near Lake Tahoe, CA compared to unburned controls (Oliver et al., 2011).

Sediment production and movement in small mountain catchments locally impacts aquatic organisms, plants, and wildlife. It also affects downstream water supply, hydroelectric operations, recreation, and downstream ecosystem services such as fisheries. Increased sediment production and transport following heavy or clear-cut logging has been well studied (Beschta, 1978; Grant and Wolff, 1991; Croke et al., 1999). However, the impacts of current, lighter, forest-management strategies, such as SPLATS, on sediment production and transport in the Sierra Nevada is less understood. The Sierra Nevada Adaptive Management Project helps to fill

some of these knowledge gaps. Our working hypothesis is that the proposed light treatments will not alter the timing or magnitude of flows. Likewise, no changes are expected to be seen in water quality due to no increased discharges. No catastrophic fires affected our field sites while we collected data.

Methods

Water quality instrumentation was installed and data collection began over the 2009-2010 winter and continued to water year 2014. Bi-weekly to bi-monthly manual sampling began around the same time. Instrumentation and manual sampling sites were co-located with the stream node instrumentation in all watersheds except Frazer Creek, where water quality was measured approximately 50-m downstream of the snow and soil moisture nodes. A detailed description of instrumentation and site configurations can be found in (CA Department of Water Resources, 2012; CA Department of Water Resources, 2014).

In Situ Continuous Water Quality

Water temperature, conductivity, dissolved oxygen, and turbidity were collected in all study catchments using multi-parameter, continuously-running sondes. Starting in water year 2012, a second multi-parameter sonde, co-located with the original sondes, was installed in all catchments except Frazier Creek. The additional sondes measured water temperature, conductivity, and turbidity for data redundancy. Anti-fouling wipers on the turbidity and dissolved oxygen optical sensors prevented buildup of sediment or algae that could interfere with measurements. Water-quality attributes and stream stage are reported in 15-minute time intervals. The meteorological attributes of air temperature, precipitation, and snow depth, plotted on the water quality figures for reference to the water-quality data, are reported in daily time intervals. Air temperature was recorded at the study-site meteorological stations. Because the study-site rain gages were unheated and unshielded, these measurements were not used for quantity – just as a confirmation of precipitation events. Precipitation, reported for reference to the water quality data from water year 2012 and on, is from the nearby stations Blue Canyon (for Last Chance) and Westfall (for Sugar Pine). The snow-depth values plotted with the water quality data represent means of all snow-depth measurements at a given site.

Separate manual measurements of temperature, discharge, conductivity, and dissolved oxygen were made on a bi-weekly to bi-monthly basis to check data accuracy. Discharge was measured using a salt-dilution slug method. Temperature, conductivity, and dissolved-oxygen measurements were made with a separately calibrated multi-parameter sonde identical to the continuous running sondes.

Data from all the multi-parameter sondes were manually checked to remove any erroneous spikes due to maintenance of sensors, sampling in the stream, or (for optical measurements of turbidity and dissolved oxygen) periods when the sonde was buried in sediment. To reduce sensor background noise, the turbidity data were filtered to remove any values less than 5 Nephelometric Turbidity Unit (NTU). The remaining values were considered actual turbidity events and were used in analysis. Gaps after the water year 2012 installation were filled using the secondary sonde. When data from the secondary sonde were unavailable, only water temperature and stage could be gap filled using data from the stand alone stage recorders.

Turbidity events were classified according to seasons, with fall defined as first fall rain event to before the beginning of snow accumulation, early/mid-winter as beginning of snow accumulation to peak accumulation, snowmelt as peak accumulation to complete melt out, and baseflow as full melt out to first fall rains. Intensity values of storm events for the turbidity and load cell pressure sensor analysis were found by subtracting peak discharge values from background discharge values defined by a 15-day running average.

The offset of turbidity or suspended sediment peaks from discharge peaks, termed hysteresis effect, can provide insight into sediment movement within watersheds. Fifteen-minute turbidity data were plotted against discharge to analyze hysteresis loop shapes. Hysteresis analysis has long been established as a technique for examining sediment source areas or flow processes in a wide range of watershed sizes and types. The temporal relationship between the turbidity peak and the discharge peak can indicate the proximity of the sediment source and whether or not sediment depletion is occurring. Early papers by Wood (1977) and Williams (1989) identified a hysteresis effect and related each hysteresis type to physical processes in the

streams. Hysteresis loops are classified into five types (Williams, 1989). Clockwise patterns are produced when turbidity peaks occur before discharge peaks indicating a localized sediment source and/or depletion of the source. Counterclockwise patterns occur when turbidity peaks occur after discharge peaks, indicating a more distant sediment source, a discharge threshold that must be reached to entrain consolidated bank sediments, or a rainfall threshold required to initiate overland flow. Linear patterns, where peaks occur simultaneously, imply a sediment source at an intermediate distance, a lower entrainment threshold, or a continuous supply of sediment. Figure-eight and complex patterns typically occur when there are multiple sediment source locations or multiple erosion processes acting concurrently.

Manual Samples

Water chemistry in stream and precipitation water can help to identify sources and flow paths of water in a system. Water chemistry samples were collected at stream sites year round at biweekly to bimonthly intervals. Samples were taken at or near the location of the water-quality instrumentation at each stream site in order to correlate sample results to continuous water quality data. Stream samples were analyzed for major ions and stable water isotopes. Bottles and lids used during sampling were cleaned, triple rinsed with deionized water prior to field work, and then triple rinsed at the site with stream water. All samples were taken in the center of flow and bed sediment disturbance was avoided.

Major Ions

Grab samples of 500 mL of stream water were collected for major cation and anion analysis. Samples were filtered using a vacuum-filtration system with a 0.45-µm filter then split in half for ion-chromatography analysis of major cation and anions as well as titration analysis for acid neutralization capacity (ANC). If samples could not be filtered immediately, they were frozen to preserve the samples until they could be processed. Cations measured included Na^{+}, NH_4^{+}, K^{+}, Mg^{+2}, and Ca^{+2}. Anions measured included F^{-}, Cl^{-}, SO_4^{-2}, and NO_3^{-}.

Stable Water Isotopes

Isotope samples were collected in 30-mL glass vials with septum lids. Bottles were capped such that no air was present in the bottle. Samples were stored refrigerated until they

could be analyzed to prevent algae growth. Isotope samples were processed using integrated-cavity laser spectroscopy to determine the δ D and δ ^{18}O of samples.

In situ Continuous Channel Bed Scour and Deposition

Load cell pressure sensors were installed to monitor sediment movement through the stream system. Two Rickly Hydrological load cell pressure sensors were buried 30 to 50-cm below the stream bed at each stream reach. The sensors operate by measuring the pressure of the water column and the pressure exerted on a water-filled pan buried in the sediment at the same depth. The difference between the two readings is the weight of the sediment on top of the pan. Sensors were co-located at Bear Trap, Frazier, and Speckerman Creeks to provide redundant measurements. At Big Sandy Creek, one sensor was installed adjacent to the water quality instrumentation and the other was installed approximately 15-m downstream. Cross-sections at the scour-pan locations were completed several times throughout the study, typically during late-summer/early-fall low flows.

The load cell pressure sensors are designed so that the pan transducer "sees" the pressure from the sediment above it, the water column, and the atmosphere. The side transducer "sees" only the water column and atmospheric pressure. When the side sensor values are subtracted from the pan sensor values, the difference should be the signal due to sediment only. This behavior held in lab tests, but when buried in the streambed, the two transducers unexpectedly tracked each other. We suspect that sediment became packed in the side sensor orifice when buried (despite attempts at screening the opening) and the transducer was effectively "seeing" some of the bed sediment.

To deal with the lack of reliable side sensor data, manual corrections were made on the pan transducer data using independent, co-located stage and barometric pressure measurements. These data were used to calculate the sediment signal in the continuously recorded data according to the following:

$$S_{sed} = S_{total} - S_{stage} - S_{baro} - c \qquad [1]$$

where S_{sed}, S_{total}, S_{stage}, and S_{baro} are the sensor signal due to sediment, total pressure, stage, and barometric pressure respectively. The pan constant, c, is found using known barometric pressure and stage values at the time of calibration when $S_{sed} = 0$. The sediment signal (in mV) was then converted to kg of bed sediment using calibration data and an assumed sediment bulk density of 2.0 g/cm^3. This value was chosen as an intermediary between water 1.0 g/cm^3 and granite 2.65 g/cm^3. It was found that the factory and lab calibrations for each pan did not translate well to the field data. Instead, *in situ* field calibrations, performed at the end of data measurement, were used to determine the relationship between mV of signal and kg of material on each pan.

Manually corrected data from the load cell pressure sensors were compared to calculated values from manual field measurements with a cone of influence based on assumed 30 degree and 45 degree angles of repose using methods from Hamblin (2003). While the angle of repose will vary based on the size distribution of the bed material, the 30-45 degree values are thought to cover the range of variation (Glover, 1995)

Results

In Situ Continuous Water Quality

The water-quality parameters of water temperature, conductivity, dissolved oxygen, and turbidity were collected in all study catchments using multi-parameter, continuously-running sondes (Figures E19-E26).

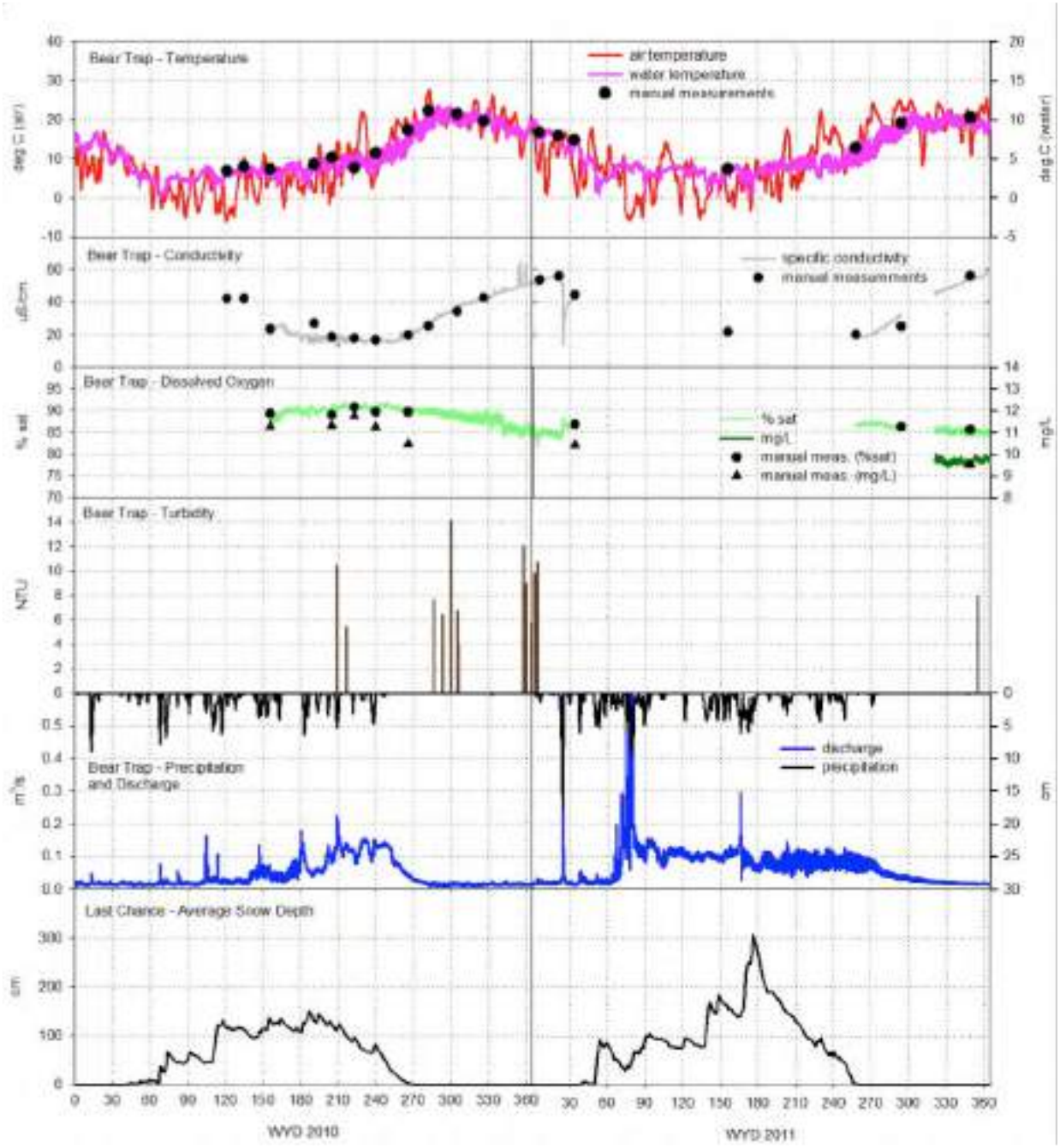

Figure E19: Bear Trap Creek water-quality data for water years 2010 and 2011. Water years run from Oct 1 to Sept 30. Water temperature, conductivity, dissolved oxygen, turbidity, and discharge are plotted as 15-minute time-interval data from Bear Trap Creek. Air temperature and precipitation were collected at Bear Trap Met and plotted on an hourly time interval. Snow depth data are plotted using daily averages and spatial averages of all sensors across the Last Chance site.

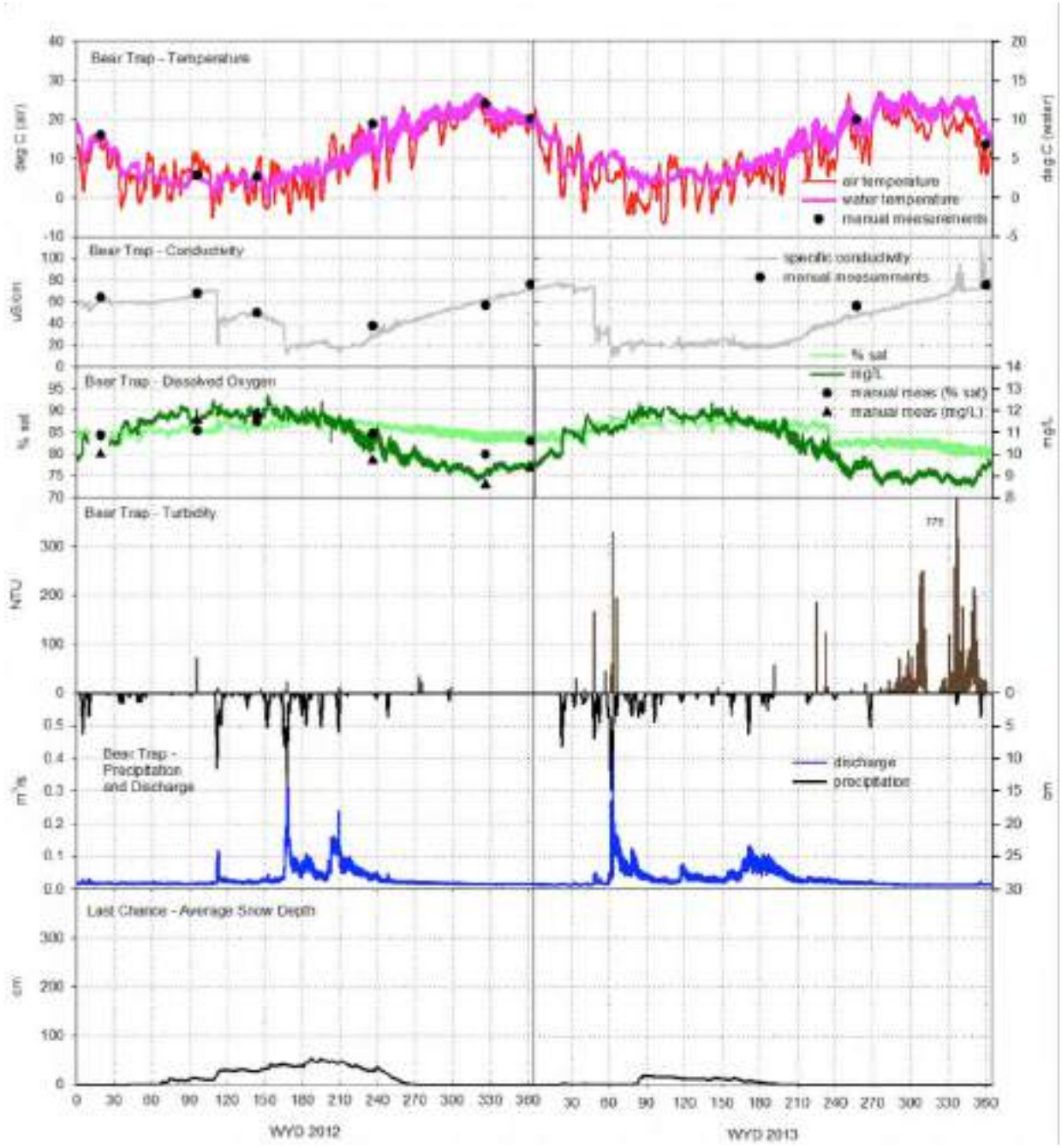

Figure E20: Bear Trap Creek water-quality data for water years 2012 and 2013. Water years run from Oct 1 to Sept 30. Water temperature, conductivity, dissolved oxygen, turbidity, and discharge are plotted as 15-minute time-interval data from Bear Trap Creek. Air temperature was collected at Bear Trap Met and plotted on a daily time interval. Precipitation data are from the Blue Canyon meteorological station operated by the US Bureau of Reclamation. Snow depth data are plotted using daily averages and spatial averages of all sensors across the Last Chance site.

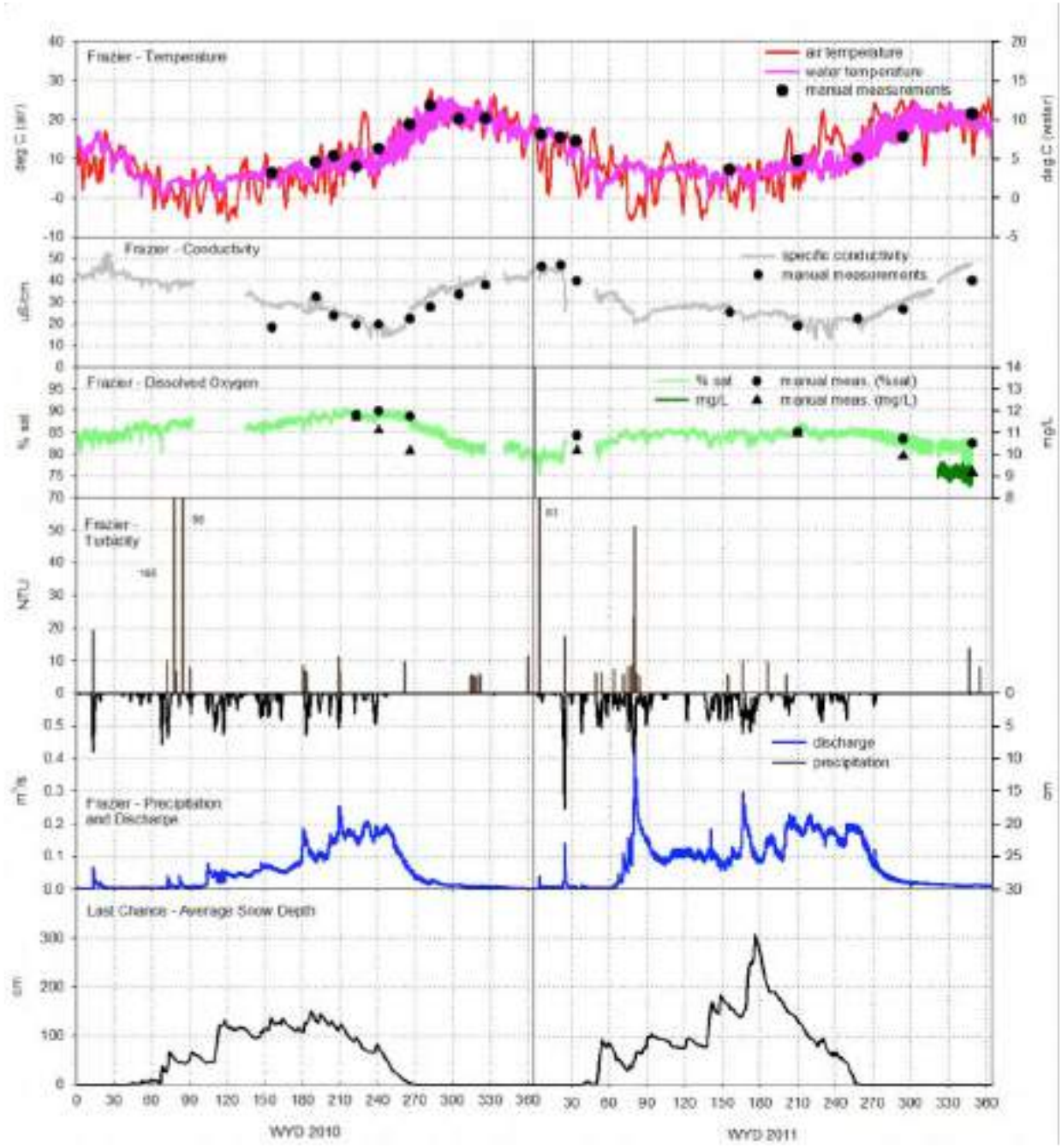

Figure E21: Frazier Creek water-quality data for water years 2010 and 2011. Water years run from Oct 1 to Sept 30. Water temperature, conductivity, dissolved oxygen, turbidity, and discharge are plotted as 15-minute time-interval data from Frazier Creek. Air temperature and precipitation were collected at Bear Trap Met and plotted on an hourly time interval. Snow depth data are plotted using daily averages and spatial averages of all sensors across the Last Chance site.

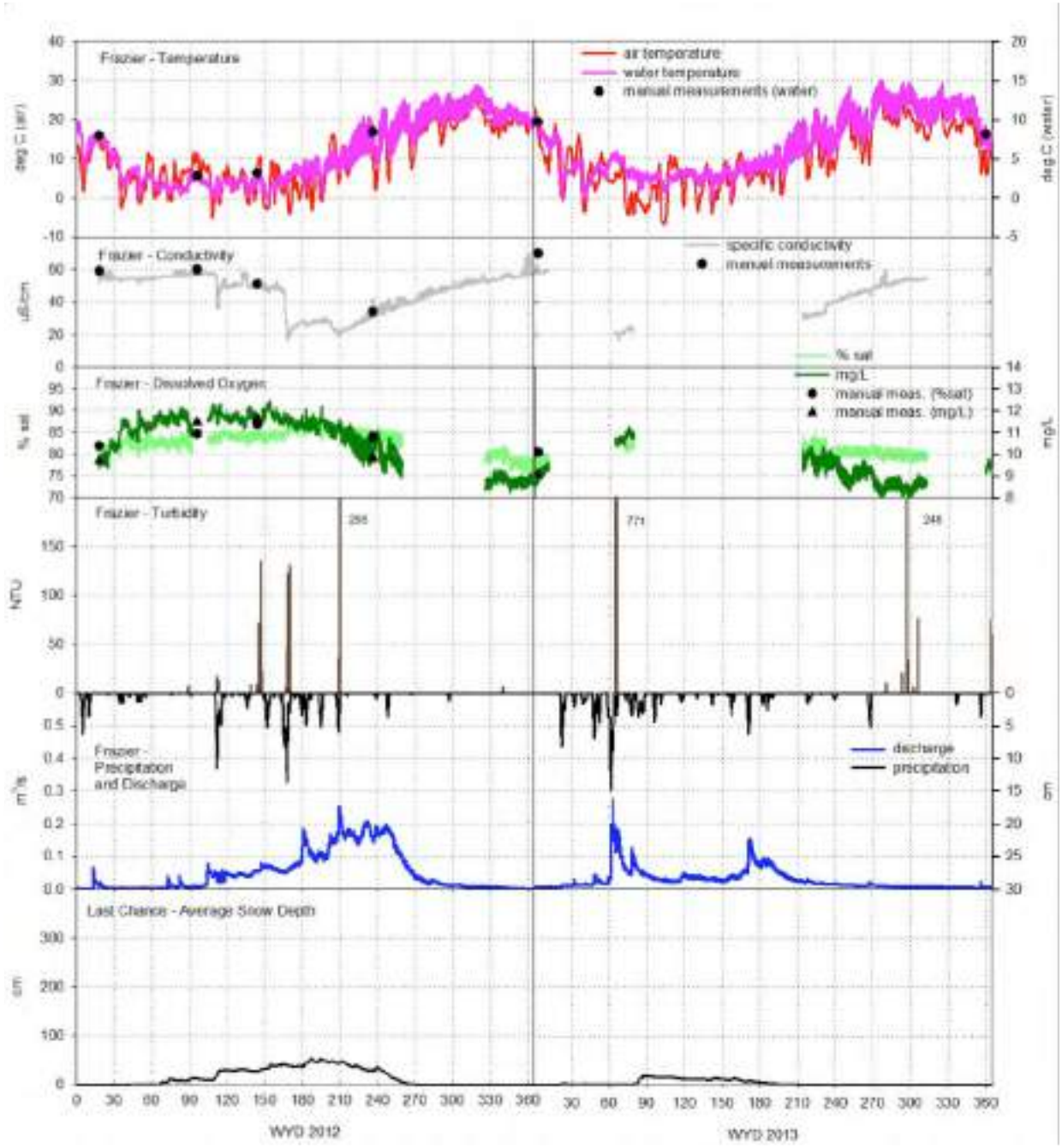

Figure E22: Frazier Creek water-quality data for water years 2012 and 2013. Water years run from Oct 1 to Sept 30. Water temperature, conductivity, dissolved oxygen, turbidity, and discharge are plotted as 15-minute time-interval data from Frazier Creek. Air temperature was collected at Bear Trap Met and plotted on a daily time interval. Precipitation data are from the Blue Canyon meteorological station operated by the US Bureau of Reclamation. Snow depth data are plotted using daily averages and spatial averages of all sensors across the Last Chance site.

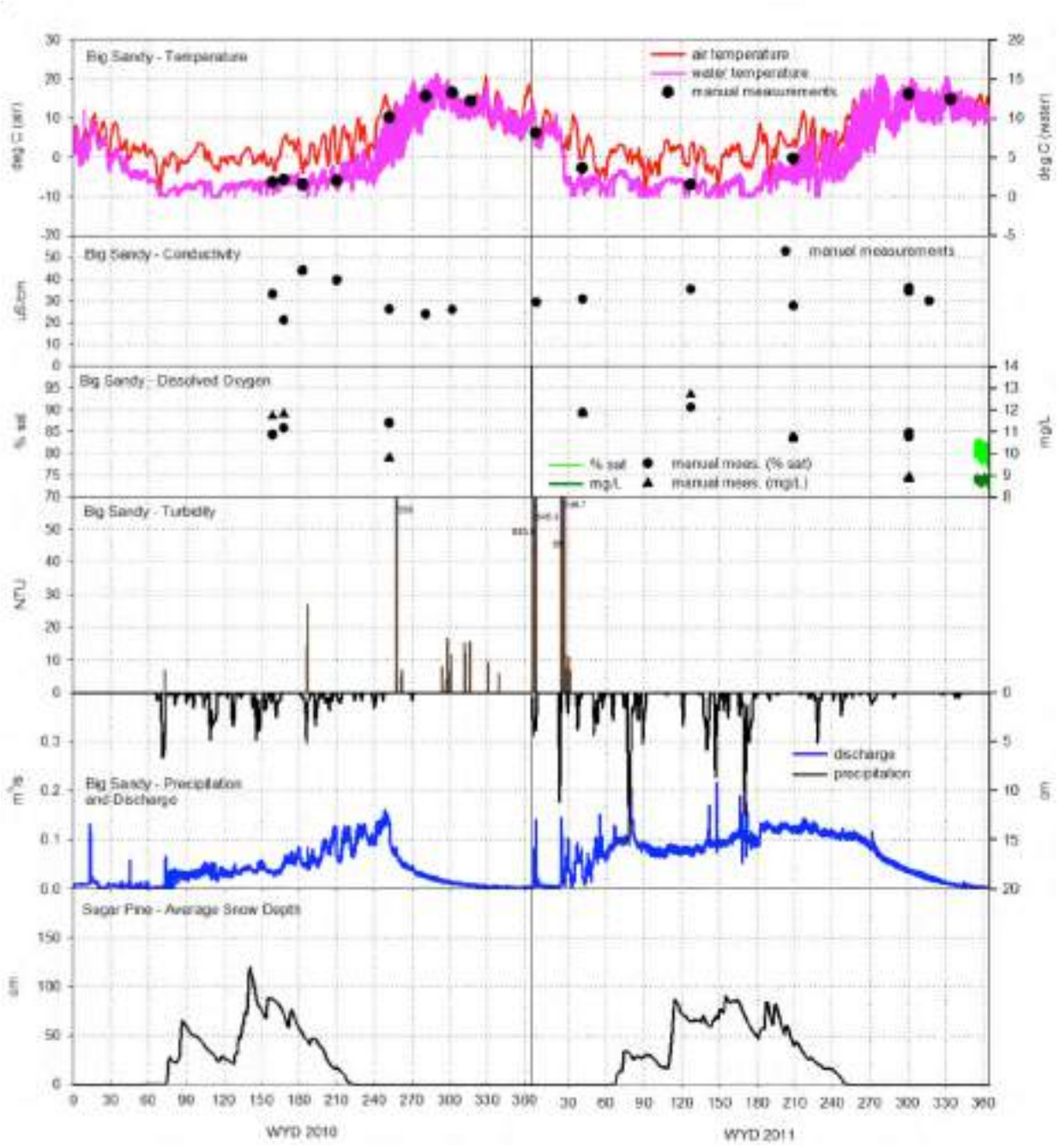

Figure E23: Big Sandy Creek water-quality data for water years 2010 and 2011. Water years run from Oct 1 to Sept 30. Water temperature, conductivity, dissolved oxygen, turbidity, and discharge are plotted as 15-minute time-interval data from Big Sandy Creek. Air temperature and precipitation were collected at Big Sandy Met and plotted on an hourly time interval. Snow depth data are plotted using daily averages and spatial averages of all sensors across the Sugar Pine site.

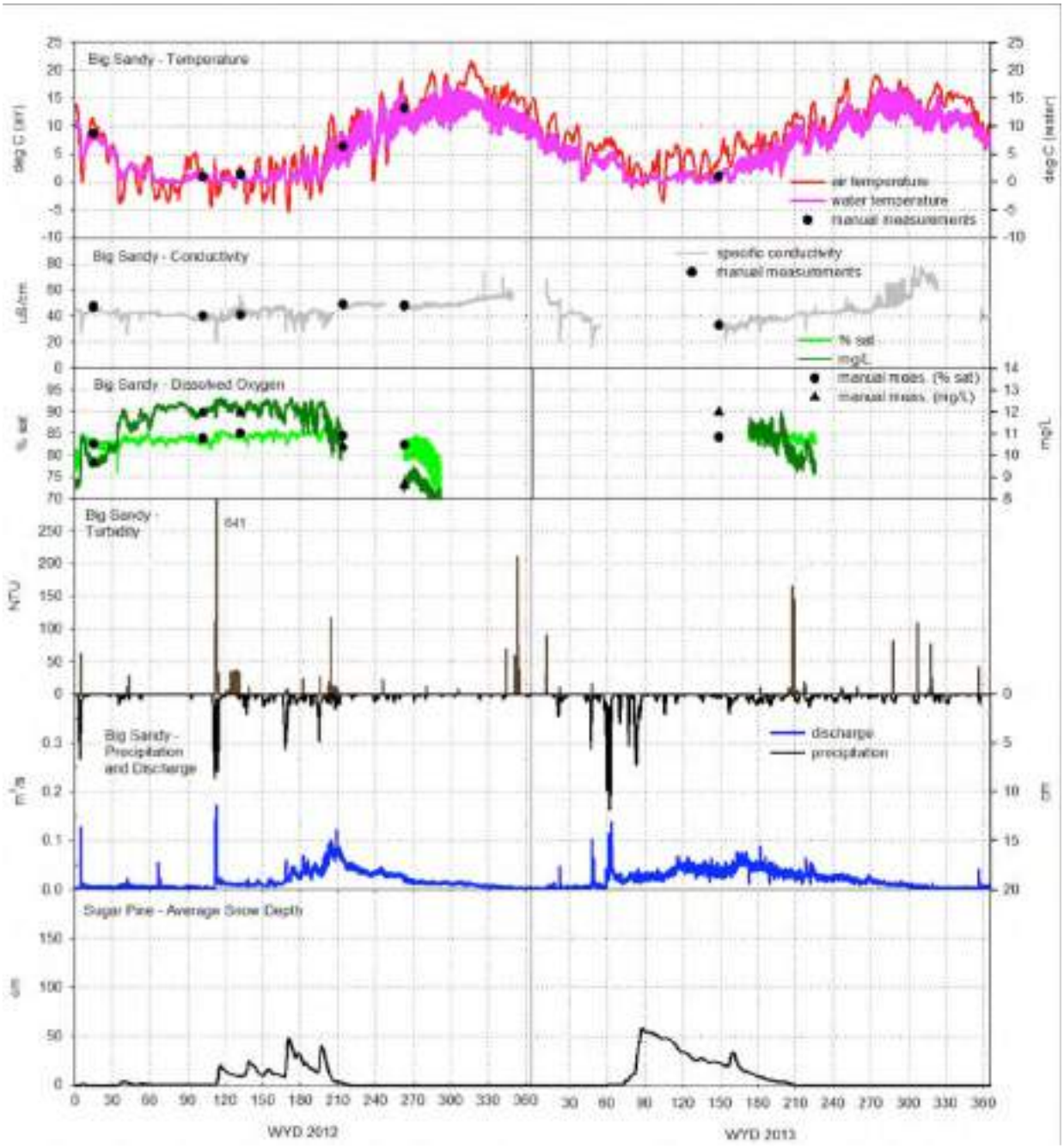

Figure E24: Big Sandy Creek water-quality data for water years 2012 and 2013. Water years run from Oct 1 to Sept 30. Water temperature, conductivity, dissolved oxygen, turbidity, and discharge are plotted as 15-minute time-interval data from Big Sandy Creek. Air temperature was collected at Big Sandy Met and plotted on a daily time interval. Precipitation data are from the Westfall meteorological station operated by the US Army Corps of Engineers. Snow depth data are plotted using daily averages and spatial averages of all sensors across the Sugar Pine site.

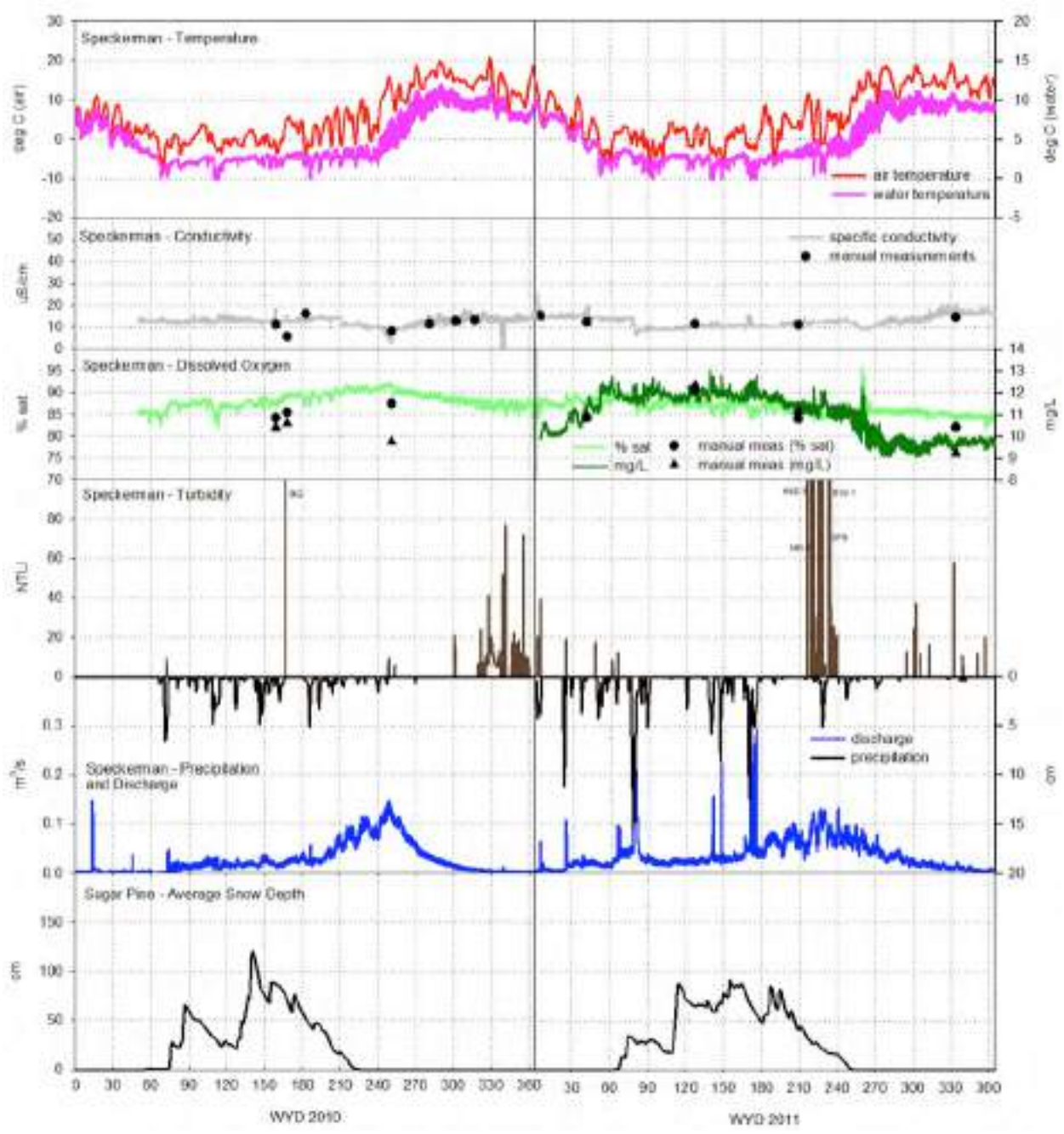

Figure E25: Speckerman Creek water-quality data for water years 2010 and 2011. Water years run from Oct 1 to Sept 30. Water temperature, conductivity, dissolved oxygen, turbidity, and discharge are plotted as 15-minute time-interval data from Speckerman Creek. Air temperature and precipitation were collected at Big Sandy Met and plotted on an hourly time interval. Snow depth data are plotted using daily averages and spatial averages of all sensors across the Sugar Pine site.

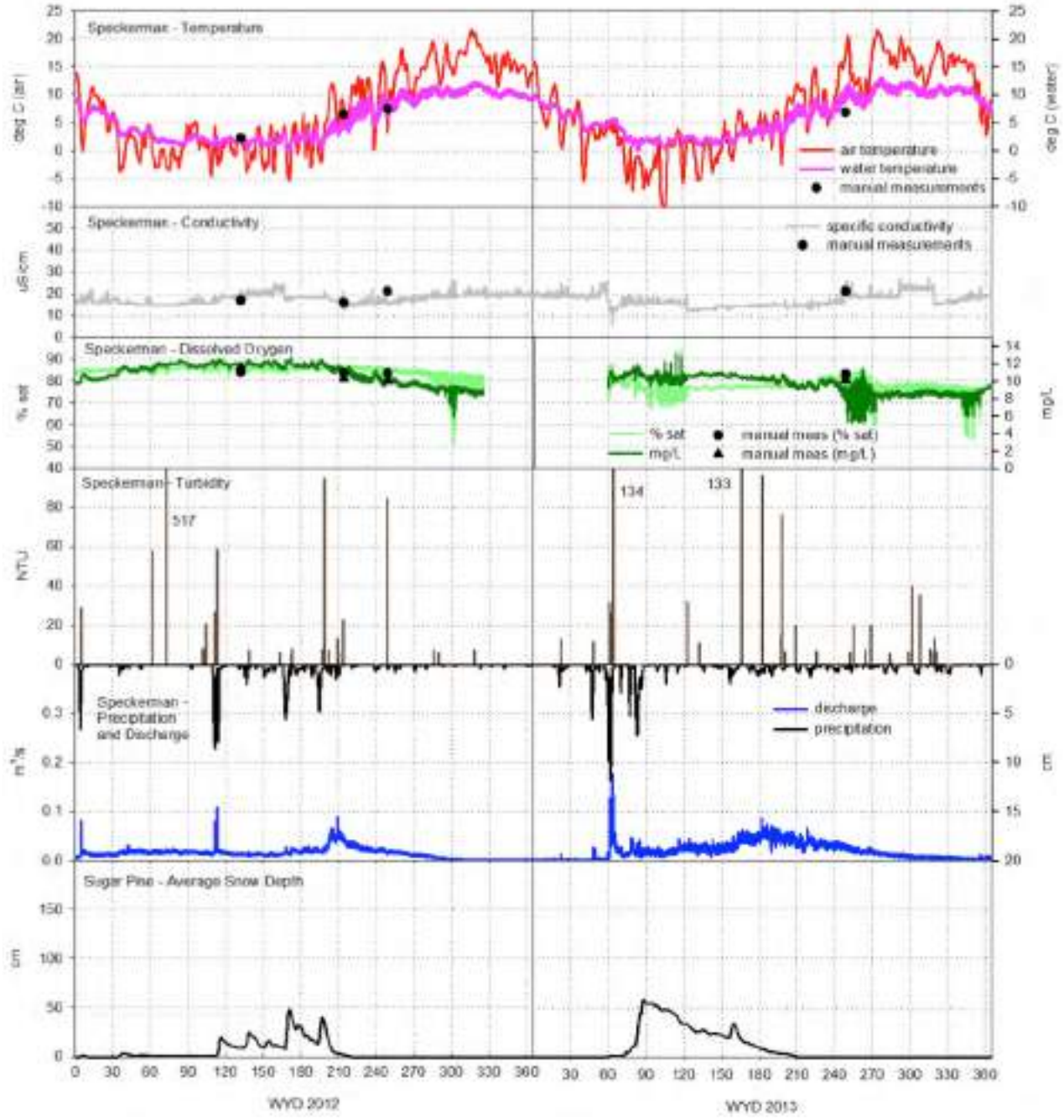

Figure E26: Speckerman Creek water-quality data for water years 2012 and 2013. Water years run from Oct 1 to Sept 30. Water temperature, conductivity, dissolved oxygen, turbidity, and discharge are plotted as 15-minute time-interval data from Speckerman Creek. Air temperature was collected at Big Sandy Met and plotted on a daily time interval. Precipitation data are from the Westfall meteorological station operated by the US Army Corps of Engineers. Snow depth data are plotted using daily averages and spatial averages of all sensors across the Sugar Pine site.

Temperature

Water temperature ranged for the period of record from 0 to 13.6 °C in Bear Trap, 0 to 15.0 °C in Frazier , 0 to 18.0°C in Big Sandy, and 0 to 13.0 °C in Speckerman (Figures E19-E26). water year 2013 showed the warmest water temperatures in all catchments except Big Sandy, where water year 2012 had roughly 1 °C higher maximum water temperature. For all four catchments, water temperatures in water year 2010 were lowest in early winter and gradually rose through the season. In water year 2011, temperatures stayed steady for much of the winter. Water temperature patterns were similar in both water years 2012 and 2013, trending with air temperature, reaching lowest values in early winter and gradually rising through the season.

Conductivity

At both the Sugar Pine catchments, manual and continuous measurements of conductivity showed low, relatively stable values with minimal seasonal variation. Mean values for water year 2010 and water year 2011 were 12.5 µS/cm and 12.4 µS/cm at Speckerman (Figure E24). Continuous conductivity and dissolved oxygen values at Big Sandy are not shown for water years 2010 and 2011 due to frequent battery failures and sediment burial. Mean specific conductivity values for water years 2012 and 2013 were 18 µS/cm and 17 µS/cm at Speckerman, and 45 µS/cm and 44 µS/cm at Big Sandy respectively (Figures E24, E26).

Mean conductivity values for the Last Chance catchments were 33.3 µS/cm and 28.8 µS/cm for Frazier for water years 2010 and 2011 (Figure E21). For Bear Trap, the mean value for water year 2010 was 27.8 µS/cm (Figure E19). Bear Trap's water year 2011 mean was not calculated due to the amount of missing data. Mean conductivity values for the Last Chance catchments were 46 µS/cm and 44 µS/cm for Frazier for water years 2012 and 2013 (Figure E22). For Bear Trap, the mean value for water year 2012 was 48 µS. Bear Trap's water year 2013 mean was found to be 43 µS/cm (Figure E20).

For all streams, the highest conductivity values were seen during baseflow conditions and the lowest during peak spring snowmelt. This was to be expected, because baseflow consists of a higher proportion of higher conductivity groundwater. In the spring, this groundwater input is

diluted by relatively low conductivity snowmelt. The dilution effect could also be seen on a storm-by-storm basis. A good example was the large discharge spike from early season snowmelt centered on WY 2011 day 80 for Frazier Creek (Figure E21). The addition of low-conductivity melt water caused a dilution of the stream, and a corresponding dip in conductivity was seen.

Dissolved Oxygen

Dissolved oxygen data in both the Last Chance catchments had percent saturation values that were fairly stable from year to year ranging between 75% and 95% saturation, with annual means for Frazier being 86%, 84%, and 83% for water years 2010, 2011 and 2012 respectively. Frazier had too many data gaps in 2013 to allow calculation of a mean (Figures E21, E22). For Bear Trap, annual means were 89%, 86%, 86%, and 85% saturation for water years 2010, 2011, 2012, and 2013 respectively (Figures E19, E20).

Sugar Pine catchments dissolved oxygen values also ranged between 75% and 95% for water years 2010 and 2011 with annual means of 88% and 87% saturation for Speckerman, 91% and 87% saturation for Big Sandy (Figures E23, E25). In water years 2012 and 2013, Speckerman's dissolved oxygen values dipped much lower ranging from 50% to 95% with annual means of 85% and 77% respectively (Figure E26). Big Sandy had values ranging between 70% and 90% for water years 2012 and 2013, but due to data gaps during baseflow, may have dipped even lower than the recorded data showed (Figure E24). Annual means were not calculated for Big Sandy due to the large data gaps.

Turbidity

Seasonal turbidity patterns were analyzed for water years 2010 through 2012. The highest turbidity values tended to occur during fall rains and during the snowmelt period (Figure E27). These large turbidity spikes often, but not always, occurred with the largest discharge events. When events were divided up by season, fall had the most turbidity-producing discharge events, with 84% of the events producing a signal (Table E14; Martin et al., 2014). However, these results did not seem to be tied to the size of the discharge events. When the three largest

discharge events per year were tallied by season, none of the largest events occurred in fall (Table E14).

Table E14: Percentage of flow events producing turbidity and number of flow events by season for all catchments**.

Season	Percentage of flow events that produce a turbidity signal	Number of large flow events *
Fall	84.2%	0
Early/Mid winter	55.6%	11
Snow melt	49.0%	18
Baseflow	44.4%	4

*Large flow events consist of the three largest discharge events of each water year for each stream.
**from Martin et al., 2014

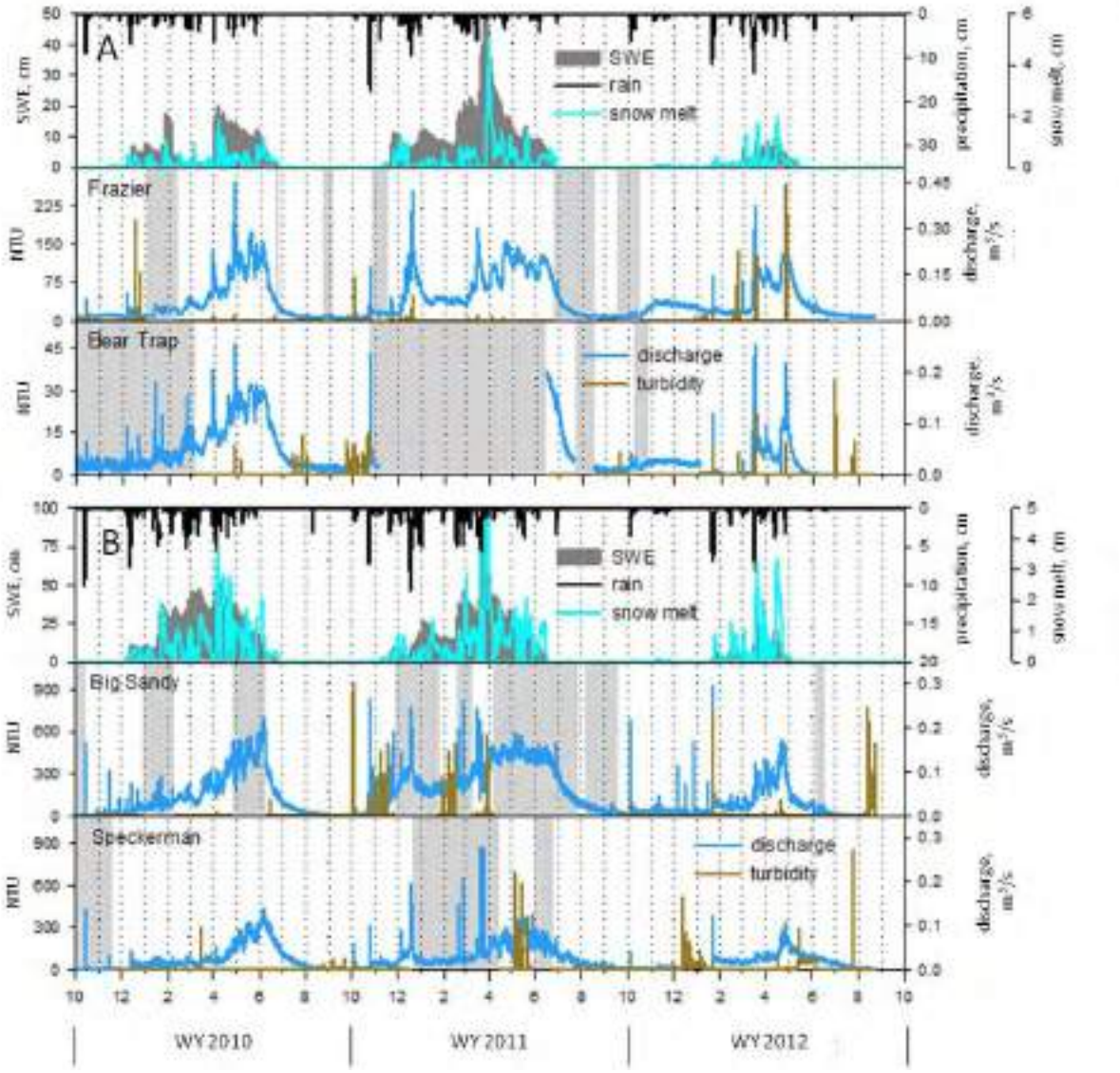

Figure E27: Daily values of precipitation, discharge, snow water equivalents, snowmelt and turbidity data for (A) Last Chance and (B) Sugar Pine sites for water years 2010–2012. Snow values are averaged across the study area. The light grey shaded areas indicate periods when turbidity data were not available.

Large storm data for water year 2011 in Bear Trap were not included in this analysis due to an extensive gap in turbidity data during the high-flow season. When intensity values (peak discharge minus 15-day running average discharge) of events were compared by season, fall had the highest average intensities (0.11 m^3/s), early to mid-winter had the second highest (0.10 m^3/s), with snowmelt and baseflow having the lowest (both 0.06 m^3/s).

Turbidity-discharge hysteresis patterns showed a dominance of clockwise patterns for all seasons except baseflow (Table E15; Martin et al., 2014). Fall and early/mid winter had the highest proportions of clockwise events. Snowmelt had the third highest proportion of clockwise hysteresis event patterns, and baseflow had the lowest proportion.

Table E15: Number of turbidity event hysteresis loop patterns by season at all study catchments*.

Hysteresis shape	Fall	Early/Mid winter	Snow melt	Baseflow
Clockwise	18	19	8	1
Counterclockwise	2	2	1	3
Linear	3	0	0	1
Figure Eight	0	2	2	2
Complex	1	3	2	0

* from Martin et al., 2014

A depletion of sediment was seen at the seasonal and at the event scale (for multi-rise events). For example, Figure E28 shows a series of discharge and turbidity events during the fall 2011 season at Speckerman Creek. The largest turbidity signal was seen early in the season, with a gradual decrease in turbidity signal values, even though the peak discharges for events increased. Multi-rise events also showed a shift in hysteresis patterns indicative of depletion of sediments. An example can be seen in Figure E29 shows a multi-rise discharge event in Big Sandy Creek that progressed from strongly clock-wise to a weakly clock-wise pattern and finally, to a linear pattern.

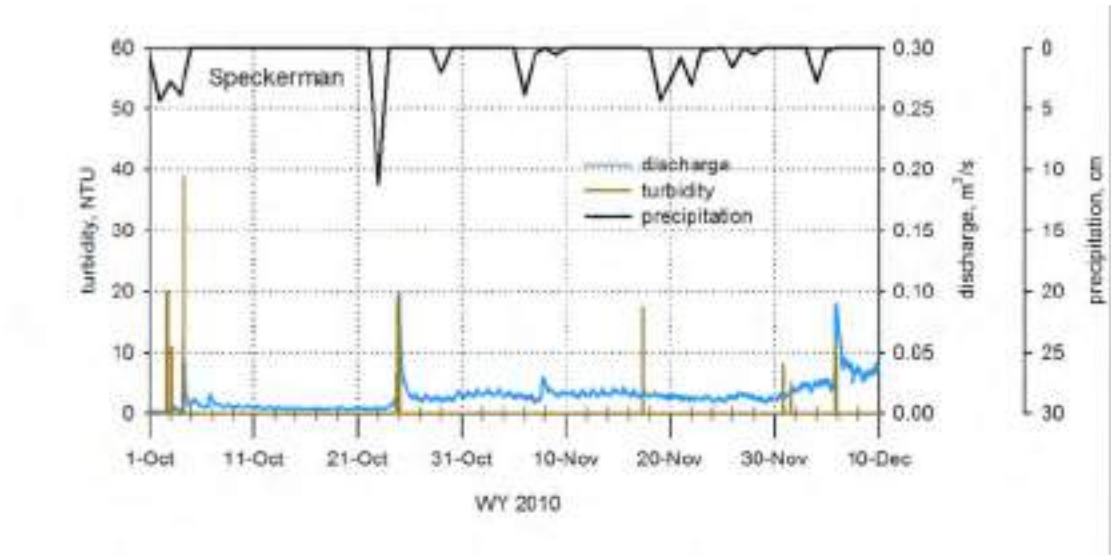

Figure E28: Turbidity, discharge, and precipitation data from Speckermen Creek for the fall rainy season, water year 2010.

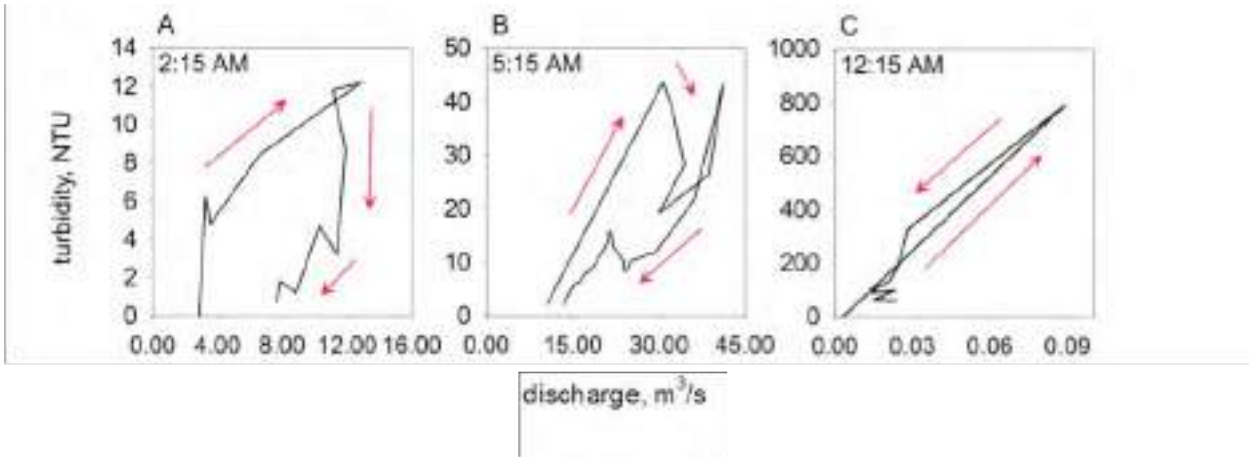

Figure E29: Hysteresis pattern progression seen within a multi-rise discharge event at Big Sandy Creek

Mean peak turbidity event values were calculated for the pre- and post-treatment periods (Table E16). Data were aggregated separately for the control watersheds and the treatment watersheds. High standard deviations and a limited amount of post-treatment data (only one year which had very few substantial events) limited the ability to conduct a robust statistical comparison of control vs treatment and pre-treatment vs post treatment turbidity response. The

percentage of turbidity events occurring during the fall, early/mid-winter, and spring melt seasons for pre- and post-treatment periods are shown in Table E16. Due to lack of consistent flow during drier years and concerns with turbidity due to algae at extremely low flows, baseflow turbidity data were not included in the analysis.

Table E16: Mean turbidity event peak values, standard deviations, and percentage of events for the fall, early/mid-winter, and spring melt seasons for the pre- and post-treatment periods*.

	Mean of turbidity event peaks	Standard Deviation	Fall	Early/Mid-Winter	Spring Melt
Control pre-treatment	44	98	26%	47%	27%
Control post-treatment	93	199	43%	14%	43%
Treatment pre-treatment	90	218	27%	36%	37%
Treatment post-treatment	67	83	59%	9%	32%

* Baseflow events were not included in analysis.

Manual Samples

Major Ions

Analysis of major cation and anions from stream water samples, and comparison of those ion concentrations with stream conductivity, showed Speckerman having the lowest concentrations and conductivities of the four watersheds (Figure E30). Big Sandy had intermediary concentrations and conductivities, while Frazier and Bear Trap showed the highest concentrations and/or conductivity depending on the ion in question. The Last Chance samples had a much larger spread of sample points than did the Sugar Pine sites.

For the cations Na^{+} and K^{+}, Frazier, Big Sandy, and Speckerman had increases in concentration that were proportional to increases in conductivity, while Bear Trap did not exhibit an increase in concentration with increasing conductivity (Figure E30). For Mg^{+2}, Speckerman did not show a concentration increase with increased conductivity and Bear Trap had only a slight increase (less steep slope) in concentration with increased conductivity. Big Sandy and Frazier had proportional increases similar to that for Na^{+} and K^{+}. For Ca^{+2} all streams except Speckerman showed higher concentrations associated with increased conductivities. The F^{-} anion showed considerable spread in the data along with relatively low concentrations. For Cl^{-} and $SO4^{-2}$, Bear Trap showed increasing ion concentrations with increasing conductivity, but the

other three streams had relatively stable ion concentrations even with increased conductivity. All four streams had proportional increases between ion concentration and conductivity for HCO_3^-.

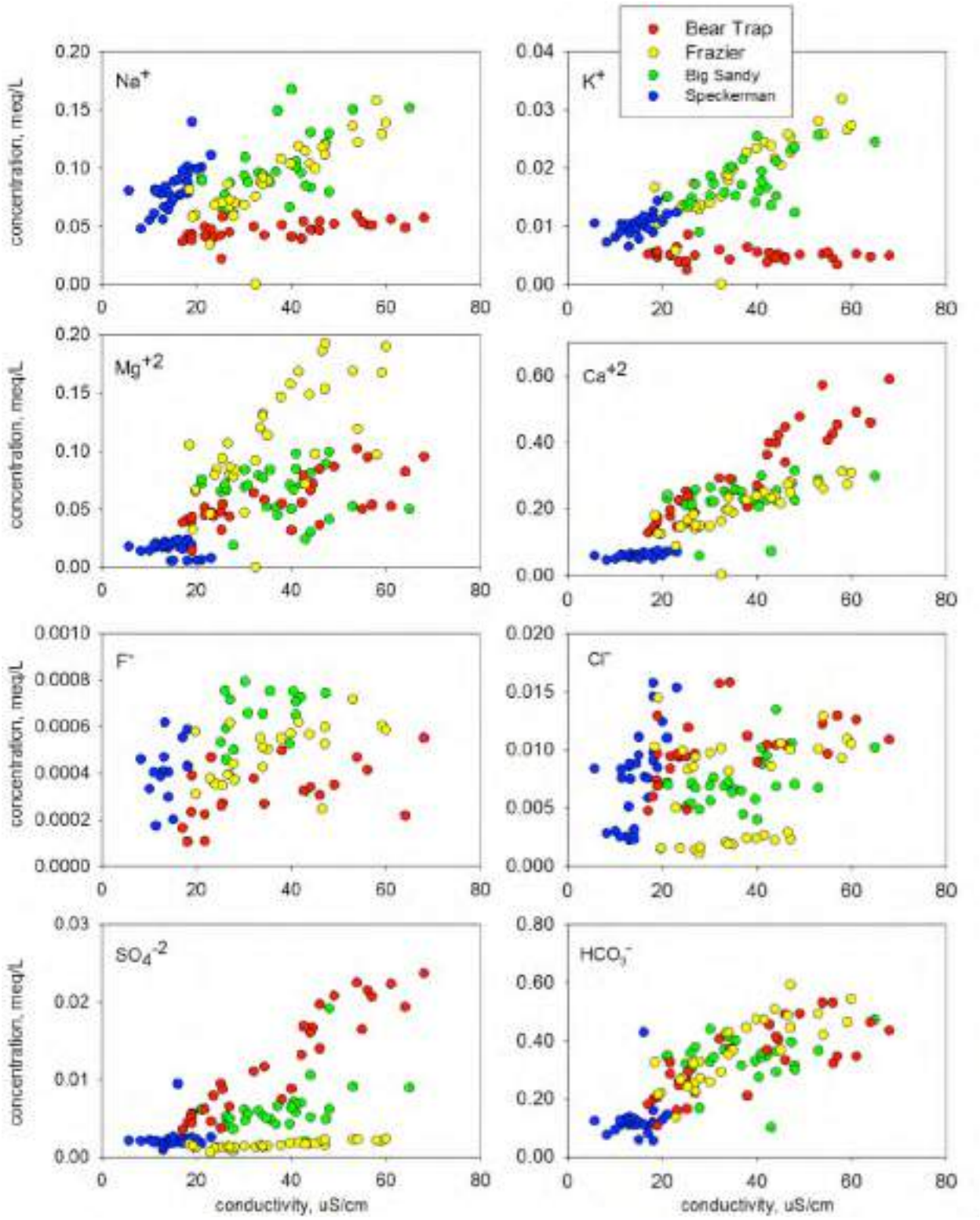

Figure E30: Major cation and anion data for stream water samples from water years 2010-2013. Charge equivalents are plotted against temperature corrected conductivity.

Stable Water Isotopes

Stable water isotopes from stream samples showed slightly more negative δ D and δ ^{18}O values for the Big Sandy and Speckerman samples (Figure E31). Paired catchments showed similar values with the northern catchments with a smaller range than the southern catchments. The isotopic signatures of the samples form a local meteoric water line (LMWL) that sits slightly to the left of the global meteoric water line (GMWL). More negative isotopic values at the Sugar Pine sites were as expected due to the southern catchment's higher altitudes. The existence and position of the local meteoric water line (LMWL) were also expected and fit well with other Sierra Nevada sites.

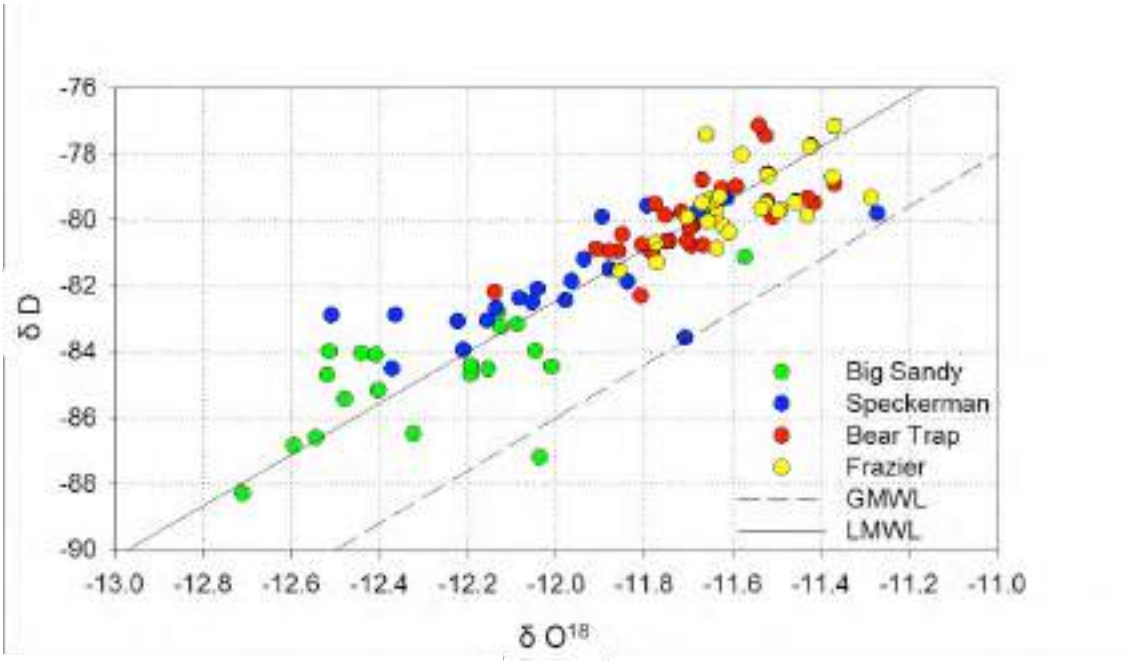

Figure E31: Stable isotopes from stream water samples in all four study catchments for water years 2010 to 2013. The local meteoric water line (LMWL) was determined based on snow and stream samples from SNAMP watersheds and from Kings River Experimental Watershed.

Baseflow Comparison

Conductivity, Ca^{+2} ion concentrations, and stable isotopes during the baseflow season were compared for each water year. Water years 2010 and 2011 were average to wet years and the water years 2012 and 2013 were both dry years. There was a general trend of increasing conductivity and increasing Ca^{+2} ion concentrations throughout the baseflow season (Figures E32, E33). For all four catchments, baseflow conductivity was higher for water years 2012 and

2013 than in the previous two water years with water year 2013 values slightly elevated over water year 2012 values. Ca^{+2} ion concentrations during baseflow showed similar elevated values in water years 2012 and 2013. Stable isotopes generally plotted along the local meteoric water line (LMWL) for all water years with the exception of a cluster of points slightly to the right of the LMWL from water year 2010 (Figure E34).

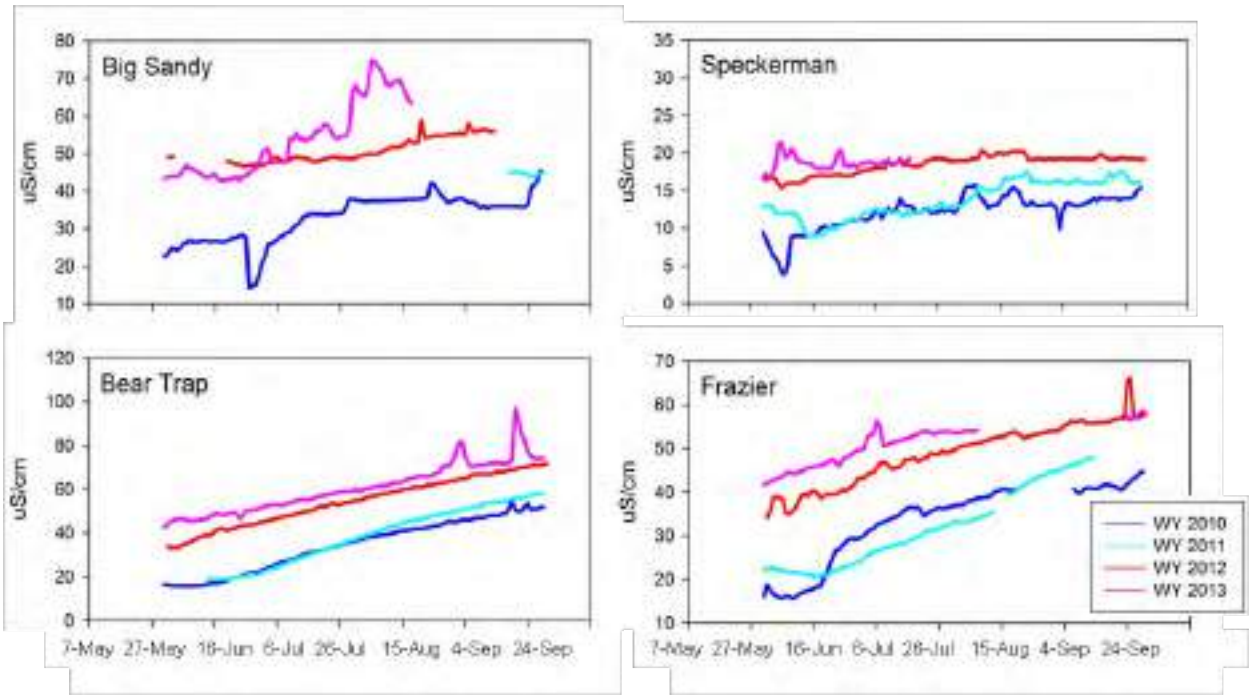

Figure E32: Baseflow conductivity values by water year. The blue and cyan lines represent water years 2010 and 2011 respectively, which were both average to wet years. The red and pink lines represent water years 2012 and 2013 respectively, which were both dry years.

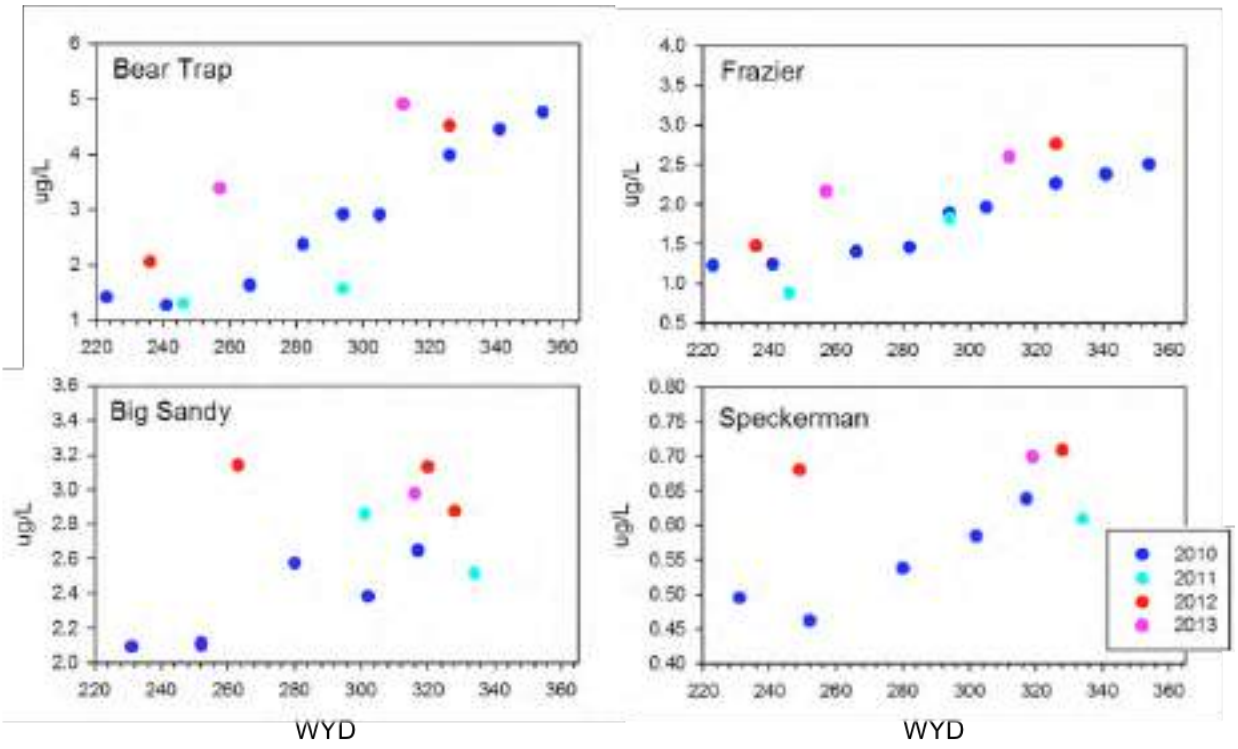

Figure E33: Baseflow calcium ion (Ca^{+2}) concentration values versus water year day by water year. The blue and cyan points represent water years 2010 and 2011 respectively, which were both average to wet years. The red and pink points represent water years 2012 and 2013 respectively, which were both dry years.

Differences between watersheds in ion concentrations and the concentration to conductivity relationship can be attributed to differences in catchment geology, water sources, and/or flow paths. The values and trends in major ion chemistry indicate that for Speckerman Na^{+}, K^{+}, and HCO_3^{-} were important constituents affecting stream conductivity, while Mg^{+2}, Ca^{+2}, and $SO4^{-2}$ contributed little to that streams conductivity. The same constituent make-up seemed to be the case for Big Sandy, however there was more scatter in the data. The similarities are likely due to very similar rock types and source waters between the two-paired watersheds.

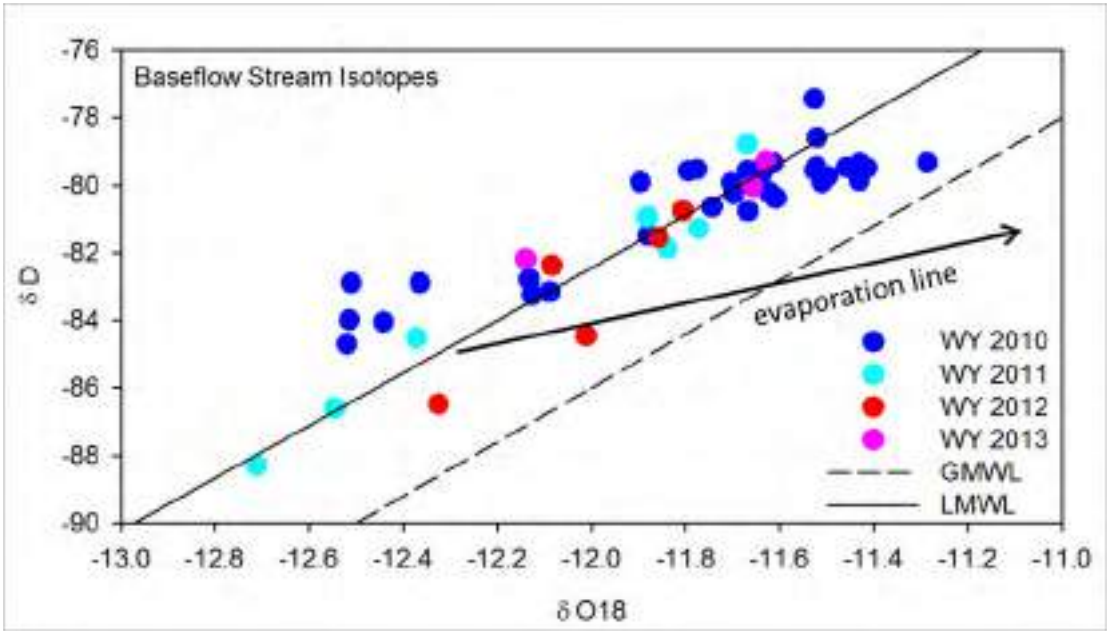

Figure E34: Baseflow stable isotope ratio values by water year. The blue and cyan points represent water years 2010 and 2011 respectively, which were both average to wet years. The red and pink points represent water years 2012 and 2013 respectively, which were both dry years and post-treatment years. The dashed line represents the global meteoric water line. The solid line shows the local meteoric water line for Sierra Nevada samples collected at Sierra Nevada Adaptive Management Project sites and at Kings River Experimental Watershed sites.

The Last Chance sites show very different constituent make-ups between the two watersheds. Ca^{+2}, Cl^{-}, and $SO4^{-2}$, and HCO_3^{-} seem to be the most important constituents for stream conductivity (Mg^{+2} to a lesser degree) for Bear Trap, while Na^{+} and K^{+} seem to be unimportant. Frazier has a nearly opposite trend, with Na^{+}, K^{+}, Mg^{+2}, and HCO_3^{-} being the more important constituents (Ca^{+2} to a lesser degree) and Cl^{-} and $SO4^{-2}$ not contributing significantly to conductivity. These differences are likely due to variations in the bedrock chemistry between the two streams. Bedrock in Frazier consists of mainly andesitic pyroclastic flow deposits with a small amount of the ShooFly Complex, a metasedimentary sandstone, siltstone, and slate (USGS 2014). Bear Trap is the opposite consisting mostly of the ShooFly Complex with limited andesitic pyroclastic flow deposits.

The lack of an evaporation signal during dry years for the baseflow isotope samples, is consistent with increases in conductivity and ion concentrations being attributed to increased amount of dissolved solids. Lengthened contact of water with subsurface materials and less dilution by low conductivity rain/snow results in increased conductivity or concentration.

Channel Bed Movement

Data from load cell pressure sensors placed in the thalweg of the four study catchments, showed patterns of abrupt channel bed disturbance (scour and/or fill) associated with discharge events. These events were overlain on a broad annual pattern of accumulation of channel bed material during fall and early/mid-winter, followed by gradual scour of material back to a stable equilibrium bed surface elevation during spring and baseflow (Figure E35). A lack of geomorphological field evidence for long-term incision or aggradation offers further evidence for inter-annual channel bed stability.

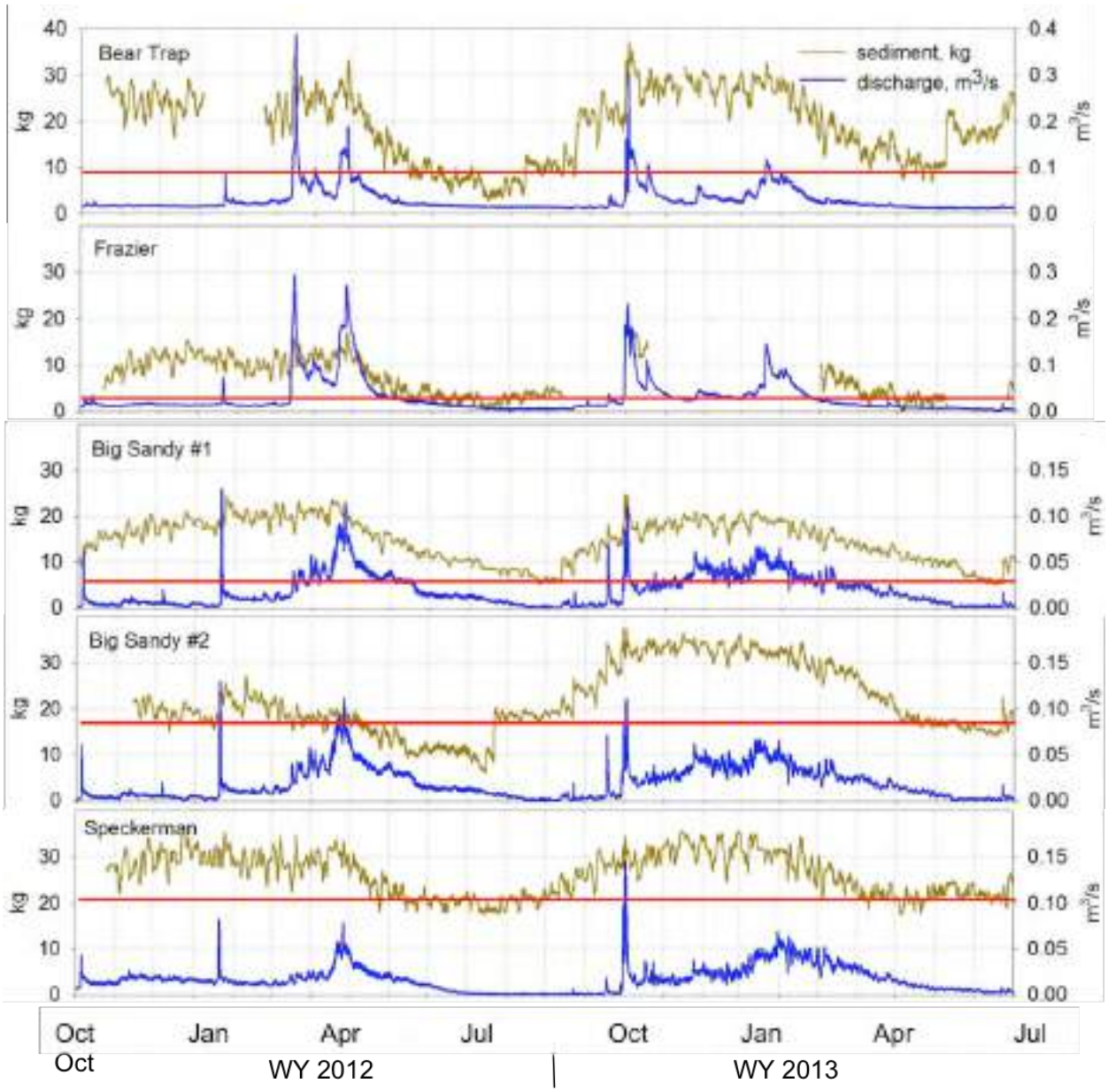

Figure E35: Load cell pressure sensor and discharge data for water years 2012-2013. Brown lines are the total kg of sediment recorded by the load cell pressure sensor. Red lines approximate the annual stable baseline level of channel bed material. Drops in sediment observed at the end of water year 2014 in BSN, SPK, and BTP are due to unburying of pans for calibration measurements.

In addition to disturbance and recovery patterns associated with storm events, a pattern of regular oscillations in pressure/sediment on a four to ten day temporal scale was observed.

These oscillations occurred year round and did not appear to be associated with changes in discharge, barometric pressure, or temperature. Rough syncronicity was seen in the timing of the oscillation peaks between the two Big Sandy Creek load cell scour sensors. It is assumed that these oscillations are due to physical sediment processes within the stream rather than sensor noise, because measurements were from independent instruments placed in different (though nearby) cross-sections.

Discussion

Turbidity

Fall typically had the greatest number of turbidity producing events without having the largest discharges due to the high intensity of fall rain events combined with the high availability of easily transported sediment that accumulated during the preceding low-flow baseflow season. These data match well with findings by Rodriguez-Blanco et al. (2010) despite major differences in land use and rainfall patterns between the two studies. These authors reported fall having the largest sediment load and hillslope runoff (50 percent of the annual) but only 29 percent of the water yield. In their study, the large fall sediment loads were attributed to fall having the highest number of rainfall events as well as to the presence of bare ground in fall due to traditional agricultural practices within their catchments.

Significant spikes in turbidity were sometimes observed during baseflows for all four streams, when no discharge events were occurring. The exact reason for these spikes is unknown, but possible explanations may be wildlife using the stream or algae growth in the water column. Because the turbidity sensors are equipped with automatic wipers, biofilm buildup on the sensor is not a likely explanation for these spikes.

Prior research has shown conflicting results on the dominant season for sediment transport, but generally the seasons of highest flow tended to also be the seasons with the highest suspended sediment concentrations. Rodriguez-Blanco et al. (2010) showed in a steep, low elevation, 16 km^2 basin in northwest Spain with no seasonal snow, that most sediment events and most suspended sediment load transport occurred in the fall, the season of highest volume of runoff and the highest number of events. Research in a mountainous catchment in Japan, which

is lower elevation but with a similar snow dominated precipitation pattern as this study's sites, found that in over 60% of the basins suspended sediment load was transported during the spring snow melt period (Iida et al., 2012). The high spring snow melt sediment load was attributed to increased discharge. Finally, Gao and Josefson (2012) did not see a dominant sediment transport season for a medium sized, low elevation, central New York catchment with patchy seasonal snow cover. Instead they showed that most of the sediment was transported throughout the year during frequent small events. The differences between their results and those of this study are likely due to differences in the amount and types of precipitation throughout the year. Their catchments had much higher year round precipitation and high intensity or high volume rainfall/melt events were not concentrated to a specific time period. Additionally, their study sites comprised of 50% agricultural lands which may have provided a steady year round hillslope sediment source to the streams. Sites in the current study are most similar to the forested, snow dominated catchments from Iida et al. (2012) and share a high spring snow melt turbidity signal. However, the strong summer accumulation–fall depletion cycle and the high intensity of fall rain events result in an additional high turbidity season in fall in this study.

As established by the work of Wood (1977) and Williams (1989), clockwise patterns indicate a localized, easy-to-transport sediment source that can be entrained and transported quickly during the early part of the discharge event. The dominance of this hysteresis pattern suggests localized in-channel sediment stores, likely at the toe of channel banks. Rodriguez-Blanco et al. (2010) similarly found clockwise to be the dominant hysteresis pattern suggesting localized sediment sources. Research in other small headwater catchments in the Sierra Nevada suggests that relatively little hillslope material reaches the stream directly (Stafford, 2011) and instead sediment comes from the channel bed and banks. Bank-pin surveys during the low-flow season in the Sugar Pine catchments confirm the existence of material accumulated at the toe of channel banks and offer supporting evidence of in-channel sediment sources (Martin et al., 2014).

In contrast to these findings, Fang et al. (2011) showed clockwise patterns at the hillslope plot scale and counterclockwise patterns at the basin scale suggesting a dominantly hillslope source at various spatial scales on the Loess Plateau of China. The difference in results between

this work and Fang et al. is likely because their site has some of the highest soil erosion rates in the world with an average annual sediment yield of 22,200 tons per km^2 and extremely steep slopes of up to 70 degrees (Fang et al., 2011). In comparison, sediment yields in the central Sierra Nevada have been estimated to be around 4.1 tons per km^2 (Stafford, 2011).

The dominance of clockwise hysteresis loops also has implications on flow pathways in the study catchments. Seeger et al. (2004) showed that clockwise loops were the most common for small Central Pyrenees catchments and that this pattern occurred under normal runoff conditions. They showed that counterclockwise loops typically only occurred under extremely wet antecedent conditions where overland flow was possible. The characteristically sandy soils in catchments (in this study and typical of Sierra Nevada headwater catchments) make overland flow occurrences extremely rare, which fits with the limited number of counterclockwise patterned events observed.

The shift away from a clock-wise hysteresis pattern during multi-rise events can be indicative of a progressive lag in sediment transport resulting from a depletion in localized stores and a shift from nearby, easy-to-transport sediments to more distant sediment sources or to more consolidated sources (consolidated banks or armored beds) that require greater flow energy to entrain. Lana-Renault et al. (2010) and Soler et al. (2008) attributed counterclockwise hysteresis patterns in their studies to distant sediment sources or to antecedent conditions that may cause a lag in sediment transport (i.e., subsurface must fill before saturation overland flow can occur).

Observed hysteresis shapes and patterns within the turbidity signal also are suggestive of the catchment undergoing phases of accumulation and depletion of localized sediment stores. One hypothesis is that during low-flow periods, sediment accumulates at the toe of banks. This accumulation period is thought to occur at the seasonal time scale (i.e., summer baseflows) as well as event scale (i.e., low flows between discharge peaks). Sediment is entrained and transported downstream during high-flow events, with multiple events in short succession depleting sediment stores (Martin et al., 2014).

The lack of significant difference seen between the means of the treatment watersheds for pre-and post-treatment turbidity events may be due to the light treatments performed and the dry conditions in the post-treatment years, but it should also be noted that the infrequency of events resulted in a relatively small sample size compared to large standard deviations for turbidity. This may have also contributed to the lack of significance. The post-treatment period showed a higher percentage of turbidity peaks during winter rather than fall for the pre-treatment, however this is more likely due to timing of precipitation/melt events in wet versus dry years than to treatment effects.

Baseflow Comparison

An increase in conductivity and ion concentrations from pre-to post-treatment years was seen in both treatment and control watersheds. The increased post-treatment conductivity and ion concentrations in water years 2012 and 2013 are attributed to drought conditions. Any potential post-treatment water chemistry signal was not distinguishable over the coinciding drought signal.

The general trend of increasing conductivity and ion concentrations during baseflow seasons were as expected due to one of two reasons: 1) as the baseflow season progresses there was an increasing proportion of sub-surface flow that had picked up dissolved materials while in contact with rock and soil, or 2) evaporation was occurring, increasing the concentration of dissolved material in the stream water throughout the summer baseflow season. The higher conductivity and ion concentration during drier water years was likely due to a greater reliance on subsurface water for maintaining stream flow, or earlier snow melt and a longer drier baseflow period where increased evaporation can occur (Figures E32, E33).

Variations in conductivity between catchments points to differences in water sources and flow paths. The higher mean conductivities and high seasonal variation imply that the groundwater input at Big Sandy and the Last Chance catchments may be older or that the soil/rock the water it is in contact with is more easily reacted. Both explanations are plausible for the Last Chance sites, given that the Last Chance catchments have a mixture of granitic and metamorphic rock types. The relatively low amount of seasonal variation in the Speckerman

catchment suggests that the water in this catchment is relatively new. The higher (roughly double) conductivity values at Big Sandy compared to Speckerman implies that Big Sandy either receives some older/higher conductivity water or there are differences between the soil and rocks within the two catchments. Given that the soil and bedrock geology of Big Sandy and Speckerman are very similar, older water sources and longer flow paths appear to be the more likely explanation.

For all streams, the highest conductivity values were seen during baseflow and the lowest during peak spring snowmelt. This was to be expected because baseflow consists of a higher proportion of higher conductivity groundwater. In the spring, this groundwater input is diluted by relatively low conductivity snowmelt. The dilution effect could also be seen on a storm-by-storm basis. A good example was the large discharge spike from early season snowmelt centered on water year 2011 day 80 for Frazier Creek (Figure E21). The addition of low-conductivity melt water diluted the stream water, and a corresponding dip in conductivity was seen.

In the nearby King River Experimental Watershed, Liu et al, (2013) showed that stream water was on average a mixture of sub-surface water (60% or more) and snow (40% or less). Higher mean conductivity values for water years 2012 and 2013, compared with those in water years 2010 and 2011, are likely due to these low water years having proportionally less low-conductivity rain/snow and proportionally more groundwater entering the stream.

Baseflow stable isotope data help to distinguish the mechanism causing higher concentration and conductivity. Isotope values are based on the isotopic signature of precipitation falling on the watershed. These values vary considerably by storm, but contact with the subsurface does not typically alter the isotopic signature of the water, so even non-event water will plot along a localized meteoric waterline. Evaporation, however, will alter the isotopic signature as samples diverge from the LMWL at a shallow angle with increasingly less negative δ D and $\delta\ ^{18}O$ values with increasing evaporation (Figure E34). The baseflow data for water years 2012 and 2013 did not show this evaporation signal in the stable water isotope data so it can be concluded that increased conductivity and ion concentrations were due to a greater proportion of sub-surface water in the stream (Figure E34). The anomalous cluster of points in

water year 2010 that plot to the right of the LMWL were all samples from the Last Chance watersheds and were from June and early July of that year (Figure E34). Due to these samples being from a fairly wet water year and early in the baseflow season this divergence is not likely due to evaporation within the stream.

Channel Bed Movement

Observed disturbance and recovery patterns over both event and annual time periods are consistent with the bed acting as a short term source or sink for sediment. As suggested in Bagnold (1973), when sediment supply is out of balance with stream power, channel beds aggrade or degrade. Active downcutting or aggradation, in which the channel bed becomes a sediment source or sink, was not observed over the long term in the streams in this study. Data suggest that under the conditions of this study, the changes in bed elevation are reflective of fluctuations in storage rather than the bed being a true source or sink and that channel beds are relatively stable inter-annually. Hassan and Woodsmith (2004) also report a relatively stable channel bed (particle sizes greater than the D50 rarely mobilized) for a northern California catchment and suggest observed changes to bed elevation are a function of upstream sediment storage and/or bank collapse. While data point toward this trend, additional years of data are required for a conclusive determination of inter-annual stability under the given conditions.

Thompson et al. (2007) found that step-pool and planar bed streams in southeastern Australia had bed surfaces that were moderately stable. Similar cycles are reported by Hassan and Church (2001) who, using pit traps in a gravel-cobble, snow dominated stream in British Columbia, show no generalized mobilization of the local bed material, but rather short term fluxes in bedload transport due to sand pulses washing through the cross-section from upstream.

Although it is recognized that a small amount of noise may exist in these systems, it is not likely that the observed 4-10 day oscillations in channel bed material are due to sensor noise. An alternative explanation is that these oscillations may be waves of fine sediment moving through the cross-section (such as those seen in sand/gravel bed rivers) or may be a small number of large particles rolling into and out of the sensor's "view" along the bed surface (Gomez et al., 1989, Gomez, 1991, Hoey, 1992). The oscillations do not appear to affect overall

behavior of storm event response-recovery and may represent a significant amount of the bedload movement in the stream. The dominant channel bed movement behavior on an annual scale reflects a return to stable stream bed elevations.

These patterns do highlight the importance of collecting concurrent discharge data, so important events can be recognized and separated from background (non-event related) patterns. Additional tests on sensor response across a range of pressures and temperatures can help confirm the extent of any possible noise occurring at this scale, and tracer studies tracking individual particle movement would help to verify the presence or absence of waves of material and its periodicity in these systems.

Management Implications

Given that monitored water chemistry parameters (DO, temperature and turbidity) are within healthy ranges for the SNAMP watersheds, we expected the biggest potential risk to water quality in these systems to be from increased sediment movement. Analysis of turbidity hysteresis loops indicate that in-channel erosion is main sediment source supplying material directly to the stream, with sediment accumulation and depletion cycles tied to low and high flows. These results fit with those from previous work in the Kings River Experimental Watershed (Stafford, 2011), which is analogous to the SNAMP watersheds, showing very low direct connectivity between the hillslopes and stream channels. Channel bed movement patterns suggest that under normal conditions (no treatment, no fire) the stream channels experience seasonal changes in storage of bed material, but remain stable on an inter-annual basis. Because in-channel sources dominate direct sediment supply, any increases in sediment transport from treatments will be due to increases in discharge. The post-treatment monitoring period was following the second year of draught. Additionally, the implemented treatments were light and located a significant distance from stream channels. These light treatments were not intensive enough to show a increase in discharge during a low precipitation year and SPLATS as implemented in SNAMP had no detectable effect on turbidity for the methods used under the climatic conditions of the study.

The data collected in SNAMP highlight the importance of detailed field measurements for watershed studies and hydrologic modeling. Despite carefully choosing catchments with very similar physical parameters, substantial differences were found in the stream chemistry and flow pathways. When choosing watersheds for study or applying data from one catchment to model another unmeasured catchment, a careful comparison of hydrologic pathways, and, if possible, biogeochemical processes may be necessary to ascertain similar characteristics.

SNAMP also highlights the need for long-term field studies. During the course of this project precipitation varied widely and a corresponding shift toward sub-surface water sources was observed in drier water years. Short term data sets may miss this variation and incorrectly characterize water sources and flowpaths under conditions that deviate from those in which measurements were taken. Long term field studies are also of particular importance in these systems because they are so episodic. Sample sizes for sediment events can be very low which is especially problematic because the storm-to-storm standard deviation for sediment measurements is typically very high. Long term field studies allow large enough event sample sizes for in-depth statistical analysis.

Spatially explicit measurements that capture both the catchment-to-catchment variability and the climatic variability will help to better understand the extent of heterogeneity within and between catchments in the Sierra Nevada. Future work in forested mountain systems, utilizing detailed long term field datasets will help provide a better understanding of the nuanced differences between seemingly similar catchments, as well as the effects of land use change and climate change which are central to future land and infrastructure planning.

References

Adams, M. A. (2013) Mega-fires, tipping points and ecosystem services: Managing forests and woodlands in an uncertain future. *Forest Ecology Management*. 294, 250–261, doi:10.1016/j.foreco.2012.11.039.

Akaike, H. (1973) Information theory and an extension of the maximum likelihood principle, in Proceedings of the Second International Symposium on Information Theory. pp. 267–281, Akademiai Kiado, Budapest.

Bagnold, R.A. (1973) The nature of saltation and bedload transport in water. in Proceedings Royal Society, London. 322A, 473-504.

Bahro, B., and K. Barber (2004), Fireshed Assessment: An Integrated Approach to Landscape Planning. USDA Forest Service Pacific Southwest Region, R5-TP-017.

Bales, R. C., J. W. Hopmans, A. T. O'Geen, M. Meadows, P. C. Hartsough, P. Kirchner, C. T. Hunsaker, and D. Beaudette (2011) Soil Moisture Response to Snowmelt and Rainfall in a Sierra Nevada Mixed-Conifer Forest. *Vadose Zone Journal*. 10(3), 786, doi:10.2136/vzj2011.0001.

Bao, Z., J. Zhang, J. Liu, G. Fu, G. Wang, R. He, X. Yan, J. Jin, and H. Liu (2012) Comparison of regionalization approaches based on regression and similarity for predictions in ungauged catchments under multiple hydro-climatic conditions. *Journal of Hydrology*. 466-467, 37–46, doi:10.1016/j.jhydrol.2012.07.048.

Bárdossy, A. (2006). Calibration of hydrological model parameters for ungauged catchments. *Hydrology and Earth Systems Science*. 11(2), 703–710, doi:10.5194/hessd-3-1105-2006.

Bateman, P. C. (1989) Geologic map of the Bass Lake quadrangle, west-central Sierra Nevada, California, Geologic Quandrangle Map GQ-1656.

Beven, K. J., and M. J. Kirkby (1979) A physically based, variable contributing area model of basin hydrology. *Hydrological Sciences Bulletin*. 24(1), 43–69.

Beschta, R. L. (1978) Long-term patterns of sediment production following road construction and logging in the Oregon Coast Range. *Water Resources Research.* 14.6, 1011-1016.

Biederman, J., A. Harpold, D. Gochis, B. Ewers, D. Reed, S. Papuga, and P. Brooks (2014) Increased evaporation following widespread tree mortality limits streamflow response, *Water Resources Research*. 50, 5395–5409, doi:10.1002/2013WR014994.

Black, T., J.-M. Chen, X. Lee, and R. Sagar (1991) Characteristics of shortwave and longwave irrandiances under a Douglas-fir forest stand, *Canadian Journal of Forest Research*. 21, 1020–1028.

Bormann, B., P. Cunningham, M. H. Brooks, V. W. Manning, and M. W. Callopy (1994) Adaptive ecosystem management in the Pacific Northwest. USDA Forest Service Pacific Northwest, PNW-GTR-34.

Bormann, B. T., R. W. Haynes, and J. R. Martin (2007) Adaptive Management of Forest Ecosystems: Did Some Rubber Hit the Road?. *Bioscience*. 57(2), 186, doi:10.1641/B570213.

Bosch, J., and J. Hewlett (1982) A review of catchment experiments to determine the effect of vegetation changes on water yield and evapotranspiration, *Journal of Hydrology*. 55, 3–23, doi:10.1016/0022-1694(82)90117-2.

Brown, M. G., T.A. Black, Z. Nesic, V.N. Foord, D.L. Spittlehouse, A.L. Fredeen, R. Bowler, N.J. Grant, P.J. Burton, J.A. Trofymow, D. Lessard, and G. Meyer (2014) Evapotranspiration and canopy characteristics of two lodgepole pine stands following mountain pine beetle attack. *Hydrologic Processes*. 28(8), 3326–3340, doi:10.1002/hyp.9870.

Burnham, K. P., and D. R. Anderson (2002) *Model selection and multimodel inference: a practical information-theoretic approach*. Springer, New York.

Burton, T. A. (1997) Effects of basin-scale timber harvest on water yield and peak streamflow, *Water Resources Research*. 33(6), 1187–1196.

California, Department of Water Resources (2013) California Water Plan, Update 2013. Sacramento, CA.

CA Department of Water Resources (2014a), Northern Sierra 8 Station Chronological monthly precipitation (in). Available from: http://cdec.water.ca.gov/cgi-progs/iodir/8stationhist (Accessed 14 July 2015).

CA Department of Water Resources (2014b), San Joaquin 5 Station Chronological monthly precipitation (in). Available from http://cdec.water.ca.gov/cgi-progs/iodir/5stationhist (Accessed 14 July 2015).

CA Department of Water Resources. Sierra Nevada Adaptive Management Project Water-Team Field Activities, Methods and Results. by Martha Conklin, Roger Bales, Ram Ray, Sarah Martin, Phil Saksa, and Patrick Womble. 2012. Print. Task Order #UC 10-6 Deliverable #4.3.2.

CA Department of Water Resources. Sierra Nevada Adaptive Management Project Water-Team Update. By Martha Conklin, Roger Bales, Phil Saksa, Sarah Martin, Ram Ray, Benjamin Tobin, and Patrick Womble. 2014. Print. Task Order #UC 10-6 Deliverable #4.3.2.

CA Environmental Protection Agency (2014) EWRIMS: Electronic Water Rights Information

System, State Water Resour. Control Board. Available from: http://www.waterboards.ca.gov/waterrights/water_issues/programs/ewrims/index.shtml (Accessed 10 June 2014)

Cerdà, A., and S. H. Doerr (2005) The influence of vegetation recovery on soil hydrology and erodibility following fire: an eleven-year investigation *International Journal of Wildland Fire*. 14(4), 423–437.

Collins, B., S. Stephens, G. Roller, and J. Battles (2011a) Simulating fire and forest dynamics for a landscape fuel treatment project in the Sierra Nevada. *Forest Science*. 57(2), 77–88.

Collins, B. M., R. G. Everett, and S. L. Stephens (2011b) Impacts of fire exclusion and recent managed fire on forest structure in old growth Sierra Nevada mixed-conifer forests. *Ecosphere*. 2(4), 14, doi:10.1890/ES11-00026.1.

Croke, J., P. Hairsine, and P. Fogarty (1999) Sediment transport, redistribution and storage on logged forest hillslopes in south-eastern Australia. *Hydrological Processes*. 13.17, 2705-2720.

Dixon, G. E. (2002) *Essential FVS: A user's guide to the Forest Vegetation Simulator*. Internal Report Fort Collins, CO: USDA Forest Service, Forest Management Service Center. 226p. (Revsed: February 25, 2015)

Doomen, A.M.C., E. Wijma, J.J.G Zwolsman,and H. Middelkoop (2008) Predicting Suspended Sediment Concentrations in the Meuse River using a Supply-Based Rating Curve. *Hydrologic Processes*. *22*, 1846–1856.

Dyrness, C. T. (1976) Effect of Wildfire on Soil Wettability in the High Cascades of Oregon. USDA Pacific Northwest Forest and Range Experiment Station, PNW-202, Portland, OR.

Dunne, T., and L.B. Leopold (1978) *Water in Environmental Planning*, 16th ed.; W.H. Freeman and Company: New York, NY, USA, pp. 713–777.

Ellis, C. R., J. W. Pomeroy, and T. E. Link (2013) Modeling increases in snowmelt yield and desynchronization resulting from forest gap-thinning treatments in a northern mountain headwater basin. *Water Resources Research*. 49, doi:10.1002/wrcr.20089.

Essery, R., J. Pomeroy, C. Ellis, and T. Link (2008) Modelling longwave radiation to snow beneath forest canopies using hemispherical photography or linear regression. *Hydrologic Processes*. 2800(June), 2788–2800, doi:10.1002/hyp.

Fang, H., Q. Li, Q, Cai,and Y. Liao(2011) Spatial Scale Dependence of Sediment Dynamics in a Gullied Rolling Loess Region on the Loess Plateau in China. *Environmental Earth Sciences*. *64*, 693–705.

Fernandez, C., J. Vega, T. Fonturbel, E. Jimenez, and J. Perez (2008) Immediate effects of

prescirbed burning, chopping and clearing on runoff, infiltration and erosion in a shrubland area in Galicia (NW Spain). *Land Degradation and Development*. 19, 502–515.

Gao, P., and M. Josefson(2012) Event-Based Suspended Sediment Dynamics in a Central New York Watershed. *Geomorphology. 139*, 425–437.

Garcia, E. S., C. L. Tague, and J. S. Choate (2013) Influence of spatial temperature estimation method in ecohydrologic modeling in the Western Oregon Cascades. *Water Resources Research*. 49(3), 1611–1624, doi:10.1002/wrcr.20140.

Glover, T. J. (1995) *Pocket Reference*. Sequoia Publishing, Second edition.

Gottfried, G. J., and L. F. DeBano (1990) Streamflow and water quality responses to preharvest prescribed burning in an undisturbed ponderosa pine watershed. USDA Forest Service, Rocky Mountain Forest and Range Experiment Station, RM-GTR-191, Flagstaff and Tempe, AZ.

Goulden, M. L., R. G. Anderson, R. C. Bales, A. E. Kelly, M. Meadows, and G. C. Winston (2012) Evapotranspiration along an elevation gradient in California's Sierra Nevada. *Journal of Geophysical Research*. 117(G3), G03028, doi:10.1029/2012JG002027.

Granger, S.J., R. Bol, J. M. B. Hawkins,S. M. White, P. S. Naden, G. H. Old, and J. K. Marsh(2011) Using Artificial Fluorescent Particles as Tracers of Livestock Wastes within an Agricultural Catchment. *Science of the Total Environment*. *409*, 1095–1103.

Grant, G. E., and A. L. Wolff (1991) Long-term patterns of sediment transport after timber harvest, western Cascade Mountains, Oregon, USA. *Sediment and Stream Water Quality in a Changing Environment: Trends and Explanation*. 203, 31-40.

Hamblin, J. M. (2003) Spatial and Temporal Trends in Sediment Dynamics and Potential Aerobic Microbial Metabolism, Upper San Pedro River Southeastern Arizona. Master's Thesis, University of Arizona.

Hartman, M. D., J. S. Baron, R. B. Lammers, D. W. Cline, L. E. Band, G. E. Liston, and C. Tague (1999) Simulations of snow distribution and hydrology in a mountain basin. *Water Resources Research*. 35(5), 1587, doi:10.1029/1998WR900096.

Hassan, M.A., and M. Church (2001) Sensitivity of bed load transport in Harris Creek: Seasonal and spatial variation over a cobble-gravel bar. *Water Resources Research*. 37(3), 813-825.

Hassan, M.A, and R. D.Woodsmith (2004) Bed load transport in an obstruction-formed pool in a forest, gravelbed stream. *Geomorphology*. 58, 203–221.

Hawthorne, S. N. D., P. N. J. Lane, L. J. Bren, and N. C. Sims (2013) The long term effects of thinning treatments on vegetation structure and water yield, *Forest Ecology and Management*. 310, 983–993, doi:DOI 10.1016/j.foreco.2013.09.046.

Helvey, J. (1980) Effects of a north central washington wildfire on runoff and sediment production. J*ournal of the American Water Resources Association*. 16(4), 627–634.

Henderson, G. S., and D. L. Golding (1983) The effect of slash burning on the water repellency of forest soils at Vancouver, British Columbia. *Canadian Journal of Forest Research*. 13, 353–355.

Heuvelmans, G., B. Muys, and J. Feyen (2004) Evaluation of hydrological model parameter transferability for simulating the impact of land use on catchment hydrology. *Physics and Chemistry of the Earth*. Parts A/B/C, 29(11-12), 739–747, doi:10.1016/j.pce.2004.05.002.

Hrachowitz, M., H.H.G. Savenije, G. Bloschl, J.J. McDonnell, M. Sivapalan, J.W. Pomeroy, B. Arheimer, T. Blume, M.P. Clark, U. Ehret, F. Fenicia, J.E. Freer, A. Gelfan, H.V. Gupta, D.A. Hughes, R.W. Hut, A. Montanari, S. Pande, D. Tetzlaff, P.A. Troch, S. Uhlenbrook, T. Wagener, H.C. Winsemius, R.A. Woods, E. Zehe, and C. Cudennec (2013) A decade of Predictions in Ungauged Basins (PUB)—a review. *Hydrological Sciences Journal*. 58(6), 1198–1255, doi:10.1080/02626667.2013.803183.

Huffman, E. L., L. H. MacDonald, and J. D. Stednick (2001) Strength and persistence of fire-induced soil hydrophobicity under ponderosa and lodgepole pine, Colorado Front Range. *Hydrological Processes*. 15(15), 2877–2892, doi:10.1002/hyp.379.

Hungerford, R. D., R. R. Nemani, S. W. Running, and J. C. Coughlan (1989) MTCLIM : A Mountain Microclimate Simulation Model; INT-414, Ogden, UT.

Hunsaker, C. T., T. W. Whitaker, and R. C. Bales (2012) Snowmelt Runoff and Water Yield Along Elevation and Temperature Gradients in California's Southern Sierra Nevada. *Journal of the American Water Resources Association*. 48(4), 667–678, doi:10.1111/j.1752-1688.2012.00641.x.

Hwang, T., S. Kang, J. Kim, Y. Kim, D. Lee, and L. Band (2008) Evaluating drought effect on MODIS Gross Primary Production (GPP) with an eco-hydrological model in the mountainous forest, East Asia. *Global Change Biology*. 14(5), 1037–1056, doi:10.1111/j.1365-2486.2008.01556.x.

Ice, G., D. Neary, and P. Adams (2004) Effects of Wildfire on Soils and Watershed Processes. *Journal of Forest Research*. 102(6), 16–20.

Iida, T.,A. Kajihara,H. Okubo,K. Okajima(2012) Effect of Seasonal Snow Cover on Suspended Sediment Runoff in a Mountainous Catchment. *Journal of Hydrology*. *428*, 116–128.

Jarvis, P. (1976) The interpretation of the variations in leaf water potential and stomatal conductance found in canopies in the field, *Philosophical Transactions of the Royal Society of London*, 273(927), 593–640.

Kattelmann, R. C., N. H. Berg, and J. Rector (1983)The potential for increasing streamflow from Sierra Nevada watersheds. *Journal of the American Water Resources Association*. 19(3), 395–402, doi:10.1111/j.1752-1688.1983.tb04596.x.

Kattelmann, R.,and M. Embury (1996). Status of the Sierra Nevada Volume III: Assessments, Commissioned Reports, and Background Information. in *Sierra Nevada Ecosystem Project Final Report to Congress*. http://pubs.usgs.gov/dds/dds-43/VOL_III/VIII_TOC.PDF (accessed on 29 November 2015).

Kerkez, B., S. D. Glaser, R. C. Bales, and M. W. Meadows (2012) Design and performance of a wireless sensor network for catchment-scale snow and soil moisture measurements. *Water Resources Research*. 48(9), 1–18, doi:10.1029/2011WR011214.

Kokkonen, T. S., A. J. Jakeman, P. C. Young, and H. J. Koivusalo (2003) Predicting daily flows in ungauged catchments: Model regionalization from catchment descriptors at the Coweeta Hydrologic Laboratory, North Carolina. *Hydrologic Processes*. 17(11), 2219–2238, doi:10.1002/hyp.1329.

Lana-Renault, N. D. Regues, E. Nadal-Romero, M. P. Serrano-Muela,J. M. Garcia-Ruiz(2010) Streamflow Response and Sediment Yield after Farmland Abandonament: Result from a Small Experimental Catchment in the Central Spanish Pyrenees. *Pirineos Revista Ecologia de Montana.* 165, 97–114.

Lane, P.N.J., G. J. Sheridan, and P. J. Noske(2006) Changes in sediment loads and discharge from small mountain catchments following wildfire in south eastern Australia. *Journal of Hydrology.* 331, 495-510.

Langlois, J.L., D. W Johnson, and G. R. Mehuys(2005) Suspended Sediment Dynamics Associated with Snowmelt Runoff in a Small Mountain Stream of Lake Tahoe (Nevada). *Hydrological Processes*. *19*, 3569–3580.

Leopold, L.B., M. G. Wolman, and J. P. Miller. *Fluvial Processes in Geomorphology*, 2nd ed.;Dover Publications: Mineola, NY, USA, 1995; pp. 27–372.

Lawler, R. R., and T. E. Link (2011) Quantification of incoming all-wave radiation in discontinuous forest canopies with application to snowmelt prediction. *Hydrological Processes*. doi:10.1002/hyp.8150.

van der Linden, S., and M. Woo (2003) Transferability of hydrological model parameters between basins in data-sparse areas, subarctic Canada. *Journal of Hydrology*. 270(3 - 4), 182–194, doi:10.1016/S0022-1694(02)00295-0.

Liu, F., C. Hunsaker, and R. C. Bales (2013) Controls of streamflow generation in small catchments across the snow-rain transition in the Southern Sierra Nevada, California. *Hydrological Processes*. 27(14), 1959–1972, doi:10.1002/hyp.9304.

Macdonald, L. H. (1987) Forest harvest , snowmelt and streamflow in the central Sierra Nevada, in Forest Hydrology and Watershed Management. in Proceedings of the Vancouver Symposium., pp. 273–284, IAHS-AISH Publication No. 167, Vancouver.

Macdonald, L. H., and E. L. Huffman (2004) Post-fire Soil Water Repellency : Persistence and Soil Moisture Thresholds. *Soil Science Society of America Journal*. 68, 1729–1734.

MacDonald, L. H., D.B. Coe, and S.E. Litschert (2004) Assessing cumulative watershed effects in the Central Sierra Nevada: hillslope measurements and catchment-scale modeling. in Murphy, D. D. and P. A. Stine (eds.), in Proceedings of the Sierra Nevada Science Symposium; USDA Forest Service Gen. Tech. Rep. PSW-GTR-193. Albany, CA. 287 p.

McDonald, D.M. and S. F. Lamoureux(2009) Hydroclimatic and Channel Snowpack Controls over Suspended Sediment and Grain Size Transport in a High Arctic Catchment. *Earth Surface Processes* and *Landforms*. *34*, 424–436.

Mackay, D. (2001) Evaluation of hydrologic equilibrium in a mountainous watershed: incorporating forest canopy spatial adjustment to soil biogeochemical processes. *Advances in Water Resources*. 24(9-10), 1211–1227, doi:10.1016/S0309-1708(01)00040-9.

Martin, S., M. Conklin, and R. Bales (2014) Seasonal Accumulation and Depletion of Local Sediment Stores of Four Headwater Catchments. *Water*. 6(7), 2144–2163, doi:10.3390/w6072144.

Marvin, S. (1996) Possible changes in water yield and peak flows in response to forest management, in Sierra Nevada Ecosystem Project: Final Report to Congress, vol. 101, pp. 154–199.

Merz, R., and G. Blöschl (2004) Regionalisation of catchment model parameters. *Journal of Hydrology*. 287(1-4), 95–123, doi:10.1016/j.jhydrol.2003.09.028.

Miller, J. D., H. D. Safford, M. Crimmins, and a. E. Thode (2009) Quantitative evidence for increasing forest fire severity in the Sierra Nevada and southern Cascade Mountains, California and Nevada, USA. *Ecosystems*. 12, 16–32, doi:10.1007/s10021-008-9201-9.

Moore, G. W., B. J. Bond, J. a Jones, N. Phillips, and F. C. Meinzer (2004) Structural and compositional controls on transpiration in 40- and 450-year-old riparian forests in western Oregon, USA. *Tree Physiology*. 24(5), 481–91.

Nash, J. E., and J. V Sutcliffe (1970) River flow forecasting through conceptual models part I --- A discussion of principles. *Journal of Hydrology*. 10(3), 282–290.

Oliver, A.A., J.E. Reuter, A.C. Heyvaert and R.A. Dahlgren (2011) Water quality response to the Angora fire, Lake Tahoe, CA. *Biogeochemistry*. 111, 361–376.

Parajka, J., R. Merz, and G. Blöschl (2005) A comparison of regionalisation methods for catchment model parameters. *Hydrology and Earth Systems Science.* 9, 157–171, doi:10.5194/hessd-2-509-2005.

Pohl, S., J. Garvelmann, J. Wawerla, and M. Weiler (2014) Potential of a low-cost sensor network to understand the spatial and temporal dynamics of a mountain snow cover. *Water Resources Research*. 50, doi:10.1002/2013WR014594.

Pomeroy, J., D. Marks, and T. Link (2009) The impact of coniferous forest temperature on incoming longwave radiation to melting snow. *Hydrology*.2525(May), 2513–2525, doi:10.1002/hyp.

Potts, J. B., E. Marino, and S. L. Stephens (2010) Chaparral shrub recovery after fuel reduction: a comparison of prescribed fire and mastication techniques. *Plant Ecology*. 210(2), 303–315, doi:10.1007/s11258-010-9758-1.

Robichaud, P. R. (2000) Fire effects on infiltration rates after prescribed fire in Northern Rocky Mountain forests, USA. *Journal of Hydrology*. 231-232, 220–229, doi:10.1016/S0022-1694(00)00196-7.

Robichaud, P. R., and T. A. Waldrop (1994) A Comparison of Surface Runoff and Sediment Yields From Low- and High-Severity Site Preparation Burns. *Journal of the American Water Resources Association*. 30(1), 27–34.

Robles, M. D., R. M. Marshall, F. O'Donnell, E. B. Smith, J. A. Haney, and D. F. Gori (2014) Effects of climate variability and accelerated forest thinning on watershed-scale runoff in southwestern USA ponderosa pine forests. *PLoS One*, 9(10), e111092, doi:10.1371/journal.pone.0111092.

Rodriguez-Blanco, M.L. M. M. Taboada-Castro, L. Palleiro, and M. T. Taboada-Castro, (2010) Temporal Changes in Suspended Sediment Transport in an Atlantic Catchment, NW Spain. *Geomorphology.* 123, 181–188.

Running, S. W., and J. Coughlan (1988) A general model of forest ecosystem processes for regional applications I. Hydrologic balance, canopy gas exchange and primary production processes. *Ecological Modeling.* 42, 125-154.

Running, S. W., and E. R. Hunt (1993) Generalization of a forest ecosystem process model for other biomes, BIOME-BGC, and an application for global-scale models, in Scaling physiological processes: leaf to globe. edited by J. R. Ehleringer and C. B. Field, pp. 141–158, Academic Press, San Diego.

Running, S. W., R. R. Nemani, D. L. Peterson, L. E. Band, D. F. Potts, L. L. Pierce, and M. A Spanner (1989) Mapping regional forest evapotranspiration and photosynthesis by coupling satellite data with ecosystem simulation. *Ecology*. 70(4), 1090–1101.

Sadeghi, S.H.R., T. Mizuyama, S. Miyata, T. Gomi, K. Kosugi, T. Fukushima, S. Mizugaki, and Y. Onda(2008) Determinant Factors of Sediment Graphs and Rating Loops in a Reforested Watershed. *Journal of Hydrology*. 356, 271–282.

Saucedo, G. J., and D. L. Wagner (1992) Geologic Map of the Chico quadrangle, Regional Geologic Map 7A.

Seeger, M., M. P. Errea, S. Begueria, J. Arnaez, C. Marti, and J. M. Garcia-Ruiz (2004) Catchment Soil Moisture and Rainfall Characteristics as Determinant Factors for discharge/suspended Sediment Hysteretic Loops in a Small Headwater Catchment in the Spanish Pyrenees. *Journal of Hydrology*. 288, 299–311.

Shakesby, R.A. (2011) Post-wildfire soil erosion in the Mediterranean: Review and future research directions. *Earth-Science Reviews.* 105, 71-100.

Shakesby, R., and S. Doerr (2006) Wildfire as a hydrological and geomorphological agent. *Earth-Science Reviews*. 74(3-4), 269–307, doi:10.1016/j.earscirev.2005.10.006.

Siebert, J. and J.J. McDonnell (2002) On the dialog between experimentalist and modeler in catchment hydrology: Use of soft data for multicriteria model calibration. *Water Resources Research. 38*(11), 23, 1-14, doi:10.1029/2001WR000978.

Silberstein, R. P. (2006) Hydrological models are so good, do we still need data?. *Environmental Modeling and Software*, 21(9), 1340–1352, doi:10.1016/j.envsoft.2005.04.019.

Sivapalan, M. (2003) Prediction in ungauged basins: a grand challenge for theoretical hydrology. *Hydrological Processes*. 17(15), 3163–3170, doi:10.1002/hyp.5155.

Soil Survey Staff, (2011), Soil Survey Geographic (SSURGO) Database. USDA Natural REsources Conservation Service. http://soildatamart.nrcs.usda.gov.

Smith, H.G., and D. Dragovich (2009) Interpreting sediment delivery processes using suspended sediment-discharge hysteresis patterns from nested upland catchments, South-Eastern Australia. *Hydrolocial Processes*. 23, 2415–2426.

Smith, H.G., G. J. Sheridan, P. N. J. Lane, P. Nyman, and S. Haydon, (2011) Wildfire effects on water quality in forest catchments: A review with implications for water supply. *Journal of Hydrology.* 396, 170-192.

Soler, M., G. Latron, and F. Gallart(2008) Relationships Between Suspended Sediment Concentrations and Discharge in two Small Research Basins in a Mountainous Mediterranean Area (Vallcebre, Eastern Pyrenees). *Geomorphology.* 98, 143–152.

Stafford, A.K. Sediment Production and Delivery from Hillslopes and Forest Roads in the Southern Sierra Nevada, California. Master's Thesis, Colorado State University, Fort Collins, CO, USA, 2011.

State of California Sierra Nevada Conservancy. Available online: http://www.sierranevada.ca.gov/our-region/sierra-water-supply-connection (accessed on 23 June 2014).

Stednick, J. (1996) Monitoring the effects of timber harvest on annual water yield. *Journal of Hydrology*. 176(1-4), 79–95, doi:10.1016/0022-1694(95)02780-7.

Stephens, S., J. Agee, P. Fule, M. P. North, W. Romme, T. Swetnam, and M. Turner (2013) Managing Forest and Fire in Changing Climates. *Science* 342, 41–42.

Stephens, S. L. (1998) Evaluation of the effects of silvicultural and fuels treatments on potential fire behaviour in Sierra Nevada mixed-conifer forests. *Forest Ecology and Management*. 105(1-3), 21–35, doi:10.1016/S0378-1127(97)00293-4.

Stephens, S. L., and J. J. Moghaddas (2005) Experimental fuel treatment impacts on forest structure, potential fire behavior, and predicted tree mortality in a California mixed conifer forest. *Forest Ecology and Management.* 215(1-3), 21–36, doi:10.1016/j.foreco.2005.03.070.

Stuemky, M. (2010) Kings River Experimental Watersheds (KREW): Providence - Instruments. USDA Forest Service Pacific Southwest Research Station. Available from: http://www.fs.fed.us/psw/topics/water/kingsriver/documents/maps/krew_providence_instruments.pdf

Tague, C., K. Heyn, and L. Christensen (2009) Topographic controls on spatial patterns of conifer transpiration and net primary productivity under climate warming in mountain ecosystems. *Ecohydrology*, 541–554, doi:10.1002/eco.

Tague, C. L., and L. E. Band (2004) RHESSys: Regional Hydro-Ecologic Simulation System—An object-oriented approach to spatially distributed modeling of carbon, water, and nutrient cycling. *Earth Interactions*. 8(19), doi:http://dx.doi.org/10.1175/1087-3562(2004)8<1:RRHSSO>2.0.CO;2.

Thompson, C., E. Rhodes, and J. Croke (2007) The storage of bed material in mountain stream channels as assessed using Optically Stimulated Luminescence dating. *Geomorphology*. 83, 307–321

Traylor, C. R., and E. E. Wohl (2000) Seasonal changes in bed elevation in a step-pool channel, Rocky Mountains, Colorado, U.S.A. *Arctic, Antarctic, and Alpine Research*. 32(1), 95-103.

Troendle, C. A., and R. M. King (1985) The effect of timber harvest on the Fool Creek watershed, 30 years later. *Water Resources Research*. 21(12), 1915–1922.

Troendle, C. A., M. S. Wilcox, G. S. Bevenger, and L. S. Porth (2001) The Coon Creek Water Yield Augmentation Project: implementation of timber harvesting technology to increase streamflow. *Forest Ecology and Management*. 143, 179–187, doi:10.1016/S0378-1127(00)00516-8.

United States Geological Survey(2014) National Geologic Map Database. (web database) http://ngmdb.usgs.gov/ngmdb/ngmdb_home.html

USDA (2004) Sierra Nevada Forest Plan Amendment, Record of Decision. USDA Forest Service Pacific Southwest Region, Vallejo, CA.

Wagener, T., and A. Montanari (2011) Convergence of approaches toward reducing uncertainty in predictions in ungauged basins. *Water Resources Research*. 47(6), 1–8, doi:10.1029/2010WR009469.

Westerling, A. L., H. G. Hidalgo, D. R. Cayan, and T. W. Swetnam (2006) Warming and earlier spring increase western U.S. forest wildfire activity. *Science*. 313(5789), 940–3, doi:10.1126/science.1128834.

Wigmosta, M. S., L. W. Vail, and D. P. Lettenmaier (1994) A distributed hydrology-vegetation model for complex terrain. *Water Resources Research*. 30(6), 1665, doi:10.1029/94WR00436.

Williams, G.P. (1989) Sediment Concentration *Versus* Water Discharge during Single Hydrologic Events in Rivers. *Journal of Hydrology*. *111*, 89–106.

Wilson, C.G., A. N. Thanos Papanicolaou, and K. D. Denn(2012) Partitioning Fine Sediment Loads in a Headwater System with Intensive Agriculture. *Journal of Soils and Sediment*. 12, 966–981.

Wood, P.A. (1977) Controls of Variation in Suspended Sediment Concentration in the River Rother, West Sussex, England. *Sedimentology.* 24, 437–445.

Zhang, L., W. R. Dawes, and G. R. Walker (2001) Response of mean annual evapotranspiration to vegetation changes at catchment scale. *Water Resources Research*. 37(3), 701–708.

Zierl, B., H. Bugmann, and C. L. Tague (2006) Water and carbon fluxes of European ecosystems: an evaluation of the ecohydrological model RHESSys. *Hydrological Processes*. 21(24), 3328–3339, doi:10.1002/hyp.

Zou, C. B., P. F. Ffolliott, and M. Wine (2010) Streamflow responses to vegetation manipulations along a gradient of precipitation in the Colorado River Basin. *Forest Ecology and Management*. 259(7), 1268–1276, doi:10.1016/j.foreco.2009.08.005.